



National Library
of Canada

Bibliothèque nationale
du Canada

Canadian Theses Service

Services des thèses canadiennes

Ottawa, Canada
K1A 0N4

CANADIAN THESES

THÈSES CANADIENNES

NOTICE

The quality of this microfiche is heavily dependent upon the quality of the original thesis submitted for microfilming. Every effort has been made to ensure the highest quality of reproduction possible.

If pages are missing, contact the university which granted the degree.

Some pages may have indistinct print especially if the original pages were typed with a poor typewriter ribbon or if the university sent us an inferior photocopy.

Previously copyrighted materials (journal articles, published tests, etc.) are not filmed.

Reproduction in full or in part of this film is governed by the Canadian Copyright Act, R.S.C. 1970, c. C-30.

**THIS DISSERTATION
HAS BEEN MICROFILMED
EXACTLY AS RECEIVED**

AVIS

La qualité de cette microfiche dépend grandement de la qualité de la thèse soumise au microfilmage. Nous avons tout fait pour assurer une qualité supérieure de reproduction.

S'il manque des pages, veuillez communiquer avec l'université qui a conféré le grade.

La qualité d'impression de certaines pages peut laisser à désirer, surtout si les pages originales ont été dactylographiées à l'aide d'un ruban usé ou si l'université nous a fait parvenir une photocopie de qualité inférieure.

Les documents qui font déjà l'objet d'un droit d'auteur (articles de revue, examens publiés, etc.) ne sont pas microfilmés.

La reproduction, même partielle, de ce microfilm est soumise à la Loi canadienne sur le droit d'auteur, SRC 1970, c. C-30.

**LA THÈSE A ÉTÉ
MICROFILMÉE TELLE QUE
NOUS L'AVONS REÇUE**

THE UNIVERSITY OF ALBERTA

Attenuation from Vertical Seismic Profile Data

by

(C) Nicholas Alexander Keehn

A THESIS

SUBMITTED TO THE FACULTY OF GRADUATE STUDIES AND RESEARCH

IN PARTIAL FULFILMENT OF THE REQUIREMENTS FOR THE DEGREE

OF Master of Science

IN

Geophysics

Department of Physics

EDMONTON, ALBERTA

Spring, 1987

Permission has been granted to the National Library of Canada to microfilm this thesis and to lend or sell copies of the film.

The author (copyright owner) has reserved other publication rights, and neither the thesis nor extensive extracts from it may be printed or otherwise reproduced without his/her written permission.

L'autorisation a été accordée à la Bibliothèque nationale du Canada de microfilmer cette thèse et de prêter ou de vendre des exemplaires du film.

L'auteur (titulaire du droit d'auteur) se réserve les autres droits de publication; ni la thèse ni de longs extraits de celle-ci ne doivent être imprimés ou autrement reproduits sans son autorisation écrite.

ISBN 0-315-37764-X

THE UNIVERSITY OF ALBERTA

RELEASE FORM

NAME OF AUTHOR Nicholas Alexander Keehn
TITLE OF THESIS Attenuation from Vertical Seismic
 Profile Data
DEGREE FOR WHICH THESIS WAS PRESENTED Master of Science
YEAR THIS DEGREE GRANTED Spring, 1987

Permission is hereby granted to THE UNIVERSITY OF ALBERTA LIBRARY to reproduce single copies of this thesis and to lend or sell such copies for private, scholarly or scientific research purposes only.

The author reserves other publication rights, and neither the thesis nor extensive extracts from it may be printed or otherwise reproduced without the author's written permission.

(SIGNED) *Nick Keehn*.....

PERMANENT ADDRESS:

.....*388 Spodino Rd*.....
.....*Toronto, Ontario*.....
.....*M5P 2V9*.....

DATED *December 5*.....1986

THE UNIVERSITY OF ALBERTA
FACULTY OF GRADUATE STUDIES AND RESEARCH

The undersigned certify that they have read, and recommend to the Faculty of Graduate Studies and Research, for acceptance, a thesis entitled Attenuation from Vertical Seismic Profile Data submitted by Nicholas Alexander Keehn in partial fulfilment of the requirements for the degree of Master of Science in Geophysics.

..... E. R. Karamant
.....

Supervisor

..... *E. R. Karamant*
.....

..... *Philippe Volpe*
.....

..... *D. G. Hughes*
.....

Date. *December 5 1986*

Dedication

My research, time, and energy of the past few years, which culminate with this thesis, have all been for Wanda Kamocki without whom they would have lost all meaning.

Abstract

Seismic waves are observed to attenuate while propagating through anelastic inhomogeneous media. Intrinsic attenuation is that component of the attenuation which is due solely to the anelasticity of the media and is described in terms of a quality factor, Q . In this study, the variation of intrinsic attenuation with depth is investigated in the neighborhood of a 5 kilometer deep borehole located on Melville Island in the Canadian Arctic. The data from a Vertical Seismic Profiling (VSP) survey performed in the well is analysed with the spectral ratio method. The results indicate good correlation between a highly attenuating zone and a sandstone unit of the Lower Triassic period, located between 1400 meters and 2500 meters. The specific attenuation for the region is found to be approximately .04458 ($Q \approx 22$) with a standard deviation of .03998. This compares with a low Q of 25 quoted in the literature for a study in the North Sea basin. However, in the Lower Triassic layer the sandstone has an anomalously high specific attenuation of .10501 ($Q \approx 10$) with a standard deviation of .05783. Immediately above 4000 meters there exists a second low- Q zone where the specific attenuation is .08337 ($Q \approx 12$) with a standard deviation of .04202. These results are somewhat higher than those found in the North Sea basin. A portion of the sandstone layer exhibits a relatively high Q -value with respect to the rest of the layer. This could be the result of either the presence of a fluid of relatively lower

viscosity, a difference in saturation, an increase in pore aspect ratio, or a decrease in porosity. From an analysis of seismic velocity dispersion it was concluded that scattering of seismic energy and the effects of intrabed multiples may be the cause of 62% of the observed attenuation. The results illustrate that correlation of Q with lithology remains feasible despite the presence of fine impedance structures which generate intrabed multiples and exaggerate scattering.

Acknowledgements

I would like to express my greatest appreciation to Dr. E. R. Kanasewich for his thoughtful guidance and many instructive discussions throughout the course of this research. As well, I am indebted to Mr. J. Thompson for allowing the use of the data collected by Panarctic Oils Ltd. I also wish to thank him for expressing interest in the research and for very informative discussions with both Dr. Kanasewich and myself. Many of the computer programs used during this study were developed by Dr. D. C. Ganley. C. McCloughan provided colorful dialogue and an abundant knowledge of the computer system, both of which were greatly appreciated. Finally, I wish to express my sincere gratitude to my parents, Dr. J. D. Keehn and N. L. Keehn, who have taught me the importance of striving to attain a goal, and to my wife, Wanda, for making the completion of this goal possible.

Table of Contents

Chapter	Page
1. Characteristics of Attenuation	1
1.1 Introduction and Research Goals	1
1.2 Formulation and Notation	3
1.3 Significance of Attenuation Studies	13
1.4 Loss Mechanisms	14
2. Procedure for Estimating Attenuation	24
2.1 Optional Procedures	24
2.2 Vertical Seismic Profiling	25
2.3 The Spectral Ratio Method	30
2.4 Interference Correction Factor	33
2.5 Depth Resolution	37
3. Case Study	44
3.1 Survey Geometry and Location	44
3.2 Description of Data	47
3.3 Generation of Synthetic Traces	56
3.4 Generation of Amplitude Spectra	60
3.5 Selection of Trace Pairs	64
3.6 Calculation of Q	66
3.7 Elimination Procedure	68
3.8 Presentation of Results	72
3.9 Discussion of Results	79
Conclusions	88
Bibliography	93
Appendix A : Log Plots	100
Appendix B : Listing of Programs	128

List of Tables

Table	Page
3.1 Interval Attenuation Statistics	77

List of Figures

Figure		Page
2.1	General layout of the VSP and Check Shot surveys	27
2.2	Example of oscillatory patterns observed in spectral ratio studies	34
3.1	Location of survey site	45
3.2	Geological cross-section of Sherard Bay F-34 survey site	46
3.3	Lithologic cross-section of Sherard Bay F-34 survey site	48
3.4	Surface geometry of the F-34 well	49
3.5	Example of filtered data from Sherard Bay	50
3.6	Sequence of 1st arrivals, a) those generated by the Aquaflex source, b) those generated by the Geogel source	52
3.7	Velocity profiles: a) every layer present b) 5% change in velocity required to define a new layer	55
3.8	Comparison of first-arrival amplitude-spectra generated from the Aquaflex (top) and Geogel (bottom) sources	62
3.9	Plot of all accepted Q-values versus depth below K.B.	71
3.10	Plot of specific attenuation versus depth with accompanying Q-axis	74
3.11	a) 200-meter running average of the specific attenuation profile b) 200-meter weighted running average of the specific attenuation profile	75
3.12	Profiles: a) weighted $1/Q$ smoothed with a 200 meter running average b) lithology c) interval $1/Q$ d) interval velocity	78
3.13	Dispersion curves for $Q(45\text{Hz}) = 60$ ($Q = 64$) and $Q(45\text{Hz}) = 23$ ($Q = 27$), a) frequency range 0 to 20 kHz, b) frequency range 0 to 200 Hz	86

Chapter 1

Characteristics of Attenuation

1.1 Introduction and Research Goals

The crust of the earth has many properties that are of interest to researchers in geophysics, geology, and geochemistry. In exploration geophysics the important properties include the compressional and shear seismic velocities, the density of a rock, its magnetic characteristics and electrical conductivity, porosity, and levels of gas or fluid saturation. A property that has recently been shown to be useful in the exploration for oil is the degree of anelasticity of a rock. The more anelastic a material the greater is the intrinsic attenuation of an elastic wave passing through it. To date, many laboratory experiments have demonstrated that intrinsic attenuation correlates well with rock properties such as the level of fluid saturation, microstructure, the viscosity of pore fluid, and porosity. These parameters are difficult to obtain from *in situ* rocks, however, there are indications that the amount of intrinsic attenuation undergone by a travelling wave will yield information regarding these parameters.

In exploration geophysics waves of seismic frequencies are used because they are easy to generate and they propagate large distances within the earth. Laboratory attenuation experiments, unfortunately, require sonic

frequencies because the attenuation of the lower seismic frequencies is not sufficient to be measured on small laboratory rock samples and the wavelengths are too long to make measurements possible. Seismic and sonic signals do not attenuate in the same manner, thus, *In situ* measurements of seismic attenuation are required for direct application in exploration geophysics. Very few such surveys have been conducted, consequently, it remains to be shown that *In situ* experiments can reliably yield intrinsic attenuation measurements.

This study attempts to extract values of intrinsic attenuation from seismic data collected *In situ*, to correlate the results with the local lithology, and to suggest how microstructure, saturation, viscosity, and porosity may vary with depth. The lithology of the study area is available and it is important, for the sake of confidence in the attenuation profile, to be able to associate anomalous attenuation measurements with specific rock types known to have certain rock properties. Once confidence is gained, rock properties, such as those listed above, can be inferred.

Data collected from a Vertical Seismic Profiling survey is analysed in this study with the spectral ratio method. It is found that the effects of intrabed multiples and scattering cause an apparent attenuation that may obscure the true intrinsic attenuation. Nonetheless, a positive correlation between the lithology and the attenuation

profile is found, indicating that variations of intrinsic attenuation are, in fact, being observed.

1.2 Formulation and Notation

The apparent attenuation caused by intrabed multiples and scattering contains no interesting information regarding attenuation measurements, consequently, attempts are made to remove it. Intrinsic attenuation, on the other hand, is a direct consequence of the anelasticity of a medium which, in turn, is characteristic of the rock properties mentioned earlier. Following is a detailed discussion of the formulation and notation used in studies of intrinsic attenuation.

Elastic materials are those which return to their initial shape after an applied stress, which has deformed the material, is subsequently removed. If, however, some of the input energy required to deform the material is lost during the stressing process, for example in the form of heat, the potential energy integrated over a stress cycle will not equal the integrated input energy. Consequently, an equal and opposite strain does not result and there remains some deformation, or strain. Such is the case with anelastic materials.

Hooke's law states that for an isotropic elastic medium the magnitude of a stress acting on an elementary volume is proportional to the magnitude of the resulting strain. But, if the stress is zero, as in the final state of the

anelastic material discussed above, and a strain remains, then Hooke's law is violated. Thus, it can be said that anelastic materials do not obey Hooke's law. However, it is true that a sinusoidal stress of angular frequency, ω , acting on an anelastic elementary volume will result in a sinusoidal strain also of angular frequency, ω , and exhibiting a phase lag with respect to the stress. The amplitude of a sinusoidally varying stress is proportional to the amplitude of a sinusoidally varying strain, whereas the magnitudes are not related by a constant of proportionality.

To gain further insight into the nature of intrinsic wave attenuation consider an anelastic elementary volume undergoing sinusoidal extension such as that caused by a compressional wave travelling in the x-direction. The magnitudes of the stress and strain are,

$$p_{xx} = P_{xx} e^{i\omega t} \quad (1 a)$$

$$e_{xx} = \xi_{xx} e^{i\omega t} \quad (1 b)$$

where P_{xx} and ξ_{xx} are the amplitudes of the stress and strain respectively. The lack of proportionality of the magnitudes and their difference in phase is accounted for

simultaneously by requiring the amplitudes to be complex quantities.

From the discussion above,

$$P_{xx} \propto \xi_{xx}$$

Note, for perfectly elastic media the magnitudes become proportional as mentioned earlier, and are related by a constant of proportionality as follows,

$$P_{xx} = (\lambda + 2\mu)e_{xx}$$

The constant of proportionality, $(\lambda + 2\mu)$, is called the elastic modulus, where λ and μ are Lamé constants. In the anelastic case there must be a constant of proportionality between the complex amplitudes, thus a complex elastic modulus is introduced,

$$P_{xx} = [\lambda + 2\mu + i(\lambda^* + 2\mu^*)]\xi_{xx} \quad (2)$$

$$= (M + iM^*)\xi_{xx}$$

where $M = \lambda + 2\mu$, $M^* = \lambda^* + 2\mu^*$, and $*$ denotes the imaginary component. Note that as M^* becomes small with respect to M the stress-strain relation for elastic media is approached.

Rewriting equation (2),

$$\xi_{xx} = \frac{P_{xx}}{M + iM^*} = \frac{P_{xx}}{M(1 + iM^*/M)}$$

The Maclaurin series expansion of the term in brackets is,

$$\frac{1}{(1 + iM^*/M)} = 1 - i\left(\frac{M^*}{M}\right) - \left(\frac{M^*}{M}\right)^2 + i\left(\frac{M^*}{M}\right)^3 + \dots$$

Note, also, the following expansion,

$$e^{-iM^*/M} = 1 - i\left(\frac{M^*}{M}\right) - \frac{1}{2}\left(\frac{M^*}{M}\right)^2 + i\frac{1}{3!}\left(\frac{M^*}{M}\right)^3 + \dots$$

If it is assumed that the quantity $\left(\frac{M^*}{M}\right) \ll 1$, which is equivalent to saying the material is near-elastic, then powers of $\left(\frac{M^*}{M}\right)$ greater than 1 can be neglected. Thus,

$$\xi_{xx} \approx \frac{P_{xx}}{M} e^{-iM^*/M}$$

or,

$$P_{xx} \approx M \xi_{xx} e^{iM^*/M}$$

Substituting P_{xx} back into equations (1 a) and (1 b),

$$P_{xx} \approx M \xi_{xx} e^{i(\omega t + M^*/M)} \quad (3 a)$$

$$\epsilon_{xx} \approx \xi_{xx} e^{i\omega t} \quad (3 b)$$

Consequently, the constant of proportionality between the amplitudes of a sinusoidal stress and the resulting strain is,

$$M e^{iM^*/M}$$

The magnitudes are not related by a constant of proportionality, and there is a phase difference of $(\frac{M^*}{M})$ between the stress and strain.

Consider now, a travelling plane wave in an anelastic medium. It has been observed that such a wave experiences an exponential decay of its amplitude with distance (Aki and Richards, 1980), and that the power of the decay-exponential varies linearly with frequency (Knopoff, 1964). An extensive review of the literature can be found in Ganley (1979).

The scalar wave equation for a plane compressional wave travelling in an elastic solid in the x-direction is,

$$(\lambda + 2\mu) \frac{\partial^2 u(x,t)}{\partial^2 x} = \rho \frac{\partial^2 u(x,t)}{\partial^2 t}$$

where ρ is the density of the solid, and u is the particle displacement along the x-axis. The corresponding equation for a homogeneous anelastic solid is,

$$[\lambda + i\lambda^* + 2(\mu + i\mu^*)] \frac{\partial^2 u(x,t)}{\partial^2 x} = \rho \frac{\partial^2 u(x,t)}{\partial^2 t}$$

$$(M + iM^*) \frac{\partial^2 u(x,t)}{\partial^2 x} = \rho \frac{\partial^2 u(x,t)}{\partial^2 t} \quad (4)$$

The previous arguments apply to a stationary sinusoidal stress of angular frequency, ω . Such a stress gives rise to a sinusoidal displacement, also of angular frequency, ω ,

$$u(t) = U_0 e^{i\omega t}$$

where U_0 is the initial displacement amplitude. If the stress is propagating with a wave number, k , then so will the displacement,

$$u(x,t) = U_0 e^{ikx} e^{i\omega t} \quad (5)$$

where U_0 is the initial displacement amplitude at the x origin. Inserting equation (5) into equation (4) gives,

$$-(M + iM^*)U_0 k^2 e^{ikx} e^{i\omega t} = -\rho U_0 \omega^2 e^{ikx} e^{i\omega t}$$

$$k^2 = \frac{\rho \omega^2}{M + iM^*} = \frac{\rho \omega^2}{M(1 + iM^*/M)} = (k_r + ik_i)^2$$

where k_r and k_i are the real and imaginary parts of the complex wave number which results from the introduction of complex elastic constants. Again, if $(\frac{M^*}{M}) < 1$ then the

following is true,

$$k^2 \approx \frac{\rho\omega^2}{M} (1 - i\frac{M^*}{M}) \approx \frac{\rho\omega^2}{M} e^{-i(M^*/M)}$$

$$k \approx \pm\omega\left(\frac{\rho}{M}\right)^{1/2} e^{-iM^*/2M}$$

$$\approx \pm\omega\left(\frac{\rho}{M}\right)^{1/2} \left(1 - i\frac{M^*}{2M}\right)$$

The velocity is given by,

$$v = \left(\frac{M}{\rho}\right)^{1/2}$$

therefore,

$$k \approx \pm\left[\frac{\omega}{v} - i\frac{\omega M^*}{2vM}\right]$$

$$k_r \approx \pm\frac{\omega}{v} \text{ and } k_i \approx \mp \frac{\omega M^*}{2vM}$$

The result being that the displacement due to a travelling wave in the positive x-direction becomes,

$$u(x, t) \approx U_0 \exp\left[-\left(i\frac{\omega}{v} + \frac{\omega M^*}{2vM}\right)x\right] \exp[i\omega t]$$

$$\left\{ \approx U_0 \exp\left[i\left(\omega t - \frac{\omega}{v}x\right)\right] \exp\left[-\frac{\omega M^*}{2vM}x\right] \right. \quad (6)$$

Often the argument of the last exponential on the right is related to a spatial attenuation coefficient, a , such that,

$$a(\omega) = k_i \approx \frac{\omega M^*}{2vM} \quad (7)$$

Recall that during the stressing of an anelastic material energy is lost to the material. For an oscillating stress the ratio of the strain energy lost per cycle, ΔE , to the peak strain energy of the cycle, E , is an indication of the degree of anelasticity, and is referred to as the specific attenuation after Knopoff (1964), Murphy III (1982), and McCann and McCann (1985), or simply attenuation when used in this context. The process of intrinsic attenuation is frequency dependent but the specific attenuation (attenuation) is a parameter which is generally

independent of frequency. This ratio is inversely proportional to the quality, Q , of the material. Infinite quality corresponds to a perfectly elastic solid. The specific attenuation may be defined as,

$$\text{Specific Attenuation} \equiv \frac{1}{Q} \approx \frac{\Delta E}{2\pi E} \quad (8)$$

By relating energy flow to stress and strain, given by equations (3 a) and (3 b), it is found that, for $Q \gg 1$,

$$\frac{\Delta E}{2\pi E} \approx \frac{M^*}{M}$$

Consequently, by equation (8),

$$\frac{M^*}{M} \approx \frac{1}{Q} \quad (9)$$

Some authors prefer to define the specific attenuation as $\frac{1}{Q} = \frac{M^*}{M}$. These two definitions agree closely for weakly attenuating media. Regardless of the definition of specific attenuation, equations (6) and (7), in terms of Q , become,

$$u(x,t) \approx U_0 \exp[i(\omega t - \frac{\omega}{v}x)] \exp[-\frac{\omega}{2vQ}x] \quad (10 a)$$

$$a(\omega) \approx \frac{\omega}{2vQ} \text{ for } Q \gg 1 \quad (10 b)$$

1.3 Significance of Attenuation Studies

A number of experiments have been conducted in an attempt to find Q-values for a variety of rock types under different levels of porosity, fluid and gas saturation, degree of consolidation, temperature, and level of hydration. The experiments have been conducted both in the laboratory and in the field and, while a great deal more work is required in this area, the likelihood of being able to discern the lithology of a borehole, or the level of fluid/gas saturation, via its Q-log is high (Stainsby and Worthington, 1985).

Winkler and Nur (1979) suggest that one would be able to monitor steam injection zones by measuring attenuation since this quantity is very sensitive to the level of fluid saturation in porous media. In their studies on Massillon sandstone they found P-wave velocities to vary approximately 15% between fully saturated and dry rock. However, the

attenuation was noted to vary by 500% or more depending on the confining pressure. In addition, they speculate upon the usefulness of attenuation studies in earthquake prediction. Winkler and Nur (1982) indicate that with knowledge of the velocity profile, the porosity, and other rock parameters including specific attenuation, it may be possible to determine fluid content, permeability, and microstructure of the lithology, information which is of interest in oil exploration.

In addition to the above, seismic inversion and the quality of synthetic seismograms would be improved with a more complete understanding of attenuation (Kan et al., 1982).

1.4 Loss Mechanisms

There exist a number of energy loss mechanisms which have been proposed to account for the observed intrinsic attenuation of a seismic wave as it propagates through the earth.

A thermoelastic loss mechanism was studied by Treitel in 1959 in which the heat generated by the compression due to a passing P-wave was examined. Because the heat conductivity of rocks is not zero, heat generated by a local compression is allowed to dissipate and so the radiated energy is not available when the rock rarefacts. This mechanism will attenuate compressional waves but not shear waves as no compression or rarefaction takes place during a

shearing stress. Treitel, however, calculated theoretical values of the attenuation coefficient for rock due to the thermoelastic mechanism and concluded that its effects were far too small compared to actual seismic attenuation to be of any significance.

Knopoff and MacDonald (1960) as well found the effects of thermoelastic loss to be too small to be of concern in seismology. They also studied Rayleigh scattering losses and loss in ferro-magnetic media. Again, at seismic frequencies these mechanisms could not account for the observed energy losses.

In experiments employing temperatures of 120°C , kilohertz frequencies, and confining pressures of 200 bars, Jones and Nur (1983) dismissed a thermal relaxation process as an attenuation mechanism. Instead, they proposed that viscous fluid flow controlled the dissipation.

Gordon and Nelson (1966) considered many loss mechanisms. One of them was stress induced ordering in which a redistribution of atoms in a dry crystal takes place due to the heat generated by stress. They found that this did not allow for the large amounts of attenuation experienced by a seismic wave.

Jackson and Anderson (1970), Gordon and Nelson (1966), and Johnston et al. (1979), all considered frictional sliding between crack walls or grains in unconsolidated dry rock at low pressure. Under an alternating stress the grains, or walls, are thought to slide past each other with

the resulting heat radiating away.

In another sense, viscous fluid in a saturated porous medium may flow from pore to pore due to a passing seismic disturbance. This assumes a continuous network of pores and channels through which the fluid is able to pass. Biot's theory (1959 a, b) describes the propagation of elastic waves in such a saturated porous elastic solid. He considered a compressible fluid which has the same density as the solid, such as a water-saturated rock. The flowing liquid experiences friction with the pore walls and results in the wave being attenuated.

The last mechanism considered here, by which energy may be dissipated, is described by the viscous squirt flow theory. The model involves a partially saturated porous elastic media where the pore spaces are isolated from one another. Within each pore there exists an incompressible fluid and a gas. Under wave excitation the pore walls are deformed decreasing the volume within the pore. The viscous fluid then flows, or squirts, and viscous losses occur due to heat generation.

In the final analysis there are three predominant theoretical models which are able to account for the observed attenuation of seismic waves in porous media. These are frictional grain sliding, Biot's mechanism, and viscous squirt flow.

Attenuation has been observed to depend on a great variety of physical parameters. Jones and Nur (1983) have

studied the effects of fluid viscosity and temperature on attenuation in the kiloHertz frequency range. They found attenuation to decrease with increasing temperature. Nyland (1985 a, b) carried out a theoretical analysis of the temperature dependence of attenuation in oil sands and concluded that attenuation is very sensitive to temperature fluctuations. The dependence on strain amplitude was studied by Winkler and Nur in 1982. There is also a dependence on pore fluid pressure (Winkler and Nur, 1982; Jones and Nur, 1983), confining pressure (Winkler and Nur, 1982, Jones and Nur, 1983, Winkler, 1986), frequency (Winkler and Nur, 1982, Jones and Nur, 1983, Murphy III, 1982, Winkler, 1986, Hovem and Ingram, 1979, McCann and McCann, 1985), and saturation (Winkler and Nur, 1982, Spencer, 1981, Murphy III, 1982, Winkler, 1986). Murphy III (1982) states that energy loss is "very sensitive" to partial water saturation. He continues to show that, in his studies on partially saturated Massillon sandstone and Vycor porous glass, the specific attenuation is "strongly frequency dependent" through the acoustic range 1 kHz to 10 kHz, otherwise known as the sonic frequency band. However, from 10 to 100 Hz his data shows almost no dependence on frequency, and in dry sandstone they are completely independent. Spencer (1981) states that vacuum-dry rocks demonstrate "negligible attenuation" while water-saturated samples of sandstone, limestone, and granite show large attenuation peaks with frequency. Winkler and Nur (1979, 1982) observed that partial water saturation

"significantly" increases the attenuation of both P- and S-waves when compared to the attenuation in dry rock. In 1979 they demonstrated that P-wave attenuation in Massilon sandstone reached its maximum value at a saturation of 95%.

The three possible attenuation models mentioned above are all found to produce results comparable to observation. However, they are individually applicable only to specific frequencies and saturations, or only become important under certain pressure conditions. There are six such major regimes of concern in attenuation studies:

1. dry porous rocks
2. partially saturated porous rocks
3. saturated porous rocks
4. ultrasonic frequencies (100 - 1000 kHz)
5. sonic frequencies (1 - 10 kHz)
6. seismic frequencies (10 - 500 Hz)

Winkler and Nur (1982) interpreted an attenuation dependence on strain amplitude as evidence for frictional sliding at grain contacts. They observed, however, that at typical *in situ* seismic strains and confining pressures there was no attenuation dependence on the amplitude of the induced strain. The conclusion they drew was that frictional sliding was "not a significant" source of seismic attenuation *in situ*. The same conclusion was reached by Murphy III in 1982 in his studies on Massilon sandstone and

Vycor porous glass in regards to sonic frequencies. The importance of grain sliding is debatable since Ganley (1979), and Johnston et.al. (1979) rate this mechanism as the most important cause of absorption.

Biot's mechanism and the viscous squirt flow mechanism have been compared to observations by many authors in the past decade. Hovem and Ingram (1979) studied saturated marine sediments in the 20 kHz to 1000 kHz range. They studied the frequency dependence of attenuation and their results agree well with Biot's theory from 60 kHz and up, however, in the lower frequencies shown the discrepancy increases. Their conclusion was that for seismic frequencies, and in media with less permeability, the Biot viscous losses will be much smaller while other mechanisms are likely to be of higher importance. McCann and McCann (1985) have formulated a modified Biot theory for fully saturated media with which they found "excellent" agreement with recent observed data, but again, only in the 10 kHz to 2.25 MHz range.

Winkler and Nur (1982) have studied P- and S-wave attenuation for fully saturated Massilon sandstone in the 500 Hz to 9000 Hz band (seismic to sonic) and observed a 3:1 ratio in the absorption of S-waves to P-waves. They state that Biot's theory is "reasonably consistent" with this observation but that a ratio such as this ($a_s/a_p > 1$) may imply that Biot's absorption is dominated by other mechanisms in the samples they were considering. Their

argument is based on the overall magnitude of the absorption observed.

Johnston et al. (1979) applied Biot's theory to Berea sandstone and they agreed with the results of Winkler and Nur (1982) and Hovem and Ingram (1979). They said that at low frequencies Biot's theory predicts values of attenuation which are an order of magnitude lower than that observed.

There are, of course, researchers who prefer mechanisms other than those pointed out here to explain their observations. Liu et al. (1976) have discussed the concept of the superposition of twelve relaxation mechanisms in a linear viscoelastic solid which is able to account for observed levels of attenuation, however, this concept is not related to levels of fluid saturation. The overriding opinion is that the squirt flow attenuation mechanism dominates other mechanisms in the seismic to sonic frequency range, at those pressures found *in situ*, and at the levels of saturation observed in exploration seismology.

Specific attenuation has a very interesting dependence on both frequency and fluid saturation. Jones and Nur (1983) observed a peak in specific attenuation at about 8 kHz and 120°C while they were studying fully water saturated Berea sandstone. At room temperature the attenuation peak shifted down to 2 kHz and if viscous oils are present they suggest the peak will move into the seismic frequency band. Nyland (1985 b) estimates that for bitumen at a temperature of 27°C the peak will be as low as 20 - 50 Hz. Murphy III (1982)

observed the same signature. His finding is based on limited data but clearly shows the nature of the compressional specific attenuation dependence on water saturation and seismic to sonic frequencies. P-wave specific attenuation rises to a peak at approximately 95% water saturation, and energy loss drops significantly as the sandstone becomes completely dry or completely saturated. The specific attenuation strongly peaks between 1 kHz and 10 kHz of the sonic band.

Winkler and Nur (1982) also show specific attenuation data where a strong frequency dependence is evident in fully saturated Berea sandstone, whereas there was essentially no dependence at zero water saturation. The data, which ranges from 500 to 8000 Hz, also suggests a peak in specific attenuation at approximately 4 kHz in the saturated rock.

Murphy III (1982) feels his observed specific attenuation dependence on water saturation is "entirely consistent" with the squirt flow theory. Winkler and Nur (1982) point out an absorption dependence where P-waves are preferentially attenuated over S-waves in partially saturated rocks ($a_s/a_p < 1$). This is interesting since the opposite is true for fully saturated rocks, as mentioned earlier. They support the viscous squirt flow mechanism because Mavko and Nur (1979) demonstrated comparable energy loss with their description of squirt flow, to what they had observed in their experiments. Regarding oil sands, Nyland (1985 b) considers viscous squirt flow to be the most likely

attenuation mechanism.

By studying the parameters in the final version of the viscous squirt equation presented by Mavko and Nur (1979) one can see that as the fluid volume increases without increasing the volume of the rock (increasing saturation), attenuation is predicted to rise. Mavko and Nur (1979) pointed out that with this mechanism only partially saturated pores or saturated pores connected to unsaturated pores will contribute to the attenuation. As successive regions saturate, the attenuation will drop. As complete saturation is approached the squirt flow theory predicts a dramatic decrease in attenuation as was observed by Murphy III (1982).

The attenuation is found to be highly sensitive to the aspect ratios of the pores. The further a pore shape departs from a sphere the greater is the pores ability to attenuate energy (Mavko and Nur, 1979). Nyland (1985 b) suggests that attenuation in oil sands is a good indicator of zones where pore aspect ratios differ from the surrounding media. Because only the flattest pores are important, it is the degree of saturation of the flattest pores, rather than that of the whole rock, that determines the attenuation. In studying how attenuation varies with saturation it is therefore important to recognize that the resulting relation will depend on the manner in which fluid is distributed within the rock as a whole. If one flat pore after another becomes fully saturated while the rest of the flat pores

remain dry the theory shows that attenuation of the low frequencies will increase linearly with fluid content. But, if all the flat pores are filled simultaneously the attenuation should increase as the third power of fluid content.

Palmer and Traviolia (1980) carried out a similar calculation on a variety of pore shapes and found that for configurations of pores similar to the shapes considered by Mavko and Nur (1979) their results were in general agreement. Of the different configurations they examined only the pore shape analyzed by Mavko and Nur (1979) showed an attenuation dependence on saturation. They then compared the results of Gardner, et al. (1964) and found that again, only this configuration agreed with the data.

The squirt flow model is capable of generating the required amount of attenuation and would, therefore, seem to be the predominant mechanism. Not only does the squirt flow mechanism result in a reasonable magnitude of attenuation, it generates the observed absorption dependence on fluid saturation and frequency.

Chapter 2

Procedure for Estimating Attenuation

2.1 Optional Procedures

The derivation presented in chapter 1 of the attenuation coefficient, a , and its relationship to the quality factor, Q , is one of many approaches available in the literature. As mentioned, different approaches result in varying definitions of the specific attenuation and, thus, the attenuation coefficient. In addition to the various derivations for the spatial attenuation coefficient and quality factor discussed in chapter 1, one could study the temporal attenuation coefficient and quality factor (Aki and Richards, 1980). Each of the above could be studied in terms of shear waves and compressional waves (Jones and Nur, 1983), or bulk compression (Winkler and Nur, 1979, 1982). Also, researchers have studied attenuation under a variety of geometries that allow Q -estimates to be obtained for rocks ranging in size from small laboratory scale samples (Jones and Nur, 1983) to large volumes of the Earth's crust (Rebollar et al., 1985, Campillo et al., 1985). Even the Earth as a whole has been studied in terms of the attenuation of the Earth's free oscillations (Aki and Richards, 1980).

Furthermore, because high frequencies are preferentially attenuated over low frequencies, a travelling wavelet will not only have its amplitude spectrum changed in

character, but the wavelet itself will broaden. Attenuation studies may observe the amplitude decay of a wavelet, the change in character of the spectrum, and the broadening of the wavelet. The change in character is usually observed by carrying out a spectral ratio analysis (Hatherly, 1986)

Many attenuation experiments have been carried out in the laboratory but relatively few *in situ* measurements are reported. The present study attempts to determine the variation of P-wave attenuation with depth down a borehole and its correlation with the local geology.

2.2 Vertical Seismic Profiling

The Vertical Seismic Profiling survey (VSP) is the best approach for analysing the elastic properties of *in situ* rocks because it samples the waveform at many depths and can, therefore, spatially monitor the attenuation.

Vertical Seismic Profiling originated in 1917 with the patenting of a downhole survey by R.A. Fessenden in the United States (Hardage, 1983). VSP is a geophysical survey which uses seismic waves to investigate the structure of the earth's upper crust to depths of 5 kilometers with the use of a borehole. Since its origin, the field of VSP has seen intermittent activity in Canada and the United States, while attention was placed on a related survey, the Check Shot Survey.

E.I. Gal'perin, a noted Soviet seismologist, described the VSP survey in a book he wrote in 1974. The book includes

an extensive bibliography of Soviet work in the field, the earliest of which is dated 1934. From the bibliography it would seem that a significant amount of work was carried out by the Soviets in the late 1950's and early 1960's, and this work has continued to date.

The VSP survey is similar to a Check Shot survey, yet one that yields far more information, and this information can be used to enhance surface seismics to a considerable degree. Both surveys consist of a surface source and a downhole geophone. In contrast with the Check Shot survey, which focuses on the arrival time of the first break for the purpose of measuring velocities, the VSP displays the waveform for several seconds beyond the first break and, in addition, records the waveform at many more depths.

The typical VSP survey requires a borehole, down which is lowered one or more geophones. The geophone is electrically connected to a recording unit at the head of the borehole and is sensitive to seismic waves which have been generated at the surface by an explosive source. Figure (2.1) is a schematic diagram showing the geometry of a VSP survey, which is identical to that of a Check Shot survey.

The VSP survey is carried out by lowering the geophone to a certain depth, clamping the geophone to the walls of the hole, and then triggering a seismic source. The resulting waveform is recorded for several seconds. In the case of a Check Shot survey only the first break would be recorded. The geophone is then released from the walls and

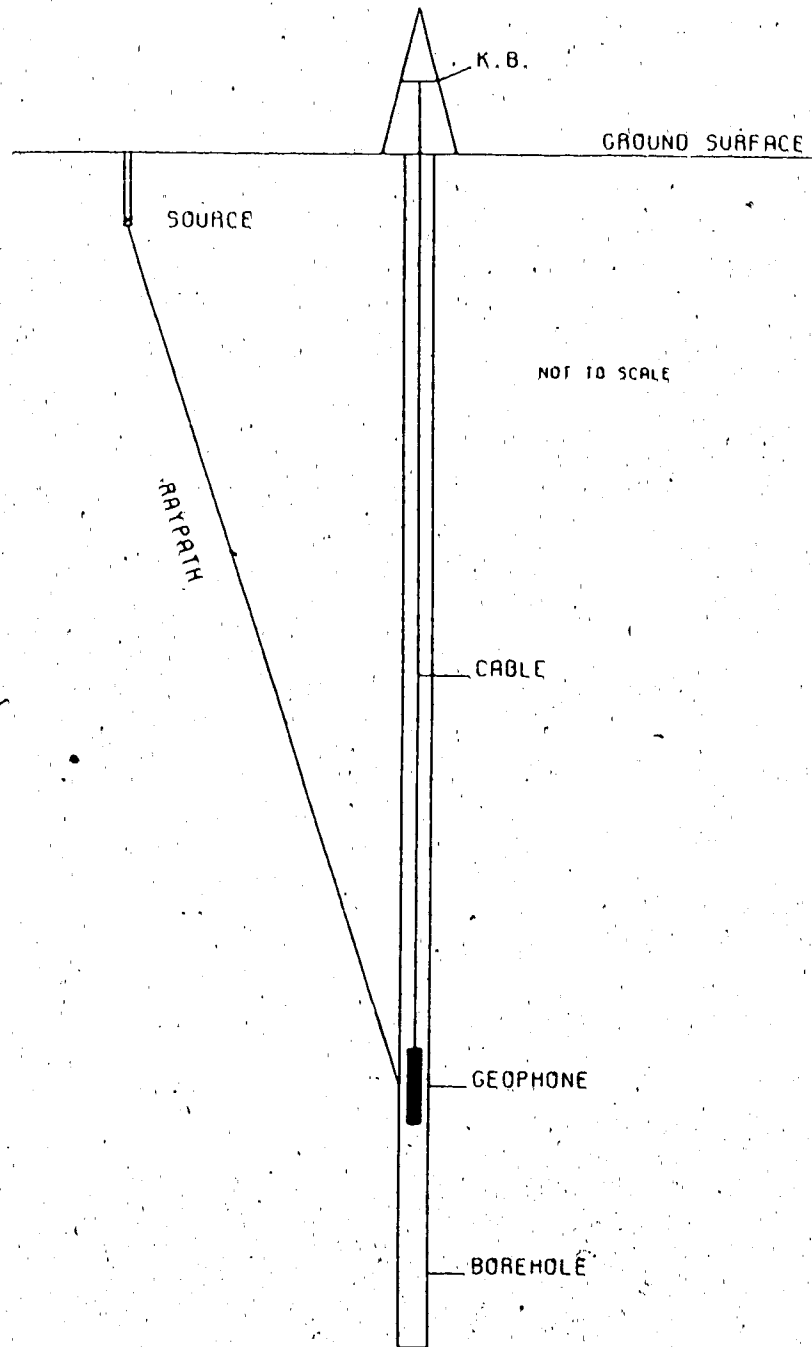


Figure 2.1 General layout of the VSP and Check Shot surveys

lowered a few tens of meters before reclamping. The procedure is carried out for the full length of the hole. A Check Shot survey, on the other hand, would have spacings, in general, on the order of a few hundred meters.

VSP has a wide variety of applications, most of which pertain to the oil industry. It is possible to predict the horizontal and vertical distances as well as the azimuth to drilling targets, and to determine structural discontinuities near the borehole. Also, hole-to-hole tomography can be used to find the boundaries of a reservoir, or alternatively, to determine the volume occupied by a steam injected zone (Simaan, 1984).

Few attempts involving field data have so far been successful in obtaining attenuation profiles from VSP surveys. P.S. Hauge (1981) used the spectral ratio approach to calculate a cumulative attenuation profile for five wells in the southern United States with the aid of a VSP survey. A cumulative attenuation curve was obtained by locating one receiver at a shallow depth. This receiver remained at this depth for the duration of the survey. A second geophone was placed further down the hole permitting a $\frac{1}{Q}$ measurement. Subsequent measurements saw the lowering of only the deeper receiver. In this manner each measurement represented the attenuation undergone by a signal travelling from the shallow receiver to the deeper receiver. Obtaining the attenuation over an arbitrary depth interval involved finding the slope of the cumulative-attenuation-versus-depth

plot over the depth interval. Hauge's profile showed a correlation of high attenuation with porous sands in contrast with neighbouring shales.

Ganley and Kanasewich (1980) analysed the results of a Check Shot survey conducted in the Beaufort Sea. They applied the spectral ratio method over two independent depth intervals arriving at a value for Q between 62 and 73 for the depth interval 945 to 1311 meters and between 42 and 45 for the more shallow interval of 549 meters to 1193 meters.

Kan et al. (1982) obtained two Q -profiles, one extending from 61 meters to 610 meters and the other from 490 meters to 2200 meters. The holes they used were located in predominantly shale formations and they drew no conclusion regarding the association of various levels of attenuation with lithology.

Dietrich and Bouchon (1985) carried out a theoretical VSP survey in which they present theoretical cumulative attenuation profiles, again using the spectral ratio method. Stainsby and Worthington (1985) present results from VSP data gathered in the North Sea, however, they cite one value of Q corresponding to one depth interval. They used the spectral ratio method to obtain a value of 25 ± 3 for the zone lying between 1500 meters and 1700 meters.

It is apparent from the literature that there is a lack of substantial evidence for the ability of *In situ* seismic attenuation measurements to yield information about lithology and other rock parameters. However, the potential

exists for obtaining such information and it is hoped that the present study will do so.

2.3 The Spectral Ratio Method

The spectral ratio method was adopted in this study for the purpose of determining the specific attenuation of seismic waves. Consider a pulse propagating in the positive z -direction (positive z increasing with depth). If it is assumed that the principle of linear superposition of waves applies, then the pulse can be viewed as consisting of an infinite number of sinusoidal waves, each of unique frequency, and travelling with some phase velocity. Note that phase velocity is weakly dependent on frequency (Richards and Menke, 1983). Each component wave is described by equation (10 a), and if equation (10 a) is integrated over all frequencies the total displacement, $P(z,t)$, as a function of depth, z , and time, t , is obtained.

$$P(z,t) = \int_{-\infty}^{+\infty} u(z,t,\omega) d\omega \quad (11)$$

$$= \int_{-\infty}^{+\infty} U_0(\omega) \exp[i(\omega t - \frac{\omega}{v}z)] \exp[-az] d\omega$$

where $U_0(\omega)$ is now a function of frequency, and is the spectrum of the source which generated $P(z,t)$.

The VSP survey is capable of recording the pulse at many individual depths as a function of time. If the pulse is recorded at depths z' and z'' then the spectral ratio method permits the determination of the attenuation coefficient, a , by taking the ratio of the two amplitude spectra, $U'(\omega)$ and $U''(\omega)$. $U'(\omega)$ and $U''(\omega)$ are the amplitude spectra of the pulses recorded at depths z' and z'' respectively, and are given by,

$$U'(\omega) = U_0(\omega) e^{-az'}$$

$$U''(\omega) = U_0(\omega) e^{-az''}$$

from equation (11). Thus,

$$U''(\omega) = U'(\omega) e^{a(z' - z'')}$$

$$-a(z'' - z') = \ln \left[\frac{U''(\omega)}{U'(\omega)} \right] \quad (12)$$

Provided that the absorption coefficient is a linear function of frequency within the seismic band, as research

indicates, a plot of the negative of 'a' multiplied by the trace separation, versus frequency, f, will result in a linear curve with slope, m. The expression for the slope would then be,

$$m = \frac{\Delta\{-a(z'' - z')\}}{\Delta f}$$

However, by equations (10 b) and (12),

$$m = \frac{-2\pi\Delta f}{2vQ} \frac{(z'' - z')}{\Delta f}$$

$$m = \frac{1}{\Delta f} \Delta\left\{\ln\left[\frac{U''(\omega)}{U'(\omega)}\right]\right\} = \frac{-\pi(z'' - z')}{vQ} \quad (13)$$

therefore,

$$Q = \frac{-\pi(z'' - z')}{vm} \quad (14)$$

for $Q \gg 1$.

In essence then, a value for Q can be obtained for a depth interval if one obtains the amplitude spectrum of a

pulse recorded at the top of the interval and one for the same pulse that has travelled to the bottom of the interval with known phase velocity, v . The slope of a graph of the logarithm of their ratio versus frequency can then be used to calculate Q .

2.4 Interference Correction Factor

The spectral ratio method is successful when applied to pulses propagating in a theoretical homogeneous anelastic medium, as demonstrated by Ganley and Kanasewich (1980). However, when interfaces were incorporated into the medium such that pulses were reflected and transmitted at each boundary, situations occurred whereby other pulses, called intrabed multiples (or short-path multiples), were superimposed on the pulse being analysed, thus forming a wavelet. The wavelets at the top and bottom of a depth interval displayed unique interference patterns because the intrabed multiples are different at each depth. When the resulting wavelets were analysed the plot of the logarithm of the amplitude-ratio versus frequency (hereafter called the log plot) oscillated about a straight line. Figure (2.2) shows examples of oscillations based on field data, where the solid line is the least-squares linear regression curve. Spencer et al. (1982) agree that oscillations are due to the difference in the local stratigraphy surrounding each receiver. Ganley and Kanasewich (1980) found that they could suppress the effects of intrabed multiples (that is, the

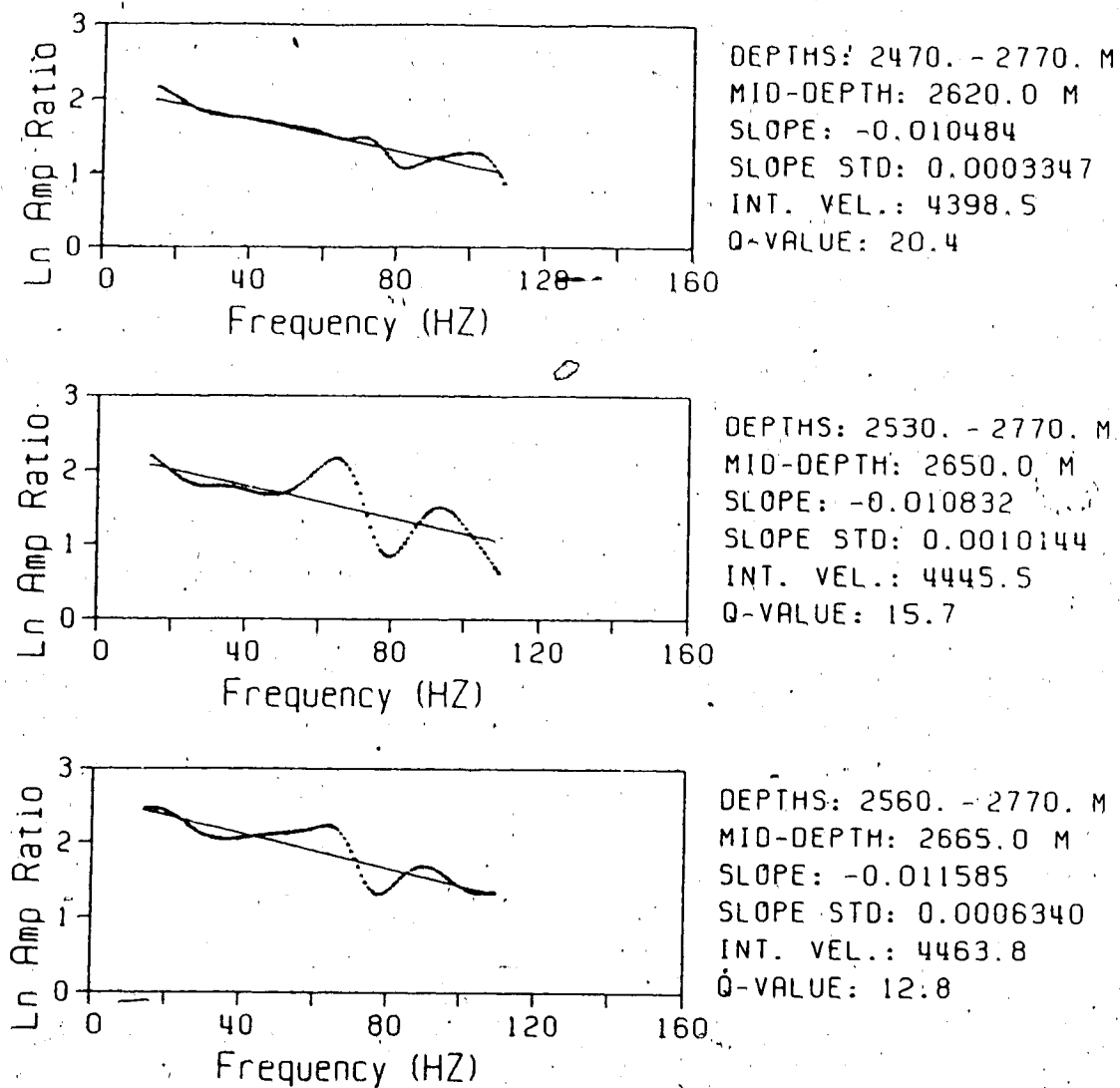


Figure 2.2 Example of oscillatory patterns observed in spectral ratio studies

oscillations and alteration of the slope of the regression curve) and could obtain a more reliable value for Q if they divided the amplitude ratio of the wavelets by the amplitude ratio of two corresponding synthetic wavelets, $S'(\omega)$ and $S''(\omega)$, that did not include the effects of absorption and dispersion but did include the effects of the intrabed multiples (see Ganley (1981) for their algorithm). Hence,

$$m = \frac{1}{\Delta f} \Delta \left\{ \ln \left[\frac{U''(\omega)}{U'(\omega)} \frac{S'(\omega)}{S''(\omega)} \right] \right\} \quad (15)$$

where equation (14) remains valid. The logarithm of the quotient, when plotted against frequency, yielded excellent results.

The generation of the synthetic wavelets required the use of two synthetic seismogram programs. One program generated synthetics which included the effects of absorption and dispersion for the purpose of simulating real data. Known Q -values could be incorporated in an earth model whereby the method outlined above could be tested. The second program did not include these effects, and the resulting traces, and wavelets, were used to find S' and S'' .

The synthetic seismograms required the earth model to be horizontally layered and that the rays reflect from, and transmit through, each interface at normal incidence. These restrictions are not too limiting because a great number of

geophysically interesting areas and surveys meet these conditions.

Given an earth model, the programs calculated the Fourier transform of both the upward and downward travelling wavefields at the top of a geological layer in which a trace was requested. The spectra were then propagated down to the depth requested with the aid of equations (16) and (17),

$$D(z,\omega) = D(0,\omega)\exp(-az)\exp(-i\omega z/v) \quad (16)$$

$$U(z,\omega) = U(0,\omega)\exp(+az)\exp(+i\omega z/v) \quad (17)$$

where $D(0,\omega)$ and $D(z,\omega)$ are the spectra of the downgoing waves at the top of the layer, and at a depth z below the top of the layer, respectively. $U(0,\omega)$ and $U(z,\omega)$ apply to the upgoing wavefields. 'a', the absorption coefficient, is zero in the synthetic seismogram program which does not include absorption and dispersion. 'v' is the phase velocity at which a wave of a certain previously specified frequency travels within the layer. The two resulting spectra were summed to yield the Fourier transform of the trace at the given depth. Inverse Fourier transformation results in the time domain trace. A wavelet in the time domain trace was then removed and analysed separately for its frequency

content. It was this spectrum that was considered when employing the spectral ratio method.

Usually the direct arrival is the focus of attention since this pulse is affected less by noise than are the later arrivals. The reason for this is that the number of reflected events increases with time (Spencer et al., 1982). In the derivation of the correction factor it was assumed that the pulses forming a particular wavelet, including the direct arrival, were identical. This implied that the attenuation and dispersion of each component pulse was negligible when compared to the overall attenuation and dispersion experienced by the direct arrival in propagating from the more shallow to the lower depth. Pulses which superimpose will have traveled farther, and through different volumes of rock, than the direct arrival, resulting in each pulse being unique. As a consequence, a minimum receiver separation was required above which the attenuation and dispersion of the component pulses was negligible. Thus, the interference correction imposes a reduction of depth resolution.

2.5 Depth Resolution

Whether or not the correction factor is employed, there exists a minimum receiver separation below which the effects of theoretical assumptions (horizontal layers), approximations (approximation (9)), noise (Rayleigh waves), and physical processes which appear to attenuate a signal,

will overshadow the intrinsic attenuation experienced by a signal in travelling between the receivers. Spencer et al. (1982) discuss the physical processes which are capable of upsetting attenuation estimates. They point out the high sensitivity of the correction factor to discrepancies between the velocity structure as given by a sonic survey and that of the actual geology.

The sonic survey is, in some aspects, similar to the VSP survey. A probe which is capable of detecting elastic motion is lowered down a borehole and it then relays information to a recording device located at the head of the well. In contrast to the VSP survey, the source of compressional waves is located within the probe a few meters above the sonic receiver, and the frequency of the waves lies in the sonic band. As the probe is slowly brought to the surface from the bottom of the borehole the source of sound waves is activated at regular intervals. The receiver senses the signal some time later and the velocity at which the sonic signal travelled from source to receiver is calculated. The slowness, or inverse of the velocity, is then plotted against depth to yield a sonic log. The area beneath the curve, between two depths, is thus the total time taken for a signal of sonic frequencies to travel from one depth to the other.

In drilling a borehole the walls often become cracked, the lithologic pressure in the neighbouring rock can be reduced, and sometimes the walls may collapse, filling the

resulting holes with drilling mud. All of these problems serve to make sections of rock adjacent to the borehole non-representative of the virgin rock further from the borehole (Stewart et al., 1984). Sonic velocities are obtained by sending signals through the rock adjacent to the borehole (within a meter of the hole) and, hence, the results may be misleading. VSP signals pass through the altered rock as well, however, proportionally little time is spent travelling through it. If the attenuation between two depths is not large enough then errors in the velocity profile may become significant.

The difference in stratigraphy, local to each geophone, is considered to be the cause of the oscillations present on the log plot. Spencer et al. (1982) studied this effect in a theoretical model and observed a marked decrease in the variability of the attenuation measurements as the receiver separation was increased past a critical separation. Beyond the critical separation little decrease in the variability took place. The decreasing variability could not be attributed to a decreasing importance of errors in the velocity structure because the velocities were specified in the model and thus had no accompanying errors. The critical separation lay between 60 and 90 meters which Spencer et al. used as a measure of the depth resolution for their model. Thus, intrabed multiples will cause erroneous attenuation estimates unless the receivers are spaced far enough apart, such that the intrinsic attenuation is the controlling

factor affecting the slope of the log plot.

Unlike the approximations, errors, and interference effects, which are frequency independent and can be minimized by increasing the receiver separation, the scattering of seismic energy is a frequency dependent process which may be difficult to isolate. Scattering occurs in zones of heterogeneity and is frequency dependent, high frequencies being more sensitive to fine impedance structures than low frequencies. High frequencies also tend to be more affected by rough interfaces where irregularities are comparable in size to the wavelength of the frequency component. The high frequencies are not absorbed but rather lose their coherence. Consequently, attenuation measured in zones consisting of many fine layers, and/or rough, contorted interfaces, include the effects of intrinsic absorption and the apparent absorption due to intrabed multiples and scattering.

Other processes exist which, on first consideration, may appear to be significant in attenuation studies, but, in actuality can be shown to play no part. One such process is the geometric spreading of a wave as it propagates from the source. The amplitude decays as $\frac{1}{r}$, however, all frequencies are affected equally. Consider pulses with amplitude spectra $U'(\omega)$, and $U''(\omega)$, that have travelled distances r' and r'' , from the source, respectively, and do not include the effects of geometric spreading. Let A and B be geometric spreading factors such that $AU'(\omega)$ and $BU''(\omega)$ are the

amplitude spectra observed at r' and r'' . By equation (13), the slope of the log plot would be,

$$m = \frac{1}{\Delta f} \Delta \left\{ \ln \left[\frac{BU''}{AU'} \right] \right\}$$

$$= \frac{1}{\Delta f} \Delta \{ \ln B + \ln U'' - \ln A - \ln U' \}$$

Evaluating the slope between frequencies f_1 and f_2 such that $\Delta f = (f_2 - f_1)$ gives,

$$m = \frac{1}{\Delta f} \left[\{ \ln U'' - \ln U' + \ln B - \ln A \} \Big|_{f_2} \right. \\ \left. - \{ \ln U'' - \ln U' + \ln B - \ln A \} \Big|_{f_1} \right]$$

Since A and B are independent of frequency,

$$m = \frac{1}{\Delta f} \left[\{ \ln U'' - \ln U' \} \Big|_{f_2} - \{ \ln U'' - \ln U' \} \Big|_{f_1} \right. \\ \left. + \ln B - \ln A - \ln B + \ln A \right]$$

$$= \frac{1}{\Delta f} \Delta \left\{ \ln \left[\frac{U''(\omega)}{U'(\omega)} \right] \right\}$$

which is identical to equation (13). Thus, geometric spreading does not affect the attenuation measurement.

The constants A and B could also be viewed as the instrument gain while the data for U' and U'' were being collected, or as constants associated with the integrated power of the respective source functions. Assuming integrated power and gain are frequency independent they need not be considered in attenuation studies that incorporate the spectral ratio method. The radiation pattern of the source, which may or may not be spherical, will likewise have no effect on attenuation measurements provided it is frequency independent. The constants A and B affect only the intercept of the log plot as can be seen if the general equation for the linear trend of the plot is considered,

$$\ln \left[\frac{BU''}{AU'} \right] = mf + c \quad (18)$$

Theoretically, little attenuation takes place at very low frequencies, so strictly speaking, if the sources are identical, the intercept of the curve, c, is zero. Rearranging equation (18),

$$\ln\left[\frac{U''}{U'}\right] = mf + \left[c - \ln\frac{B}{A}\right]$$

Thus, the varying instrument gain and/or source power are the cause of intercepts other than zero.

Chapter 3

Case Study

3.1 Survey Geometry and Location

Panarctic Oils Ltd. conducted a VSP survey in a well on Melville Island which is located in the Canadian Arctic. The name of the well is Sherard Bay F-34 and a map of its location is shown in figure (3.1). The survey was conducted during 1983 and 1984 on three separate occasions. On each occasion a different section of the hole was surveyed.

There were several appealing features of the survey which made obtaining an attenuation profile feasible. The trace separation was of the order of 30 meters for most of the well allowing for a relatively high depth resolution. The sources were located very close to the head of the well allowing for a vertical travel path of the seismic energy to the receiver. This, in combination with the horizontal nature of the geologic layers resulted in energy approaching all horizons at near-normal incidence. Reflection and transmission coefficients are frequency dependent at non-normal incidence, therefore, the geometry of the survey was suitable for a Q-analysis. The geological cross-section of the area is shown in figure (3.2) which illustrates the horizontal nature of the layers. Included is the Kelly Bushing which is 10 meters above the ground surface and is taken to be the zero depth level for all depths mentioned. Figure (3.3) illustrates the lithology of the well where all

WELL SITE - Arctic Islands

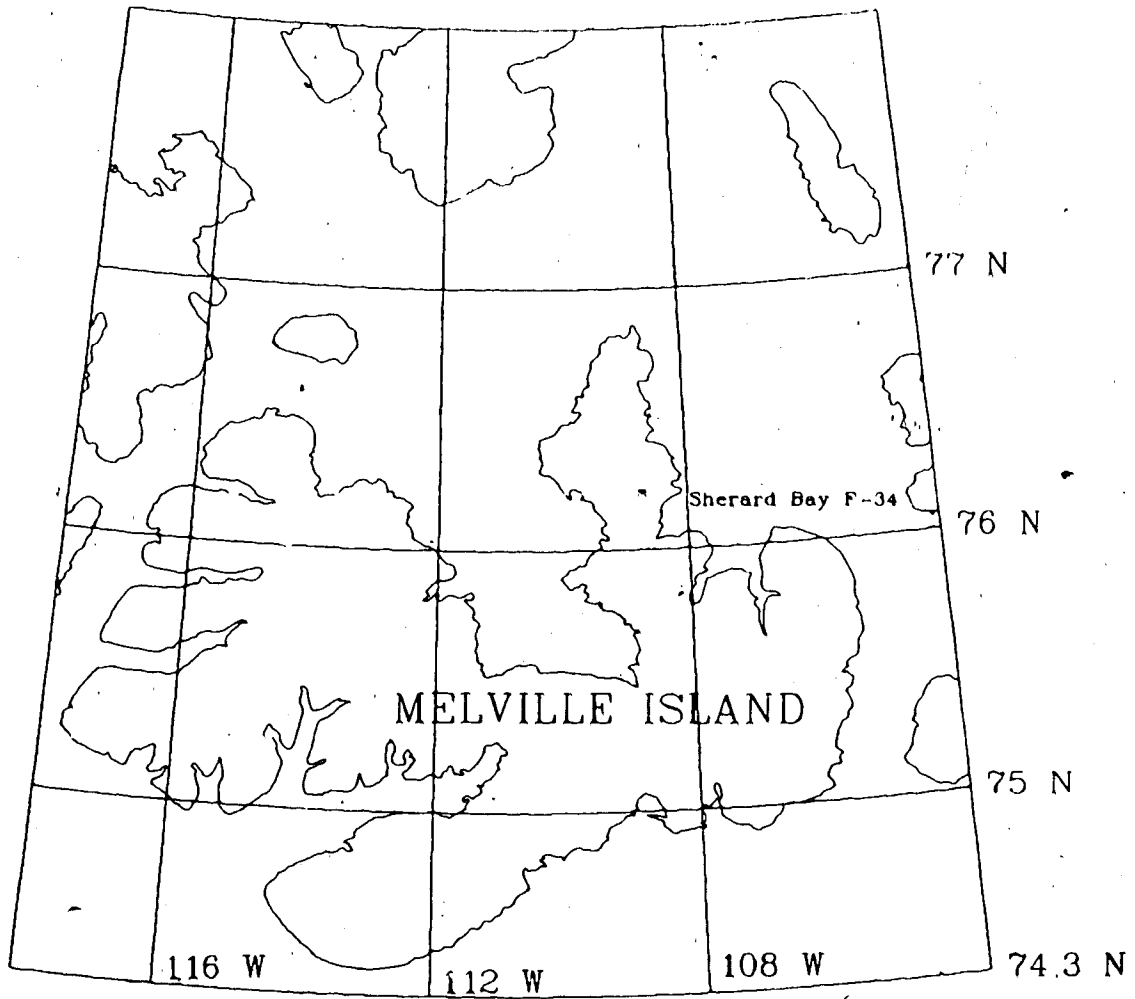


Figure 3.1 Location of survey site

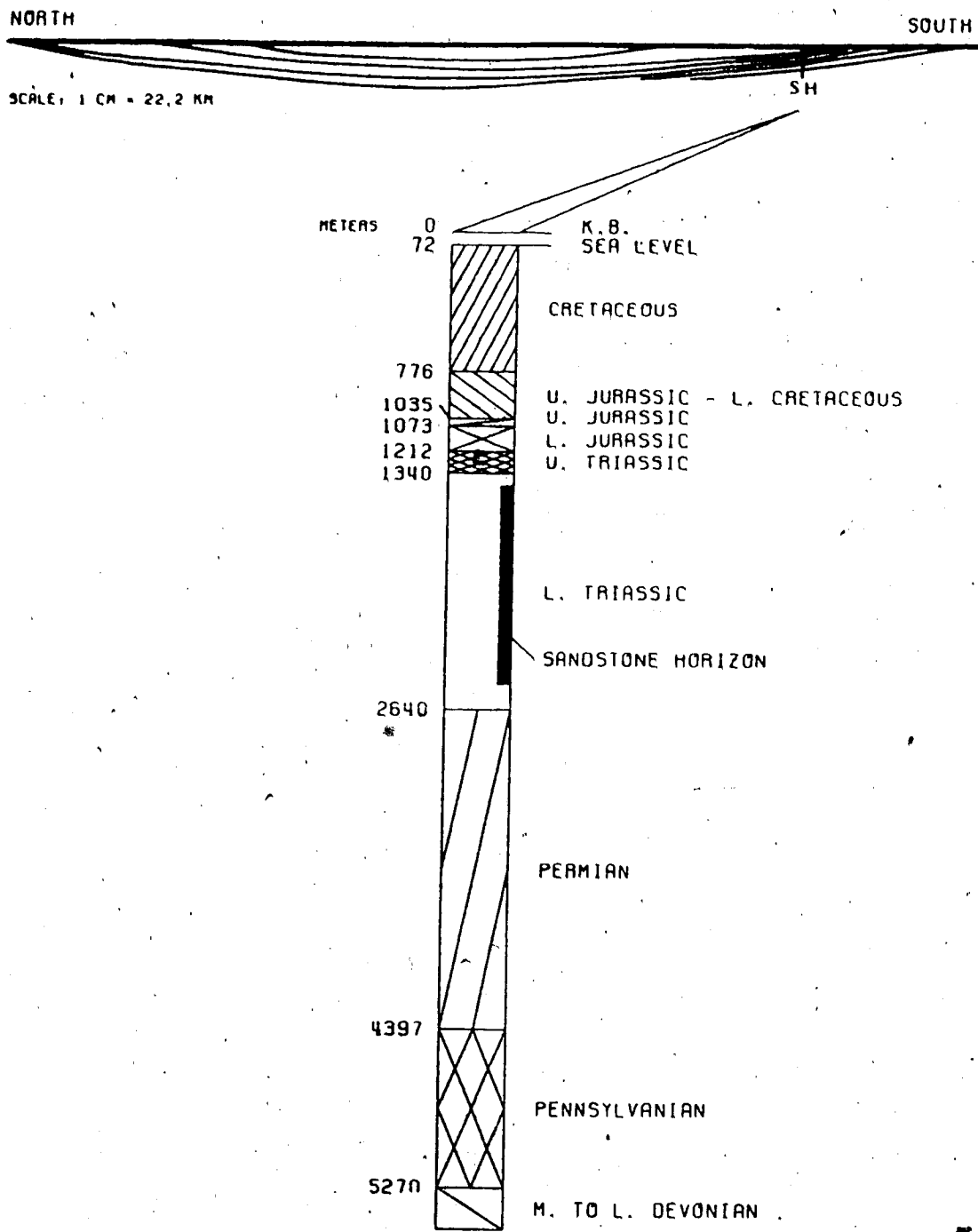


Figure 3.2 Geological cross-section of Sherard Bay F-34 survey site

major rock types are included. Zones of multiple rock types are shown as a sum of the components. The well extends to a depth of more than 5 kilometers below the surface allowing for an extensive survey. The length also lends itself to a high signal to noise ratio at depth.

Figure (3.4) shows the surface geometry of the well, including the location of the source holes. There are 21 source holes in total which reduces the amount of damage sustained by any one hole over the course of the survey. Only one source hole is employed per shot.

3.2 Description of Data

The traces provided by Panarctic Oils Ltd. were generated by one of two types of dynamite sources, Aquaflex or Geogel. The traces came in their raw form both on tape and paper, and in a variety of displays which depended on the degree of processing undergone. The fully processed VSP section from Sherard Bay is shown in figure (3.5). There is a trace approximately every 30 meters down the length of the hole except between 2800 and 3800 meters, where the separation generally varies between 100 and 200 meters. Depth is measured down the length of the page while the time axis is across the page. Each trace is 3 seconds long and has a sampling interval of 2 milliseconds.

Because the fully processed data had its frequency content limited to the range 10 - 70 Hz it was not particularly useful. The wider the frequency band the better

LITHOLOGY

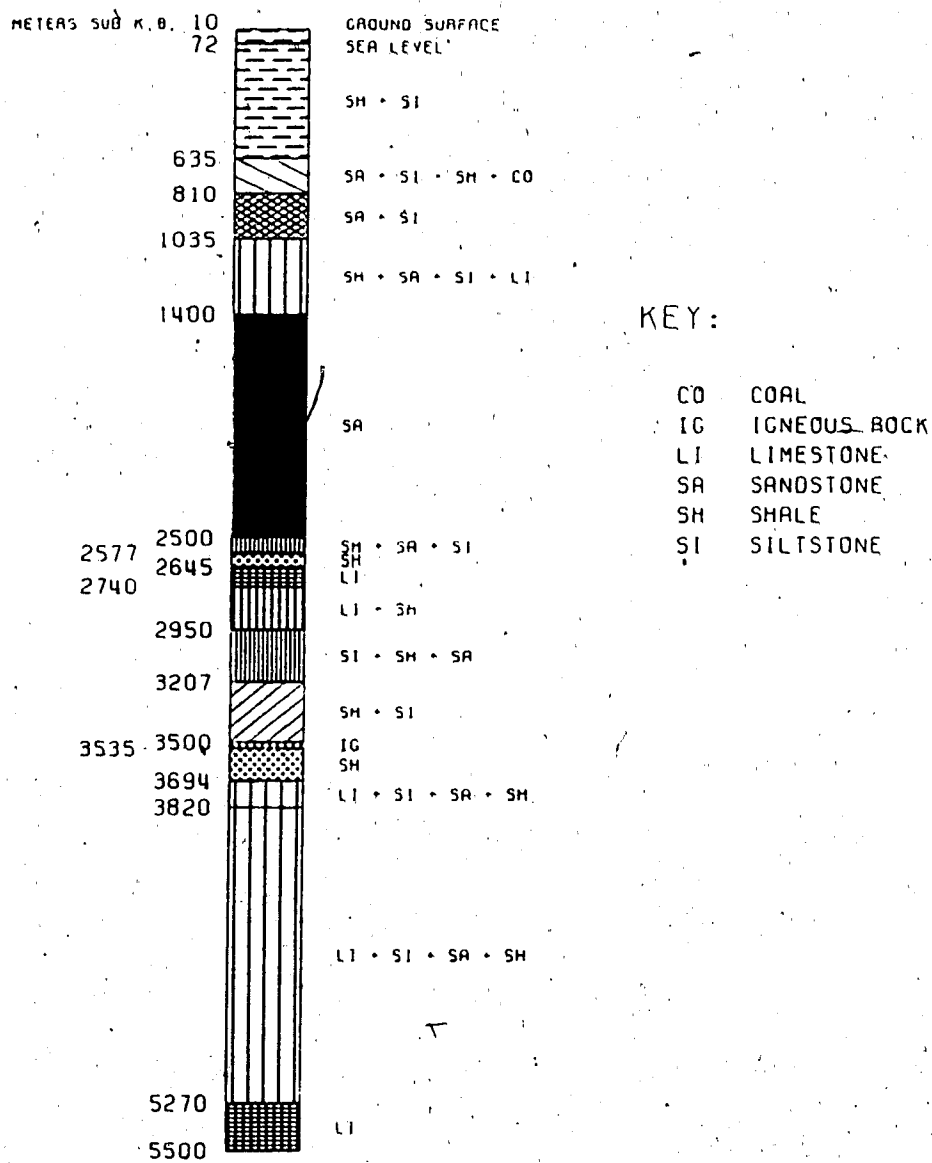


Figure 3.3 Lithologic cross-section of Sherard Bay F-34 survey site

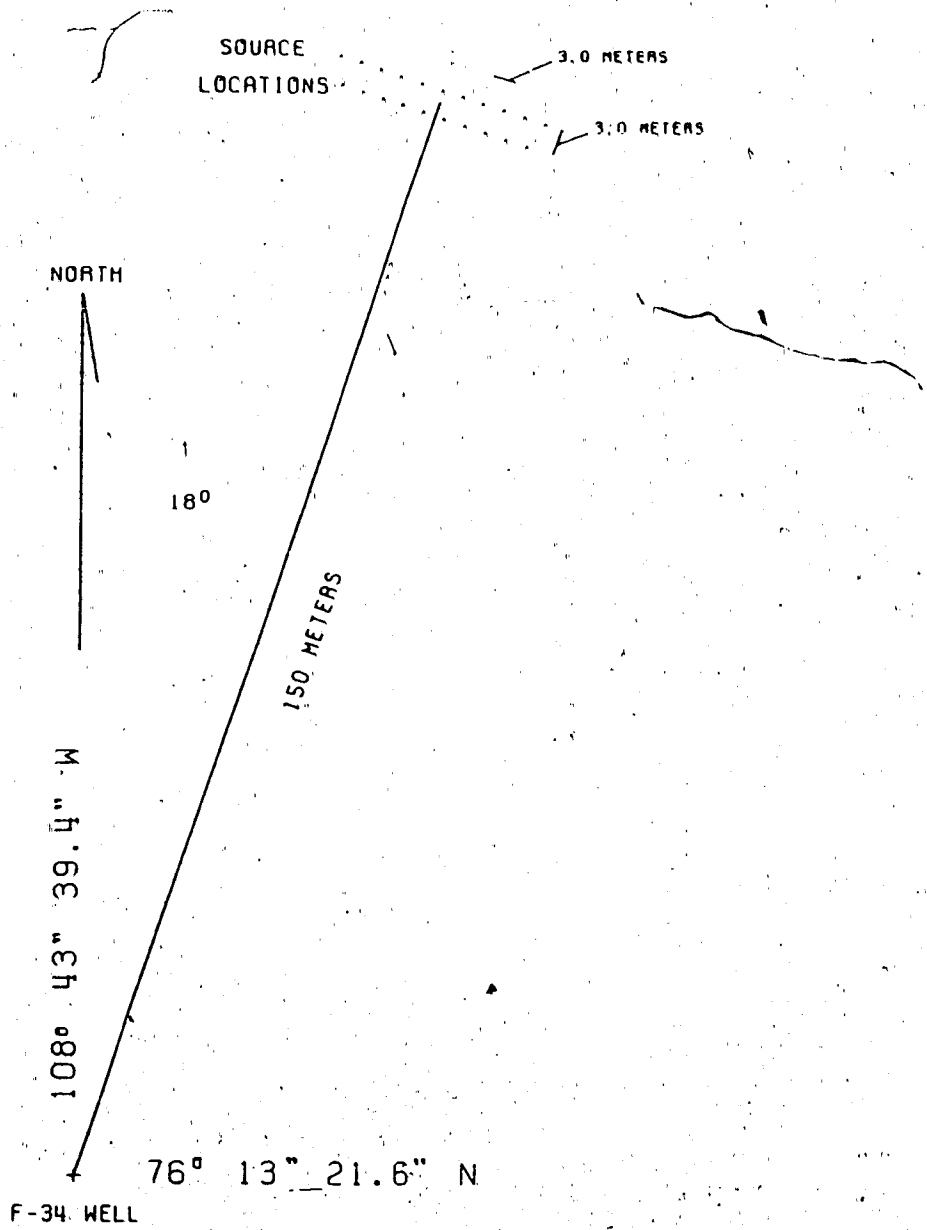


Figure 3.4 Surface geometry of the F-34 well

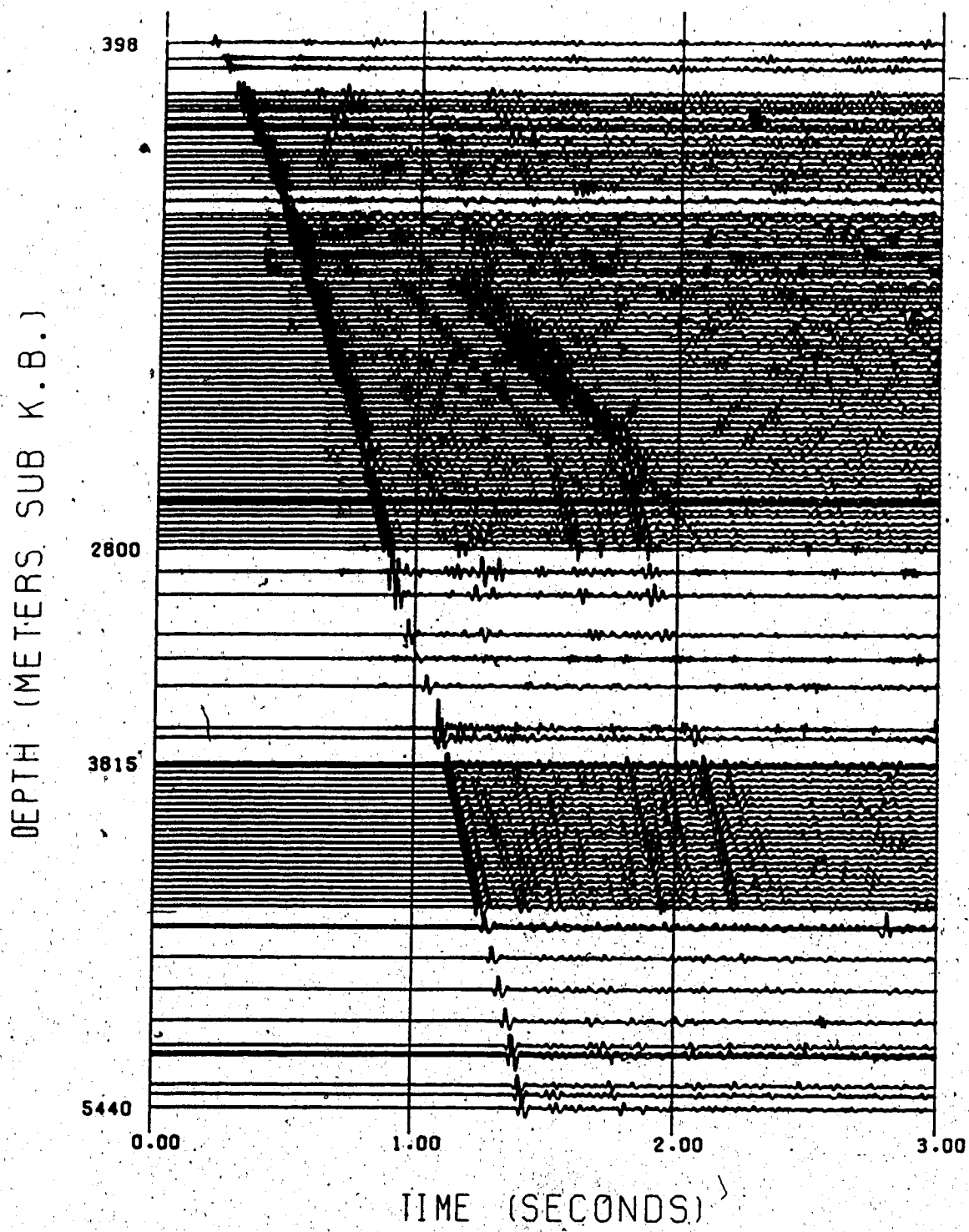


Figure 3.5 Example of filtered data from Sherard Bay

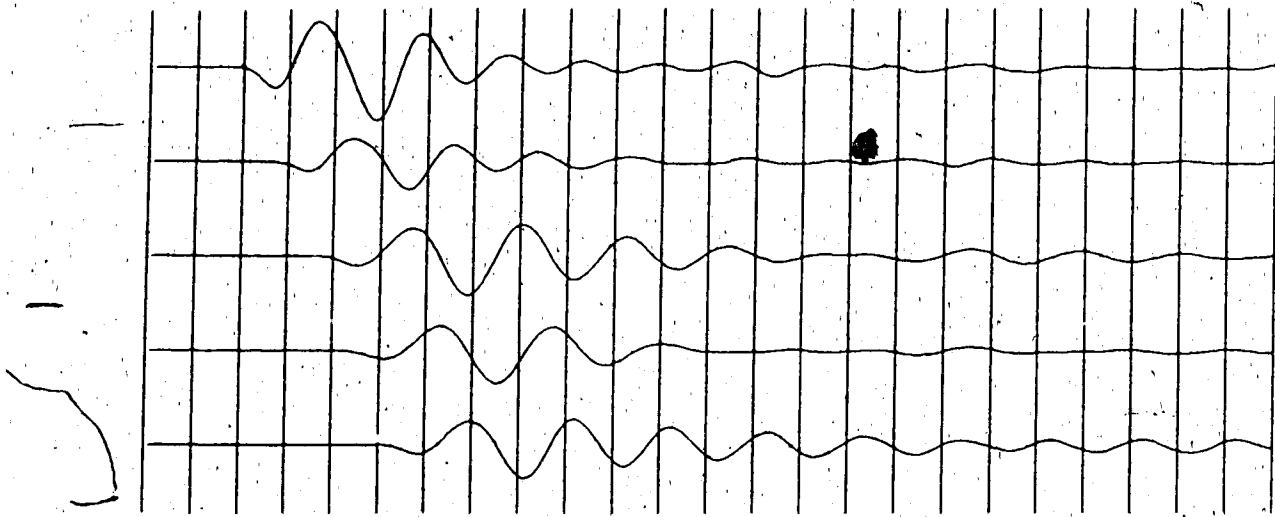
the Q-approximation. For this reason the raw traces were used in the analysis. The raw data, in many cases, had sufficient power above 160 Hz to provide reliable Q-estimates. In addition, only the direct arrivals were analysed since they contained the widest range of frequencies of all the pulses within a trace. This is due to their relatively short travel path from shot to receiver, resulting in reduced attenuation of the high frequencies. They also contain less noise as pointed out by Spencer et al. (1982). A sequence of raw first arrivals from both Aquaflex and Geogel sources is shown in figure (3.6). The raw data was recorded for 4 seconds at a rate of 1 sample per millisecond.

In addition to the seismic traces described above, Panarctic provided a velocity profile for the well. This gives the velocity of P-waves as a function of depth and was obtained through analysis of a sonic survey. The velocity profile is an important part of the Q-estimation since the interval velocity is an explicit term in the equation for Q as shown in section 2.1, and, as mentioned in chapter 2, its accuracy is important for the determination of the correction factor (Spencer et al., 1982).

To obtain a digitized velocity profile, as provided by Panarctic, the sonic log was integrated until the travel time was 1 millisecond. The velocity obtained was then applied to the depth interval in question. The integration continued for the full length of the hole. The final product

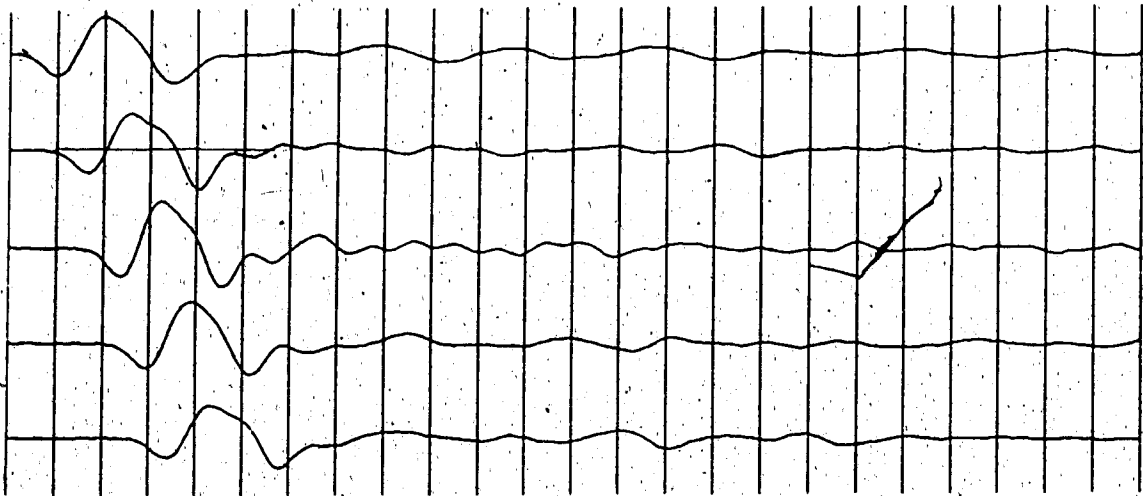
AQUAFLEX

(A)



GEOGEL

10 MILLISECOND INTERVAL



(B)

Figure 3.6 Sequence of 1st arrivals, a) those generated by the Aquaflex source, b) those generated by the Geogel source

is a velocity profile, for which the thickness of each depth interval, or geologic layer, is determined by the distance travelled in 1 msec by a sonic signal. The layer thicknesses consequently vary between 2 and 6 meters.

It is often found that a seismic signal requires more time to travel to a particular depth than is suggested by the integrated sonic travel time. This indicates that the velocity profile, as given by the sonic survey, does not apply to waves of seismic frequencies. In fact, for the most part, the discrepancy between the sonic arrival time and the seismic arrival time grows with depth, which is a phenomenon called 'drift'. There have been various explanations for drift as presented by Stewart et al. in 1984. They quantified the drift caused by variations in layer thicknesses, intrabed multiples, time picking of first arrivals, and attenuation (and dispersion). In their final analysis they concluded that the drift is due mainly to velocity dispersion between the seismic and sonic frequency bands, with the effect of intrabed multiples playing a minor role.

The method by which the oil industry corrects for drift involves performing a Check Shot survey. Recall that a Check Shot survey is the same as a VSP survey except that only the first breaks are recorded and the spacing between receiver depths increases from 30 meters to 100 meters or more. Hence, VSP data may also be used to correct for drift. Panarctic, consequently, used their VSP data to correct for

the drift that was present in their velocity data.

Essentially the arrival times, as given by the integrated sonic log, are tied down to the Check Shot arrival times at four or five depths. The sonic velocity variations provide a detailed indication regarding the seismic velocity variations, however, they become misleading over large depth intervals. The drift correction maintains the detail while correcting the general trend.

The full velocity profile is shown in figure (3.7, a) and the interval velocity is shown in part (b). The interval velocities were calculated by averaging the velocities in each layer. A new layer was defined to begin whenever the velocity changed by 5% or more from one depth to another. Because the sonic survey does not begin until the 389 meter depth the velocity down to that depth was determined by the VSP survey. At depths greater than that sampled by the sonic survey a halfspace is considered to exist with a velocity equal to that of the last layer of the velocity profile.

The interference correction factor, referred to in section 2.4, requires the generation of synthetic traces. To calculate synthetics the variation with depth of layer thickness, P-wave velocity, and rock density, must be known, that is, the earth model must be specified. The sonic survey provided all the required information except the rock densities.

Although the density variations are small from layer to layer and could, therefore, be ignored completely, they were

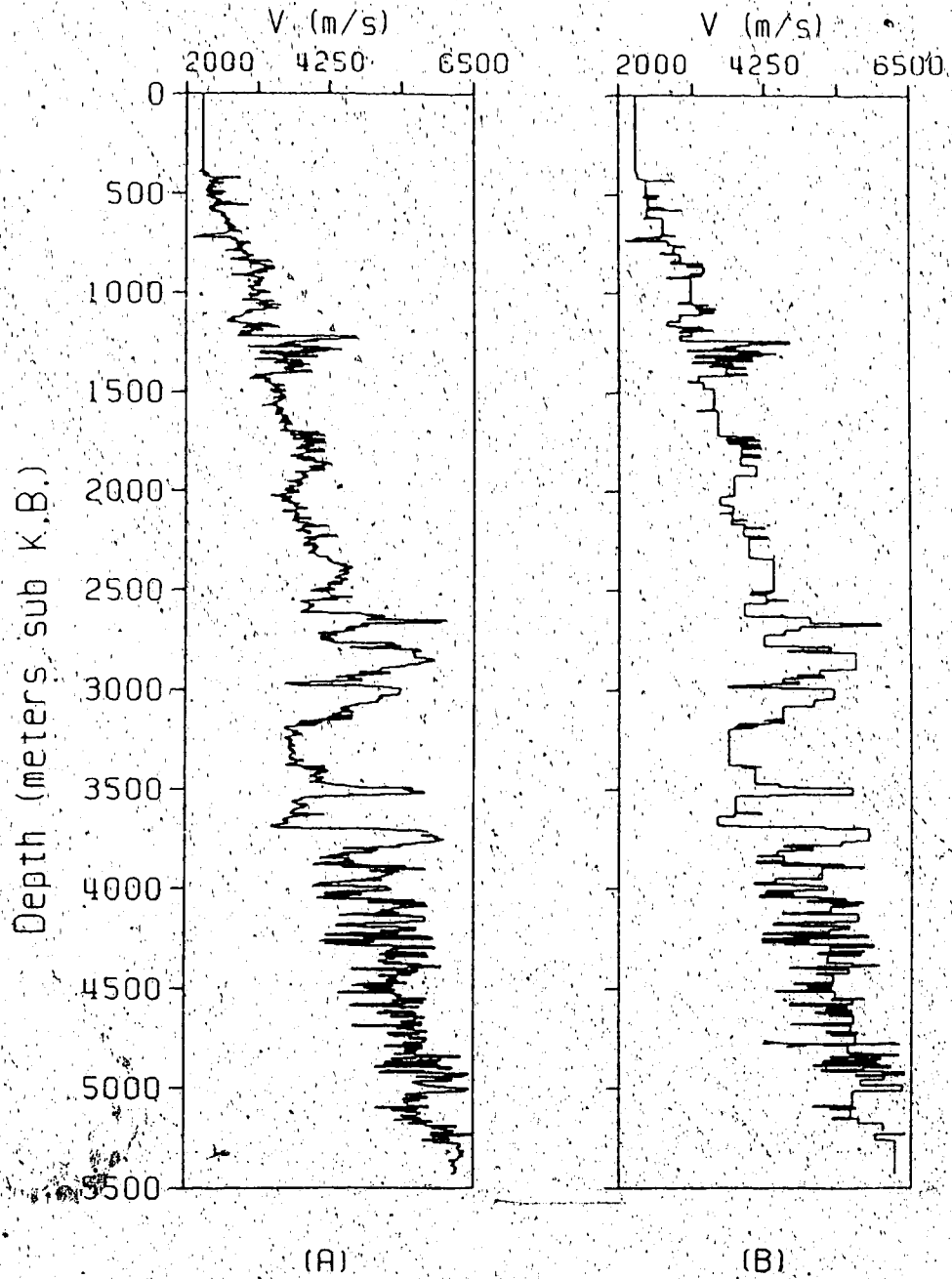


Figure 3.7 Velocity profiles: a) every layer present b) 5% change in velocity required to define a new layer

included in the synthetics calculated in this study. Panarctic did not provide a density profile, but instead, supplied the reflection coefficients for each interface from which the layer densities could be determined. The relationship between the reflection coefficients and densities is given by,

$$\rho_2 = \frac{v_1 (\rho_1 - R\rho_1)}{v_2 (R + 1)}$$

where ρ_1 and ρ_2 are the respective densities of the layers above and below the interface with reflection coefficient, R . v_1 and v_2 are the velocities of P-waves in the layers corresponding to ρ_1 and ρ_2 . ρ_2 is solved for iteratively by first assigning ρ_1 some arbitrary value.

3.3 Generation of Synthetic Traces

For each pair of raw traces analysed, a corresponding pair of synthetic traces was generated as discussed in section 2.4. However, when generating the synthetics two problems were encountered. The traces experienced both time- and frequency-domain aliasing. In trying to reduce the noise caused by the aliasing the sample interval was set at 1 msec. This was the sample interval of the raw traces. The Nyquist frequency was, therefore, well above any frequencies that would be used in the spectral analysis. A high Nyquist

frequency itself helps reduce the frequency aliasing but further measures were required. A 12-pole Butterworth filter with its corner at half the Nyquist frequency (250 Hz) was used to filter the amplitude spectra of the synthetics before their inverse Fast Fourier Transform (FFT) were calculated. A Butterworth filter was used in contrast to a box car filter as the Gibbs effect is optimally reduced. Aliasing was still apparent, thus, the corner was set at 1/4 the Nyquist frequency but this yielded no improvement. Use of the Butterworth filter effectively decreased all power above the Nyquist frequency to insignificant amounts.

Time domain aliasing is directly analogous to frequency aliasing. Events that arrive beyond the end of the calculated trace become superimposed on the beginning of the calculated trace. Because the synthetics do not allow for attenuation, the only path for energy to leave the system is via the halfspace. Therefore, there exist many arrivals after the end of the trace that will be aliased back into the trace. One way to reduce this effect is to calculate a long trace; thus, most arrivals legitimately appear on the trace. This procedure can be expensive, and since no attenuation is taking place, it may not be effective.

The alternative approach that was used in this study involved simplification of the earth model. Recall that for the Q-analysis only the first arrival is studied, and that the first arrival is actually made up of many, hopefully similar, superimposed wavelets. Considering the synthetics,

only the first arrival, with all the superimposed wavelets, need be constructed. The remainder of the trace is not important. Consequently, only those interfaces in the earth model that can reflect energy such that it arrives at the geophone at about the same time as the direct arrival need be included. If the first arrival is considered to be 100 milliseconds long then the deepest interface, below the depth of the geophone, that must be included in the earth model must be no less than 50 msec deeper, as far as vertical travel time is concerned. Since each layer requires 1 msec for the seismic wave to traverse it, the earth model must extend 50 layers below the depth of the geophone. Beyond the last layer all interfaces are blanked, thereby creating a halfspace from which no energy can emerge and hence, appear on the trace after the 100 msec mark. For the same reason, only 50 layers above the more shallow geophone of any given pair, are required. The model for the deeper trace should begin at the same interface as for the more shallow trace, yet, it must be extended to the 50th interface below the deeper trace. Time domain aliasing, however, is not completely reduced by the blanking procedure since energy can reverberate in the existing layers for any length of time.

Q was calculated using the interference correction factor for 5 depth pairs during an initial trial survey. Using blanked earth models, as described above, the synthetic trace pairs were calculated. It was found that,

although the correction factor slightly altered the character of the log plot, the oscillations of the curve were not reduced. It was thought that the failure of the correction factor was due to an overly complicated earth model whereby many small, false reflections were overshadowing a few main, real reflections. There may not have been one interface every 1 msec of travel time. To test this hypothesis, the earth model was divided into thicker layers according to two criteria. To define the commencement of a new layer the velocity had to change by a certain percentage of the previous velocity, and also, a minimum travel time across each layer was required. Using a variety of combinations of these two parameters, the correction factor remained uneffective.

It was concluded that either the dominant oscillations of the log plot were caused by the differences between the sources used by Panarctic, or, the geologic interfaces were rough or contorted in such a manner that the synthetic seismograms did not adequately resemble the VSP traces. Such contortions would not be apparent from the sonic profile from which the synthetics were calculated, and may have scattered energy in an unpredictable fashion. As a result of this analysis, and the relatively high cost of generating the synthetics, the correction term was not used in any further analysis.

3.4 Generation of Amplitude Spectra

The length of the first arrival, or window length, was determined from the field data whether or not synthetic traces were used in the Q-estimate. A subjective estimate of the length of the first arrival was required because there was no point along a trace where it was clear that the first arrival had ended. An optimum window length is required such that oscillations in the log plot are minimized while at the same time the entire pulse is retained. A number of values ranging from 50 to 200 msec were tested. An optimum value of 125 msec was determined from the degree of linearity of the log plot. When the synthetics were included the same window lengths were applied to them.

Although it was known that Panarctic employed two types of explosive sources, Geogel and Aquaflex, during the course of the survey, it was not clear which traces corresponded to a particular source. Only in the lower portion of the well was there no ambiguity since Geogel was the only source specified.

After the generation of several spectra with window lengths of 125 msec, the source used in each instance became apparent. Not only were there differences between the spectra of the two sources, but it was found as well that the Geogel source consistently caused shorter first arrivals than the Aquaflex. Consequently, all Geogel related traces were analysed with a window length of 80 msec. Refer to figure (3.6) for a comparison of Aquaflex and Geogel first

arrivals, and to figure (3.8) for a comparison of Aquaflex and Geogel spectra. Recall from section 2.4 that the shorter the window length, the more constant are the wavelets, and the closer one may adhere to theory. Neither the resulting Q-values nor their reliability were overly dependent upon the window length. In this study, window lengths may be safely varied within ± 10 msec of the above values. Because the choice of window length is dependent on the sharpness of the pulses obtained, the window used will vary from survey to survey. Hauge (1981) used a 30 msec window, and Ganley and Kanasewich (1980) used a 200 msec time window.

Due to the unprocessed nature of the data, all traces, and thus all first arrivals, exhibited a DC bias which originated during the recording of the signal. After the first arrival had been isolated from the remainder of the trace the accompanying DC bias was removed. Following the removal of the DC bias zeros were added at the end of the first arrival such that the total number of data points was 1024. This was necessary since an FFT algorithm was used to calculate the spectra, and thus, the total number of points was required to be a power of 2. The longer the data set, the better is the spectral estimate but the higher the cost of calculating it.

The number of points in the data set, N , affects the frequency resolution according to,

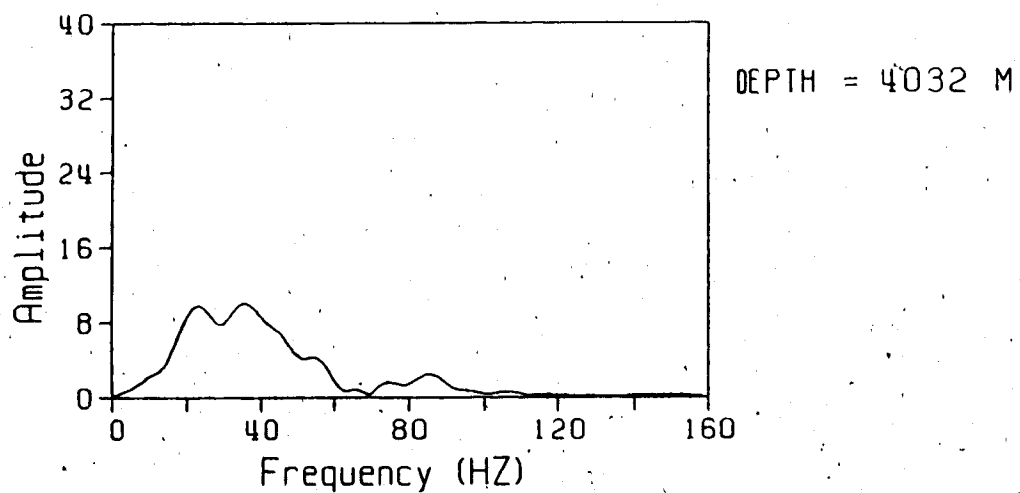
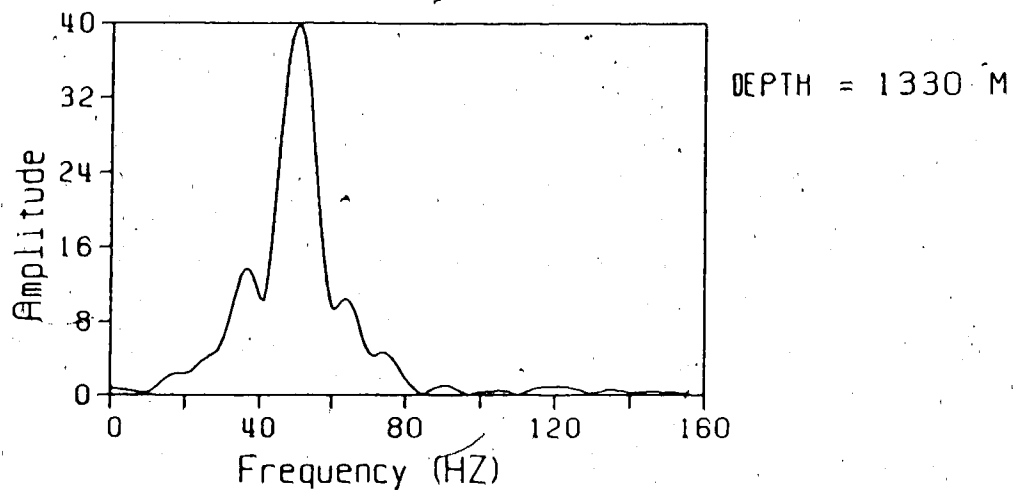


Figure 3.8 Comparison of first-arrival amplitude-spectra generated from the Aquaflex (top) and Geogel (bottom) sources.

$$\Delta f = \frac{1}{N \Delta t}$$

where Δt is the sample interval of the data set. For $N = 1024$ and $\Delta t = 1$ msec, the frequency interval is .97 Hz, which provides enough points to allow a linear regression fit.

The truncation of a trace after the first arrival, in virtually all cases, will cause a sharp discontinuity between the end of the window and the subsequent zeros. This, in turn, artificially adds high frequencies to the spectrum. It is possible to minimize the effects of truncation by applying a cosine bell to both ends of the window (Kanasewich, 1981). The cosine bell is a weighting function that gradually reduces the values of a series of points to zero. The number of points affected can be set as desired. In this study, a variety of values were tried ranging from 3 to 20 points. A 20 point cosine bell altered the nature of the beginning and end of the window too much while 3 points did not reduce the discontinuity sufficiently. As a compromise, a 10 point cosine bell was applied to both ends of the window. Furthermore, the window began 5 msec (5 points) before the first break. This allowed for errors in picking the first break in addition to

reducing the effect of the cosine bell in an area of the trace where its usefulness was minimal.

The resulting time series was Fourier transformed and the amplitude spectrum was calculated (see figure (3.8)). This procedure was carried out on all four traces (or, if no correction factor was used, only the two field traces) and the natural logarithm of the amplitude ratios at each frequency was calculated in accordance with equation (13), or equation (15) as required.

During an initial survey, it was found that the log plot was quite noisy, so a 9 point (approximately 9 Hz) running average of the amplitude spectra was included before the ratios were taken. This resulted in a smooth curve with all major oscillations still present. An attempt was made to smooth the complex Fourier coefficients instead of the amplitudes but peculiar effects arose so this procedure was abandoned. The straight line, that the theory predicts, did not materialize in most cases. Instead, an oscillatory curve with a linear trend was observed (see figure (2.2)).

3.5 Selection of Trace Pairs

In the process of selecting pairs of traces for analysis it was important not to compare traces that originated from different sources. Geogel and Aquaflex had quite distinct spectral characteristics which made them incompatible.

Due to the approximations described above, very small levels of attenuation are difficult to estimate. It was felt that the attenuation of a signal over a distance of 200 to 300 meters was measurable and that this provided a high enough depth resolution to be of value. Dietrich and Bouchon (1985) considered a depth interval greater than 100 meters as an appropriate figure. At depths greater than 3800 meters the separation was increased to 300 to 400 meters between traces in case Q increased. In general Q tends to increase with depth reducing the attenuation to levels less than that measurable over small receiver separations. In this study, Q did not increase appreciably, so a depth resolution of 200 to 300 meters was added to the data set below 3800 meters. Once the more shallow trace was chosen, a compatible trace 200 to 300 meters further down the borehole was sought.

The appearance of the trace played only a small part in the selection process. The phases of the spectral components of the first arrival could be sufficiently different between the shallow and deep traces making them seemingly incompatible. Their amplitude spectra on the other hand could be very similar, and it is this quality that was important. However, on many occasions spectra were very similar but were nevertheless incompatible. Subtle differences, due possibly to varying degrees of geophone-ground coupling, or borehole deformations such as washouts or fractures, may render anomalous results. Twenty-one different shot holes were used by Panarctic with

no indication as to which hole was used on a particular occasion. Again, subtle differences between holes may have been present. Also, the preparation of the dynamite may have varied from shot to shot. Powder densities and density variations will certainly be unique for each shot, and this will result in differences among individual source amplitude spectra.

A reliable Q -value was obtained by choosing pairs of spectra whereby the deeper spectrum was simply a copy of the more shallow one but multiplied by a ramp with any negative slope. Often this was a difficult condition to assess, and several physically non-realizable values were obtained.

3.6 Calculation of Q

Given the amplitude spectra of a pair of field traces, the depths corresponding to each spectrum, and the velocity values for the intervening layers, one may calculate Q by solving equation (14) of section 2.3. The value of v was given by the average value of the velocity of P-waves in the intervening layers as specified by the earth model.

Calculation of the slope, m , of the log plot involves several steps. First, the minimum and maximum frequencies at which both spectra had sufficient power to be reliable were determined. Typical extremes were 15 Hz and 160 Hz, with the minimum upper limit of 80 Hz in a few instances. Spencer et al. (1982) found measured attenuations to be "strongly" dependent upon the frequency band selected for the least

squares fit and observed that the optimum band was not necessarily determined by the wavelet bandwidth. They suggested that multiple measurements should be taken to obtain the optimum frequency band, an option not available with the data set available here. Hauge (1981) conducted a cumulative attenuation study using VSP and found he was able to use the frequencies from 20 to 105 Hz in one offshore hole, and the range 15 to 40 Hz for the land surveys which used a vibrator as a source. Ganley and Kanasewich (1980) did a spectral analysis over two depth intervals on the frequency bands 10 to 75 Hz and 30 to 75 Hz. In this study the Geogel spectra were more band limited than the Aquaflex spectra, which is, in part due to their relatively deep receiver locations.

Once the frequency band was obtained, the logarithm of the amplitude ratio of each frequency within the band limits was plotted versus frequency. One frequency value occurs every .97 Hz. As mentioned in the previous section, each resulting curve exhibited some oscillation. Again, a nine point running average smoothed the plot to emphasize its general character. The slope of this curve was approximated by finding the slope of the corresponding linear least squares line as was done by Ganley and Kanasewich (1980) and Hauge (1981). The power spectra were not normalized, consequently, the deeper spectrum of a given pair could indeed contain larger amplitudes. Arbitrary intercepts will result for this reason. For the sake of uniformity, the

curves were moved such that they were confined to the first quadrant.

3.7 Elimination Procedure

Frequently, curves displayed a linear trend only up to a certain point, after which large oscillations and/or deviations from the linear trend were apparent. These irregularities were attributed to differences in the source spectra above a certain frequency. Only on one occasion was it necessary to raise the lower frequency limit. Under such circumstances, the irregular sections were not included in the least squares fit and thus did not affect the value of Q . If the linear trend persisted for less than 65 Hz the curve was considered unacceptable. The average frequency range was about 15 Hz to 120 Hz. Stainsby and Worthington (1985) were able to use the 25 Hz to 125 Hz band in their studies. Frequencies below 25 Hz had been filtered out during the survey, and above 125 Hz the power was inadequate.

On those occasions where a negative value for Q arose the curve was dismissed. Negative Q 's are physically unrealizable, and imply that the source amplitude spectra were not similar. An acceptable plot will have a negative slope. All else being constant, an increasing Q decreases the magnitude of the slope. Infinite Q , corresponding to no attenuation, occurs when the slope is zero, and negative Q 's result when the slope is positive.

Just as negative Q's were dismissed, so too were extremely atypical Q-values. If the majority of results in a depth interval were in close agreement while a few were not, the anomalous values were considered to have no validity. The definition of "anomalous" was taken from Margenau and Murphy (1956) which suggested that residuals exceeding 5 times the probable error, r , be rejected on the grounds that such large errors are not random. The remaining Q-estimates had a probable error of 28, that is,

$$r = .6745 \left[\frac{\sum (d_i)^2}{(n - 1)} \right]^{1/2} = 28$$

where d_i is the residual of the i^{th} point, Q_i , and is given by,

$$d_i = Q_i - \bar{Q}$$

\bar{Q} is the arithmetic mean equal to 40 for this data. Accepted Q-estimates, Q_i , were thus found by,

$$d_i < 5r$$

$$Q_i < 5r + \bar{Q}$$

or,

$$Q < 180$$

A total of 11 points were rejected on this basis. All those points retained in the Q-profile are displayed in figure (3.9).

Appendix A includes all plots that gave rise to accepted Q-values. They are arranged in order of increasing depth according to the most shallow trace of a given pair. Appendix B contains the Fortran programs used in the generation of the Q-values. All points shown within each graph of appendix A were used in the calculation of the least squares curve. Some plots may arise from the same depth range but at least one of the traces was not repeated, thus rendering an independent measurement of Q. The mean velocity for the depth interval shown is also presented along with the resulting Q-estimate. In addition, the standard deviation of the slope of the least squares line is given. This was calculated using the formula,

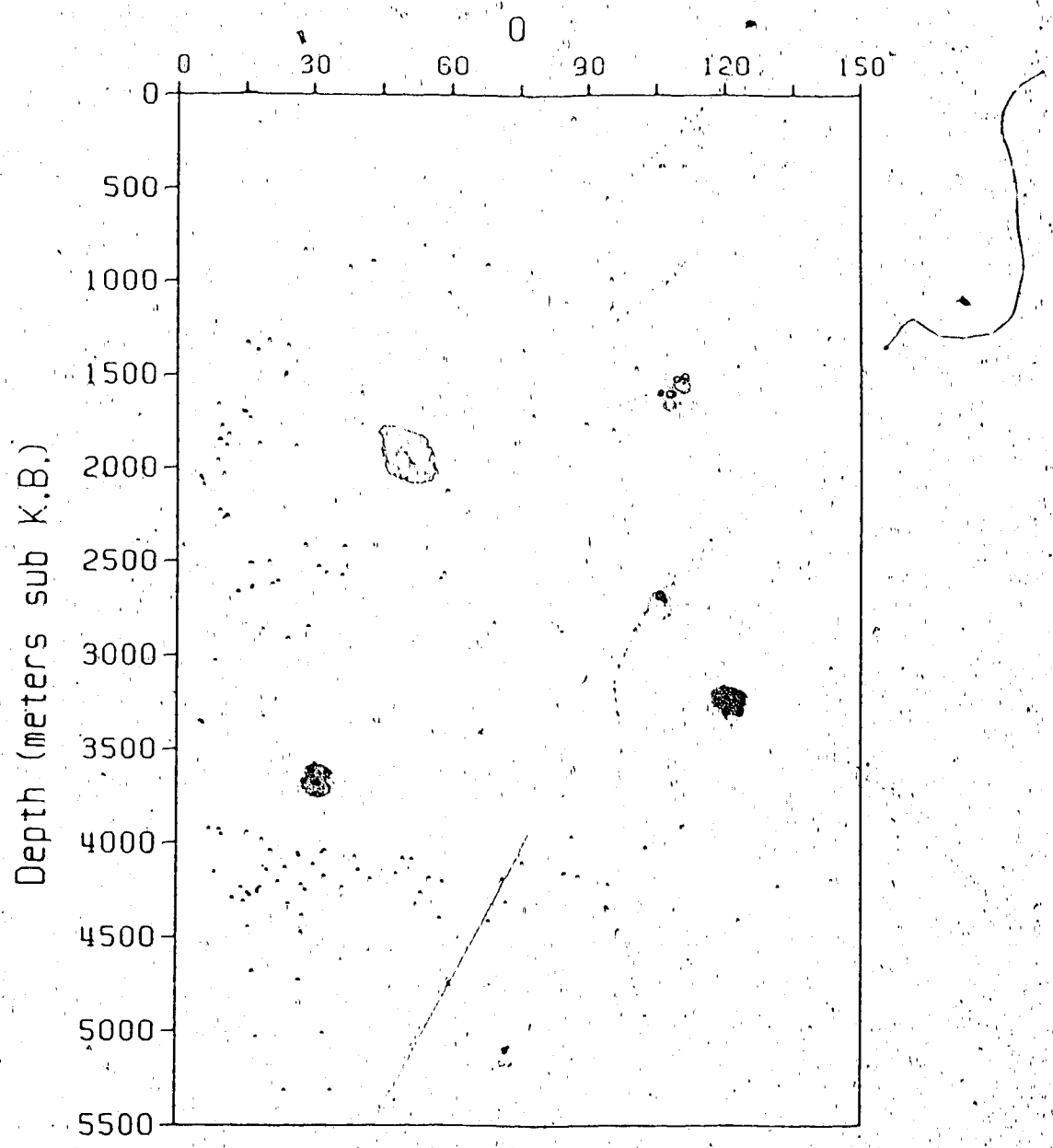


Figure 3.9 Plot of all accepted Q-values versus depth below K.B.

$$STD_{\text{slope}} = \left[\frac{1}{(n-2)\Sigma x^2} (\Sigma y^2 - b\Sigma xy) \right]^{1/2}$$

where, x represents the discrete frequencies, y gives the corresponding log-of-ratio values, b is the slope of the least squares regression line, and n is the number of points (Huntsberger, 1973).

3.8 Presentation of Results

Figure (3.9) is the raw Q -profile for the Sherard F-34 borehole composed of all acceptable Q -values. Each point is plotted at the mid-depth of the interval over which it was collected. The ordinate is depth below the Kelly Bushing (K.B.) with units of meters, where the Kelly Bushing is 10 meters above the surface of the ground (see figure (2.1)). The abscissa is the unitless quality factor, Q . The relative absence of points between 2800 meters and 3800 meters is due to the large receiver spacing used during the survey between these two depths. The raw Q -profile reveals little information other than the variability of the 108 data points.

Because attenuation is directly proportional to the specific attenuation, Q^{-1} , in the relation (10 b), it is customary instead to show the variation of this parameter

with depth. Figure (3.10) is a plot of the reciprocals of the Q-values shown in figure (3.9). An added advantage of this type of display is the reduced emphasis placed on values which stray far from the mean during further data processing.

A prominent feature is immediately apparent at 2100 meters where the specific attenuation peaks to a maximum for the hole. More detail is found by smoothing the profile with a running average as can be seen in figure (3.11, a). Each point in figure (3.10) was replaced by the arithmetic mean of all points lying within 100 meters to either side, thus, a running average with a window of 200 meters was performed. The mean value was subsequently plotted at the same depth as the point in question. The following points were then processed in the same manner, consequently the number of points in the profile remained 108. The points in figure (3.11, b) were processed in a similar fashion to those of figure (3.11, a), however, the weighted arithmetic means were calculated instead. The largest source of error in the calculation of specific attenuation comes from the determination of the slope arising from the log plot. The reliability of the interval velocity and trace separation is considerably higher than that of the slope obtained from the least squares linear regression curve. With this in mind, each point in the profile was weighted by the inverse of the standard deviation of the slope of the respective regression line. This value accompanies every plot in appendix A.

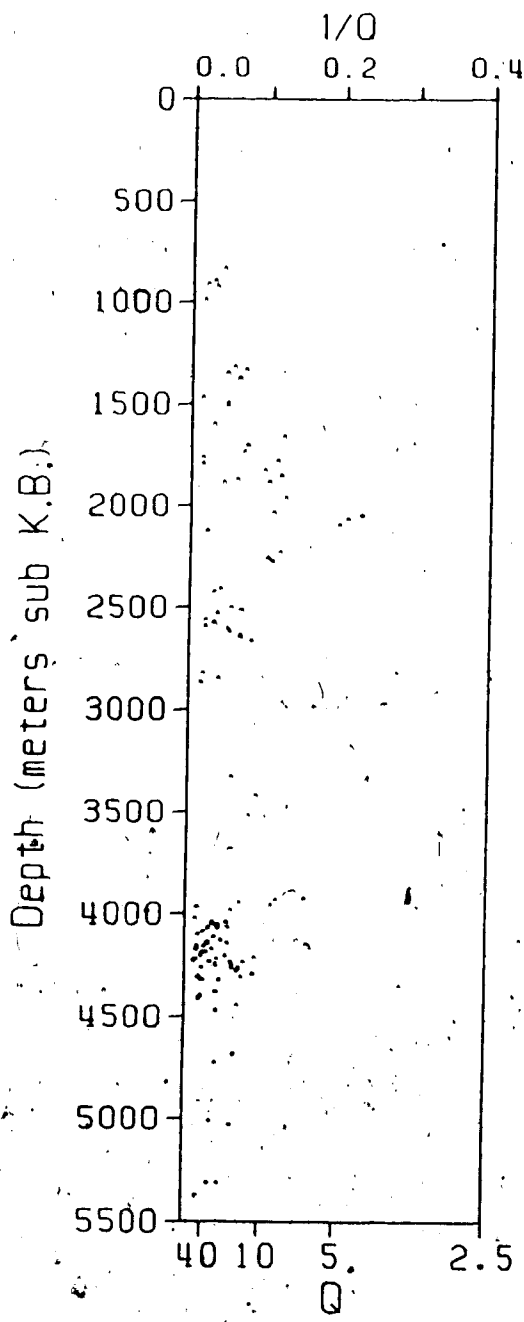


Figure 3.10 Plot of specific attenuation versus depth with accompanying Q-axis

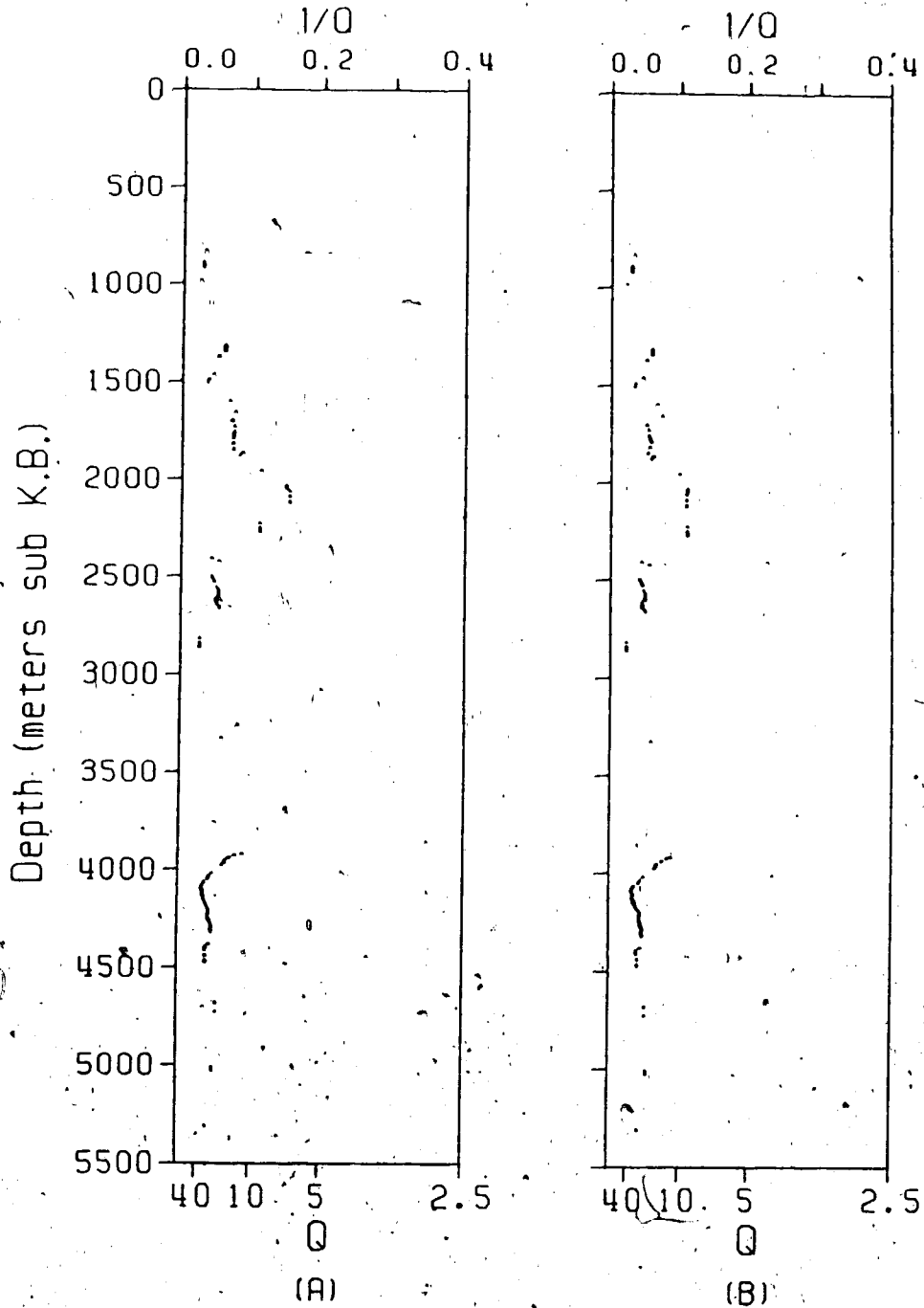


Figure 3.1.1 a) 200-meter running average of the specific attenuation profile b) 200-meter weighted running average of the specific attenuation profile

Both profiles of figure (3.11) exhibit an interesting peak between 1900 and 2300 meters, and an indication of a zone of high attenuation immediately above 4000 meters. Consider figure (3.12) where the interval-velocity, lithologic, specific attenuation, and interval- Q^{-1} profiles can be reviewed simultaneously. The interval- Q^{-1} profile was obtained by finding the weighted arithmetic mean of those Q^{-1} values lying within a specified depth interval. The depth intervals were selected according to distinct Q^{-1} zones as apparent from part (a). The interval-velocity profile was described in section 3.2 and the specific attenuation profile was duplicated from figure (3.11, b). The lithologic section was duplicated from figure (3.3) and the key remains unaltered. From figure (3.12), the weighted means of the specific attenuations for each depth interval are given in table (3.1) where the standard deviations were calculated with the unweighted means. The number of data points in each interval is given along with the range of Q^{-1} values. The range was determined from the standard deviation (STD) of the specific attenuation values in each depth interval. The final column in table (3.1) gives the most probable quality factor for each interval given by the inverse of the specific attenuation values in column three. One set of values for the entire well is presented in the bottom row of the table.

Table 3.1 Interval Attenuation Statistics

DEPTH INTERVAL (meters)	# OF POINTS	1/Q	INTERVAL 1/Q STD	Q-RANGE	MOST PROBABLE Q
750 to 1035	5	.02437	.00833	31 - 62	41
1035 to 1550	7	.04560	.01562	16 - 33	22
1550 to 1930	13	.05495	.03487	11 - 50	18
1930 to 2320	9	.10501	.05783	6 - 21	10
2320 to 3813	18	.04003	.01904	17 - 48	25
3813 to 4000	6	.08337	.04202	8 - 24	12
4000 to 5400	50	.03789	.01920	18 - 54	26
750 to 5400	108	.04458	.03998	12 - 217	22

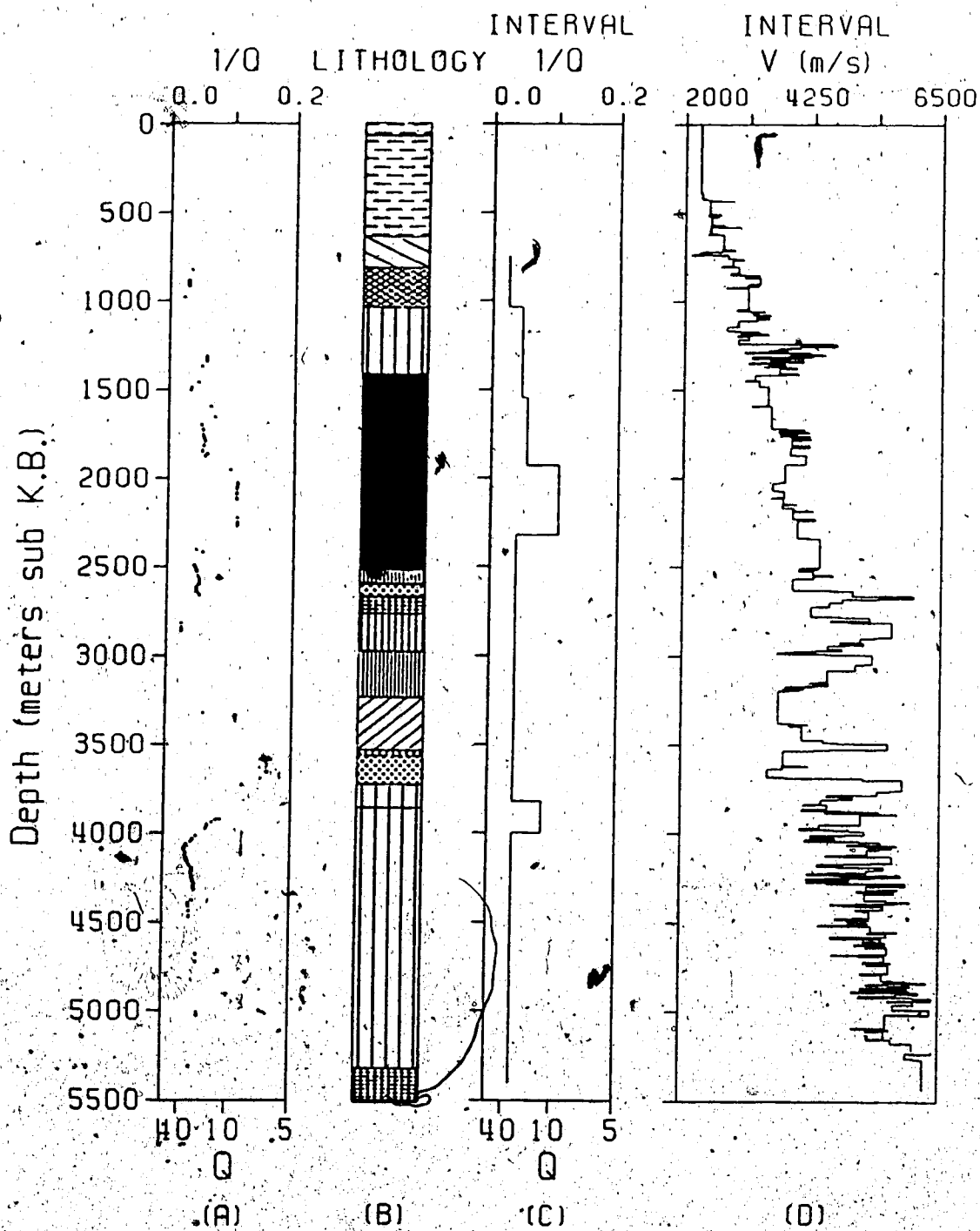


Figure 3.12 Profiles: a) weighted $1/Q$ smoothed with a 200 meter running average b) lithology c) interval $1/Q$ d) interval velocity

3.9 Discussion of Results

The strongly attenuating zone between 1930 and 2320 meters is associated with a virtually uninterrupted Lower Triassic sandstone layer which extends from 1400 meters to 2500 meters. The remainder of the sandstone layer seems to coincide with a slightly elevated attenuation level. Hauge (1981) shows clearly that attenuation increases with increasing sand content of rocks. From the results of a VSP survey he found that most of the attenuation took place in sandstone layers while relatively little occurs in the shale which comprised the remainder of the hole. Stainsby and Worthington (1985) give further examples of porous sand units being associated with high attenuation. It would appear, therefore, that the results obtained in this study further substantiate these findings.

The suggestion of a highly attenuating zone immediately above 4000 meters appears to be well correlated with a distinct velocity signature at 3750 meters. It is not related to the presence of sandstone, however, it could be interpreted as a partially saturated zone ($\approx 95\%$) in contrast with fully saturated or dry neighbouring rocks in accordance with the results of Winkler and Nur in 1979, and 1982, and Murphy III (1982). A change in microstructure may, in addition, contribute to the high attenuation, in that pore aspect ratios might be smaller with respect to the over- and underlying layers. The viscosity of the pore fluid may increase in the low-Q zone, as may the porosity. These

variations in rock properties may also be responsible for the varying attenuation within the sandstone interval.

It should be noted that the attenuation observed here will approximate the upper limits of intrinsic attenuation due to the inclusion of frequency dependent scattering and the effects of intrabed multiples. A Q-value of 26 is likely to be too low a value for depths greater than 4 Km. Scattering and intrabed multiples are thought to contribute to this value because of the highly cyclical nature of the velocity log. It is possible that some scattering is due to irregular interfaces which may be responsible for the failure of the correction factor discussed in section 3.3. This is in agreement with the findings of Spencer et al. (1982), as mentioned in section 2.5. The sandstone layer, however, is relatively homogeneous, as can be seen in the velocity and geologic profiles, thus, scattering and the number of intrabed multiples may be minimal in this zone. The highly cyclic stratigraphy between 1200 and 1400 meters and below 2500 meters could be depleting the signal of higher frequencies, hence inflating the attenuation at these depths. This serves to reduce the contrast in attenuation between the sandstone layer and bordering zones. If the effects of scattering and intrabed multiples could be eliminated, the contrast between the sandstone interval and neighbouring layers would likely be enhanced.

In 1979 Ganley obtained phase velocities that agreed well with Futterman's theory of velocity dispersion (1962).

By considering Futterman's third dispersion relation (he provides three feasible relations), it is possible to approximate the percentage attenuation that is a result of intrabed multiples and scattering versus that which is due to intrinsic attenuation. According to Richards and Menke (1982) the apparent attenuation due to intrabed multiples and intrinsic absorption are approximately additive. At the same time it will be possible to see whether or not the observed drift between seismic and sonic arrival times, as discussed in section 3.2, can be accounted for by the attenuation observed. In the following discussion it must be noted that attenuation is a necessary and sufficient condition for dispersion (Futterman, 1962), and that dispersion accounts for the vast majority of the drift (Stewart et al., 1984).

Over the depth interval 750 meters to 3695 meters the F-34 well exhibits a drift (sonic arrival time minus seismic arrival time per kilometer) of -8 msec/Km. Between 3695 meters and 4600 meters the seismic and sonic velocities are roughly comparable while below 4600 meters the seismic velocities are greater than the sonic velocities. The behaviour of the velocities below 3695 meters is not explained by Futterman's theory and may result from reduced sonic tool- or geophone-ground coupling, or errors in time picking of the first arrivals. Stewart et al. (1984) found an average drift of -6.6 msec/Km in the literature they reviewed. In 5 wells they themselves studied (4 wells in the

Anadarko basin of the southern United States, and 1 well in east Texas) intrabed multiples caused a drift of -6.6 msec/Km while dispersion (or intrinsic attenuation) resulted in a drift of -23 msec/Km.

Futterman's third dispersion relation is given by,

$$v(\omega) = c \left[1 - \frac{1}{\pi Q_0} \ln\left(\beta \frac{\omega}{\omega_0}\right) \right]^{-1} \quad (19)$$

where,

$v(\omega)$ = phase velocity for a disturbance of angular frequency ω .

ω_0 = an angular frequency below which no attenuation takes place

(let it be $2\pi \times 10^{-3} \text{ sec}^{-1}$)

c = phase velocity for frequencies below ω_0 (a constant)

$\beta = \ln \gamma = 1.78107248\dots$
 γ is Euler's constant

Q_0 = reduced quality factor (a constant)

$$= \frac{\omega}{2a(\omega)c} = Q(\omega) + \frac{1}{\pi} \ln\left(\beta \frac{\omega}{\omega_0}\right) \quad (20)$$

$Q(\omega)$ = frequency dependent quality factor

$a(\omega)$ = frequency dependent attenuation coefficient

An estimate of the reduced quality factor, Q_0 , can be obtained if the phase velocity at each of two known frequencies is available. Because c is a constant, equation (19) gives,

$$v(\omega_1) \left[1 - \frac{1}{\pi Q_0} \ln \left(\beta \frac{\omega_1}{\omega_0} \right) \right] \\ = v(\omega_2) \left[1 - \frac{1}{\pi Q_0} \ln \left(\beta \frac{\omega_2}{\omega_0} \right) \right] \quad (21)$$

Let ω_1 be a seismic frequency and $v(\omega_1)$ be the phase velocity of a seismic wave. Down to the depth of 3695 meters the average phase velocity is 3622 m/s as calculated from the travel time of a pulse generated by a Geogel source.

Futterman points out that it is the highest dominant frequency component of a pulse which arrives first. In view of figure (3.8) the velocity of 3622 m/s will be applied to a frequency, ω_1 , of 80 Hz. ω_2 can be assigned to the frequency used in the sonic survey which was 20 kHz. By considering the integrated sonic log prior to correction by the VSP survey, this frequency travelled with an average velocity of 3731 m/s over the same depth interval.

Solving equation (21) for Q_0 gives,

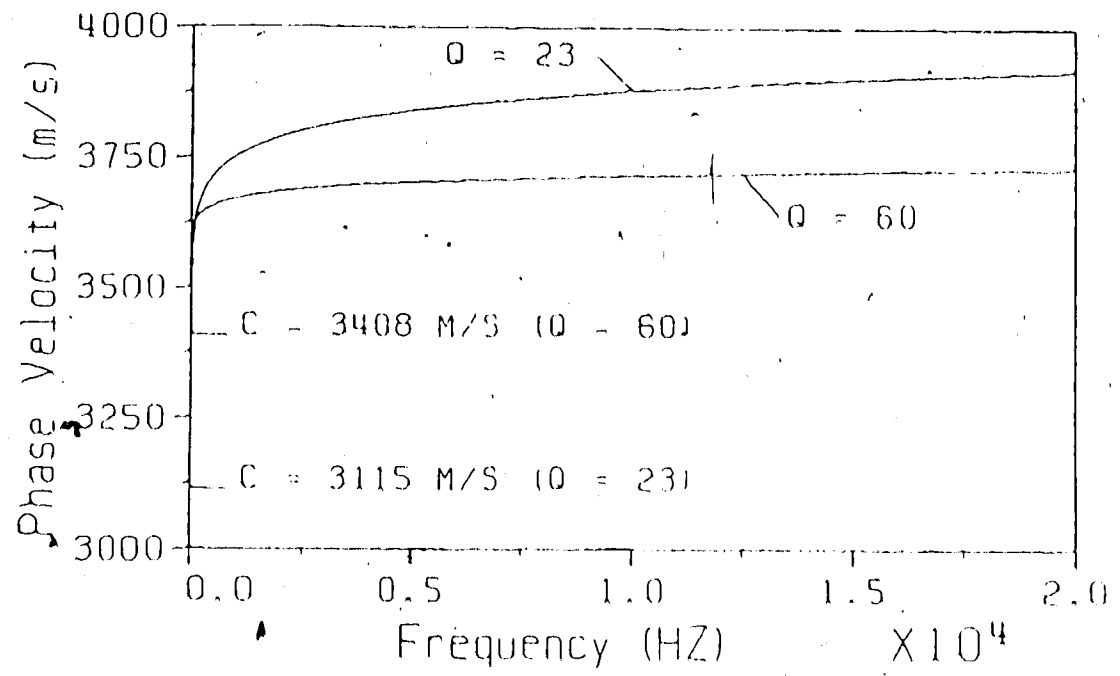
$$Q_0 = 64$$

for the zone lying between 750 meters and 3695 meters. By applying equation (20) it is possible to determine Q for a given frequency. The mean Q down to a depth of 3695 meters is 23. Because both Aquaflex and Geogel played an equal part in obtaining this value, and because this Q should be associated with the dominant frequency of the spectrum, the average of the two dominant frequencies } 50 Hz for Aquaflex and 40 Hz for Geogel (see figure (3.8)), was the frequency for which this Q -value was considered to apply. Thus, $Q(45\text{Hz}) = 23$ between 750 and 3695 meters. Equation (20), however, renders $Q(45\text{Hz}) = 60$ based on the observed drift (assuming that intrinsic attenuation caused the majority of the drift). It seems likely that the discrepancy in Q -values is due almost entirely to intrabed multiples and scattering because the Q obtained from drift measurements will be weakly affected by such processes whereas that arising from the spectral ratio method is strongly affected. This implies that intrabed multiples and scattering contribute 62% of the observed attenuation. It must be kept in mind that there is strong evidence of an attenuation peak in the mid-kiloHertz frequencies (Murphy III, 1985) which is capable of increasing drift. Futterman's relation assumes a linear function of attenuation with frequency up to an arbitrarily high frequency. The intrinsic attenuation for the seismic

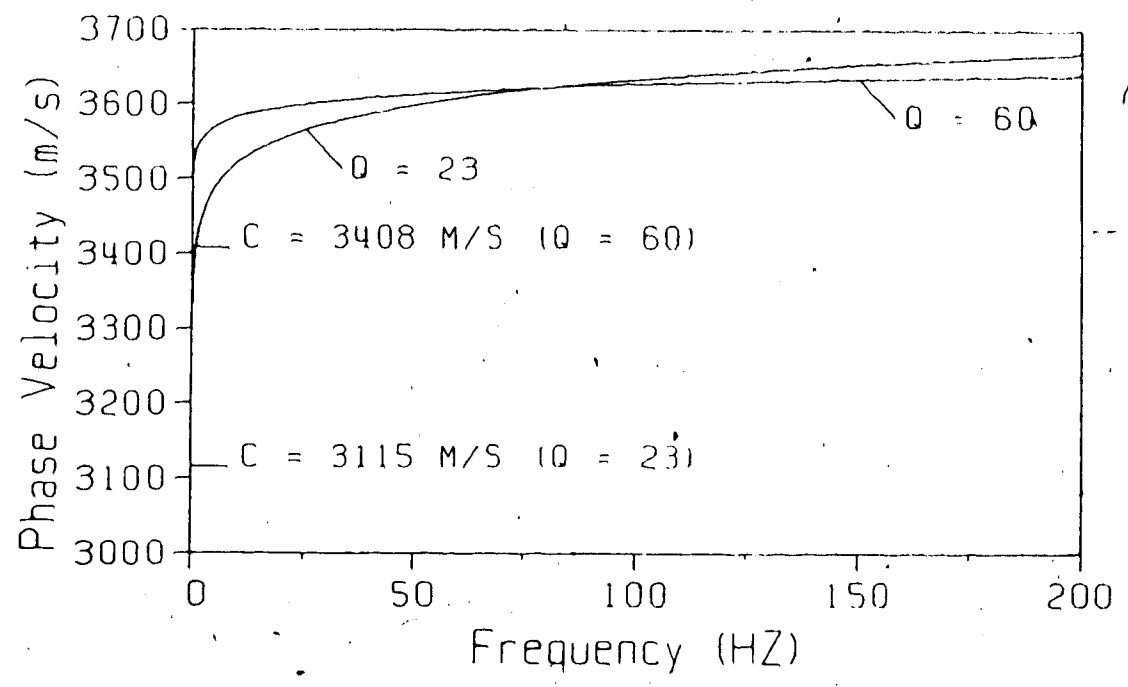
frequencies calculated strictly from Futterman's relation should, therefore, be lower in order to leave room for the attenuation peak to increase the drift to the observed level. This places the lower limit of attenuation due to intrabed multiples and scattering at 62%. In a study of two wells, Schoenberger and Levin (1978) found that intrabed multiples alone were responsible for 33% to 50% of the observed attenuation. Summarizing the results of 4 additional wells from basins around the world they found that the apparent attenuation due to intrabed multiples accounted for 14% to 77% of the observed attenuation. Kan et al. (1982) found a negligible contribution to attenuation due to intrabed multiples in an analysis of 2 wells.

The method by which the contribution of intrabed multiples to attenuation is estimated involves generating synthetic pulses that do not include the effects of intrinsic attenuation. The pulses are then analysed via the spectral ratio method in the same fashion as in the case of field data. The effect of scattering is therefore ignored and the resulting attenuation due to intrabed multiples alone is assumed to be the same for the field data.

Equation (19) can now be used to obtain the non-dispersive limit of the phase velocity, c , given Q_0 and the phase velocity at 80 Hz. If Q_0 is taken as 64 then the parameter $c = 3408$ m/s and the dispersion curve which accounts for the observed drift can be calculated (see figure (3.13)). The observed $Q(45\text{Hz}) = 23$ ($Q_0 = 27$) produces



(A)



(B)

Figure 3.13 Dispersion curves for $Q(45\text{Hz}) = 60$ ($Q_0 = 64$) and $Q(45\text{Hz}) = 23$ ($Q_0 = 27$), a) frequency range 0 to 20 kHz, b) frequency range 0 to 200 Hz

a dispersion curve also shown in figure (3.13) where c is now 3115 m/s. This level of attenuation causes a drift of -21 msec/Km.

Conclusions

The variation of intrinsic attenuation with depth plays an important role in the distortion of seismic wavetrains. Since seismic energy is a convenient probe for studying the structure of the earth, knowledge of the attenuation profile increases the power of the seismic method of geophysical exploration. The attenuation profile is diagnostic in its own right as it is capable of discerning zones of varying fluid saturation, lithology, rock microstructure, porosity, and temperature. The quality of synthetic seismograms would be improved with the use of attenuation profiles in their generation. Seismic inversion would, likewise, be improved, as would the monitoring of steam injection zones, and possibly, earthquake prediction. The synthetic seismogram generation and seismic inversion both require the Q -values themselves while the latter two require the level of fluid saturation obtained from the attenuation profile.

The consensus among current researchers favors the viscous squirt flow mechanism as being the major cause of intrinsic seismic attenuation. This is a fluid flow mechanism, consequently, it is believed that saturation, pore aspect ratio, and porosity of a medium are the dominant parameters governing intrinsic attenuation.

As with any experiment, direct sampling of a parameter usually yields the best estimates for the parameter. Laboratory experiments are useful in determining dependencies on parameters but are unable to study rocks in

their undisturbed state. The Vertical Seismic Profiling (VSP) survey is the most direct approach for studying *in situ* intrinsic attenuation. The VSP data from a borehole on Melville Island, in the Canadian Arctic, was employed in this study and subsequently analysed by the spectral ratio method. 108 depth intervals were studied. The depth intervals ranged in thickness from 200 to 400 meters and spanned more than 5 kilometers down the well.

An attempt at correcting for the effect of intrabed multiples, as described by Ganley and Kanasewich (1980), was unsuccessful. Reflection arising from smooth horizontal interfaces was assumed by them in their presentation of the correction factor, however, this may not be applicable in the Sherard Bay F-34 well. It is proposed here that the oscillations observed on the log graphs likely result from source to source variations and/or irregular scattering and intrabed multiples arising from contorted interfaces. The combined effects of intrabed multiples and frequency dependent scattering of seismic energy appears to contribute at least 62% of the observed attenuation when considering the entire well. This value was obtained through an analysis of the observed seismic velocity dispersion employing W. I. Futterman's results of 1961, which state that attenuation is a necessary and sufficient condition for dispersion. Estimates of this percentage are presented in the literature through calculation of both synthetic VSP sections for purely elastic media and also the subsequent

spectral ratios so that apparent attenuation due to intrabed multiples alone can be isolated. This approach, however, does not allow for the effects of scattering, nor for the presence of non-smooth interfaces. The possibility of poor geophone- or sonic tool-coupling to the walls of the borehole may, in addition, contribute to uncertainties in the attenuation estimates.

The majority of Q-values obtained were reasonable, lying between 4.5 and 131.1. The data shows the possibility of a highly attenuating zone immediately above 4000 meters for which the specific attenuation is .08337 ($Q \approx 12$), with a standard deviation of .04202, in contrast with a regional specific attenuation of .04458 ($Q \approx 22$), with a standard deviation of .03998. A strongly attenuating zone, where the specific attenuation is .10501 ($Q \approx 10$) with a standard deviation of .05783, lies between 1930 and 2320 meters and is associated with a sandstone horizon of the Lower Triassic period. In comparing the Q of this zone with that of neighbouring layers there is little doubt of the existence of the low-Q zone especially when the findings of other authors also indicate an association of sandstone with high attenuation. If the effects of intrabed multiples and scattering could be reduced, the contrast in attenuation between the two low-Q zones and the remainder of the borehole would likely increase.

It must be kept in mind that the data analysed in this study was gathered under less than ideal survey conditions,

the survey not being designed specifically for obtaining attenuation measurements. Several modifications could be made to the survey procedure employed by Panarctic Oils Ltd. The borehole should be cased down its entire length for better geophone-wall coupling. In addition, the shot hole should be concrete lined to prevent damage to the walls and it should be filled with water. It is advantageous for the shot to be suspended in the water for maximum repeatability of the source spectrum (Hardage, 1983). Ideally, the number of shots should be kept to a minimum while incorporating a maximum number of geophones.

A satisfactory technique for obtaining attenuation measurements entails the use of one pair of geophones separated in depth by 250 meters or so. Beginning at the bottom of the well, raise the pair in 30 meter intervals, or less, until the top of the well is reached. At each level, clamp the geophones to the well and fire a shot. In this manner, each geophone of the pair receives an identical source spectrum at each depth interval. This would greatly improve the results of the spectral ratio method, and hence, the quality of the attenuation profile.

It was the intention of this work to obtain an attenuation profile for the Sherard Bay F-34 well, to relate the profile to the local lithology, and ultimately, to infer properties of the neighbouring rocks. Excellent correlation of high attenuation with a sandstone layer provided confidence that intrinsic attenuation was in fact being

observed, and thus, allowed predictions to be made regarding rock properties for the entire well. The existence of the two low-Q zones may be attributed to one or more of the following factors which contribute to high attenuation: the presence of fluids with higher viscosity than those in the remainder of the hole, pores with smaller aspect ratios, more pore space, and a higher degree of saturation ($\approx 95\%$ saturation).

Further work is required both in the laboratory and in the field to obtain independent quantitative measures of each of the above properties such that the nature of the attenuating medium may be more accurately determined. In addition, methods must be developed which reduce the effects of scattering and intrabed multiples when contorted interfaces are involved. This is desirable since these effects obscure the intrinsic attenuation and, therefore, reduce the reliability of the attenuation profile.

Bibliography

- Aki, K., and Richards, P. G., 1980, *Quantitative Seismology*, Vol. I, II, W. H. Freeman and Co.
- Biot, M. A., 1956 a, Theory of propagation of elastic waves in a fluid-saturated porous solid. I. Low-frequency range, *Journal of the Acoustical Society of America*, 28, 168-178.
- Biot, M. A., 1956 b, Theory of propagation of elastic waves in a fluid-saturated porous solid. II. Higher-frequency range, *Journal of the Acoustical Society of America*, 28, 179-191.
- Campillo, M., Plantet, J. L., and Bouchon, M., 1985, Frequency-dependent attenuation in the crust beneath central France from Lg waves: Data analysis and numerical modelling, *Bulletin of the Seismological Society of America*, 75, 1395-1411.
- Clark, T. H., and Stearn, C. W., 1960, *The Geological Evolution of North America*, The Ronald Press Company, New York.
- Dietrich, M., and Bouchon, M., 1985, Measurements of attenuation from vertical seismic profiles by iterative modelling, *Geophysics*, 50, 931-949.
- Futterman, W. I., 1962, Dispersive body waves, *Journal of Geophysical Research*, 67, 5279-5291.
- Gal'perin, E. I., 1974, *Vertical Seismic Profiling*, Society of Exploration Geophysicists Special Publication No. 12, Tulsa, Oklahoma.

- Ganley, D. C., 1979, The seismic measurement of absorption and dispersion, Ph.D. thesis, University of Alberta, Edmonton.
- Ganley, D. C., and Kanasewich, E. R., 1980, Measurement of absorption and dispersion from check shot surveys, *Journal of Geophysical Research*, 85, 5219-5226.
- Ganley, D. C., 1981, A method for calculating synthetic seismograms which include the effects of absorption and dispersion, *Geophysics*, 46, 1100-1107.
- Gardner, G. H. F., 1962, Extensional waves in fluid-saturated porous cylinders, *Journal of the Acoustical Society of America*, 34, 36-40.
- Hardage, B. A., (editor), 1981, An examination of tube wave noise in vertical seismic profiling data, *Geophysics*, 46, 892-903.
- Hardage, B. A., 1983, *Vertical Seismic Profiling, Part A: Principles*, Geophysical Press, London-Amsterdam.
- Hatherly, P. J., 1986, Attenuation measurements on shallow seismic refraction data, *Geophysics*, 51, 250-254.
- Hauge, P. S., 1981, Measurements of attenuation from vertical seismic profiles, *Geophysics*, 46, 1548-1558.
- Hovam, J. M., and Ingram, G. D., 1979, Viscous attenuation of sound in saturated sand, *Journal of the Acoustical Society of America*, 66, 1807-1812.
- Hunstberger, D. V., 1967, *Elements of Statistical Inference* (3rd edition), Allyn and Bacon.

- Jones T., and Nur, A., 1983, Velocity and attenuation in sandstone at elevated temperatures and pressures, *Geophysical Research Letters*, 10, 140-143.
- Kan, T. K., Corrigan, K., and Huddleston, P. D., 1982, Attenuation measurement from vertical seismic profiles, *Geophysics*, 47, 466.
- Kanasewich, E. R., 1975, *Time Sequence Analysis in Geophysics* (2nd edition), University of Alberta Press, Edmonton, Alberta.
- Kennett, P., Ireson, R. L., Conn, P. J., 1980, Vertical seismic profiles: their applications in exploration geophysics, *Geophysical Prospecting*, 28., 676-699.
- Kjartansson, E., 1979, Constant Q-wave propagation and attenuation, *Journal of Geophysical Research*, 84, 4737-4748.
- Knopoff, L., 1964, Q, *Reviews of Geophysics and Space Physics*, 2, 625-660.
- Levin, F. K., and Lynn, R. D., 1958, Deep-hole geophone studies, *Geophysics*, 23, 639-664.
- Liu, H.-P., Anderson, D. L., and Kanamori, H., 1976, Velocity dispersion due to anelasticity; implications for seismology and mantle composition, *Geophysical Journal of the Royal Astronomical Society*, 47, 41-58.
- Lomnitz, C., 1957, Linear dissipation in solids, *Journal of Applied Physics*, 28, 201-205.
- Margenau, and Murphy, 1956, *The Mathematics of Physics and Chemistry* (2nd edition), D. Van Nostrand Co. Inc., Princeton, New Jersey.

- Mavko, G. M., and Nur, A., 1979, Wave attenuation in partially saturated rocks, *Geophysics*, 44, 161-178.
- McCann, C., and McCann, D. M., 1969, The attenuation of compressional waves in marine sediments, *Geophysics*, 34, 882-892.
- McCann, C., and McCann, D. M., 1985, A theory of compressional wave attenuation in noncohesive sediments, *Geophysics*, 50, 1311-1317.
- Murphy III, W. F., 1982, Effects of partial water saturation on attenuation in Massillon sandstone and Vycor porous glass, *Journal of the Acoustical Society of America*, 71, 1458-1468.
- Murphy III, W. F., 1985, Sonic and ultrasonic velocities: theory versus experiment, *Geophysical Research Letters*, 12, 85-88.
- Newman, P. J., and Worthington, M. H., 1982, *In situ* investigation of seismic body wave attenuation in heterogeneous media, *Geophysical Prospecting*, 30, 377-400.
- Nyland, E., 1985 a, Theory for estimating seismic wave velocities in oil sands, *AOSTRA Journal of Research*, 2, 53-57.
- Nyland, E., 1985 b, Seismic attenuation in oil sand, *AOSTRA Journal of Research*, 2, 47-51.
- O'Brien, P. N. S., and Lucas, A. L., 1971, Velocity dispersion of seismic waves, *Geophysical Prospecting*, 19, 1-26.
- O'Connell, R. J., and Budiansky, B., 1977, Viscoelastic properties of fluid-saturated cracked solids, *Journal of Geophysical Research*, 82, 5719-5735.

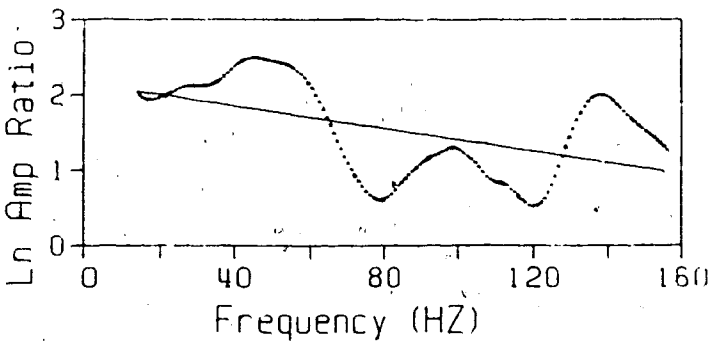
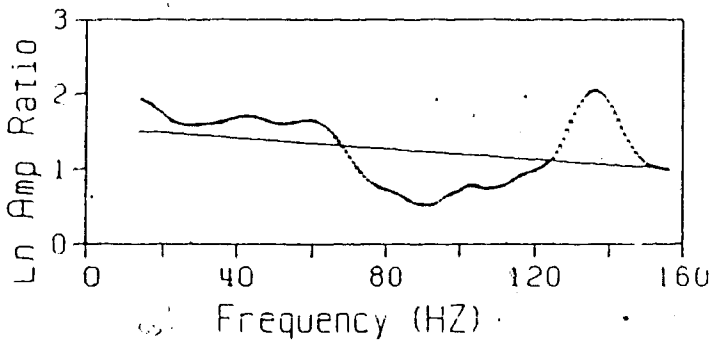
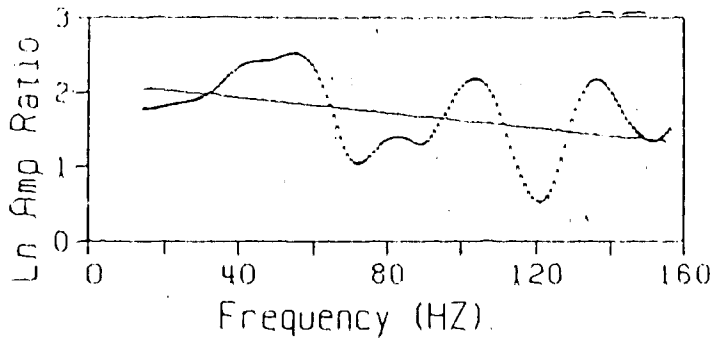
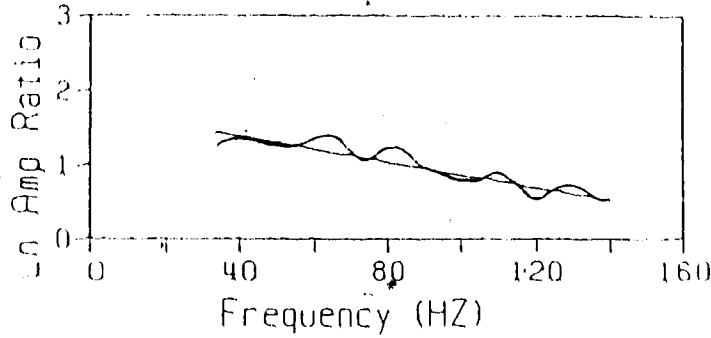
- O'Doherty, R. F., and Anstey, N. A., 1971, Reflections on amplitudes, Geophysical Prospecting, 19, 430-458.
- Palmer, I. D., and Traviolia, M. L., 1980, Attenuation by squirt flow in undersaturated gas sands, Geophysics, 45, 1780-1792.
- Raikes, S. A., and White, R. E., 1984, Measurements of earth attenuation from downhole and surface seismic recordings, Geophysical Prospecting, 32, 892-919.
- Rebollar, C. J., Traslosheros, C., and Alvarez, R., 1985, Estimates of seismic attenuation in northern Baja California, Bulletin of the Seismological Society of America, 75, 1371-1382.
- Richards, P. G., and Menke, W., 1983, The apparent attenuation of a scattering medium, Bulletin of the Seismological Society of America, 73, 1005-1021.
- Ricker, N., 1953, The form and laws of propagation of seismic wavelets, Geophysics, 18, 10-40.
- Savage, J. C., and O'Neill, M. E., 1975, The relation between Lomnitz and Futterman theories of internal friction, Journal of Geophysical Research, 80, 249-251.
- Schoenberger, M., Levin, F. K., 1974, Apparent attenuation due to intrabed multiples, Geophysics, 39, 278-291.
- Schoenberger, M., Levin, F. K., 1978, Apparent attenuation due to intrabed multiples II, Geophysics, 43, 730-737.

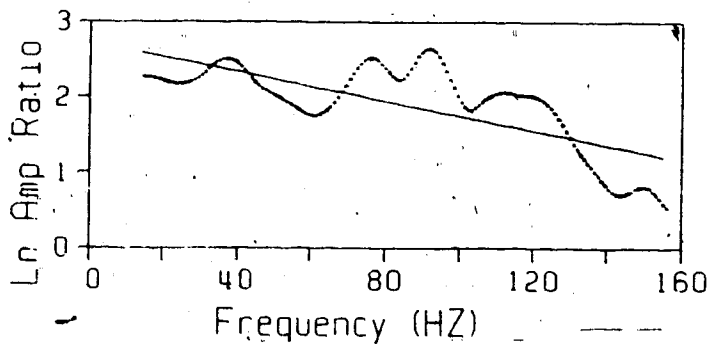
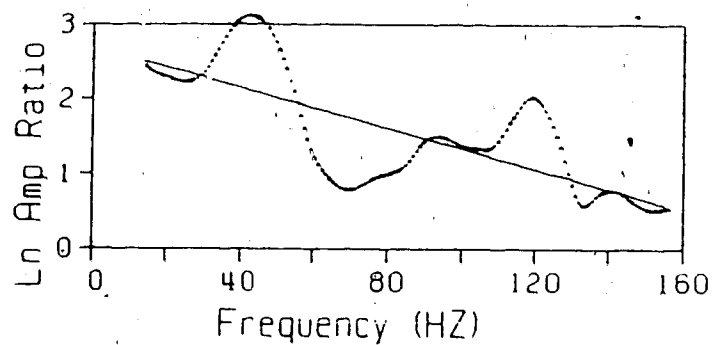
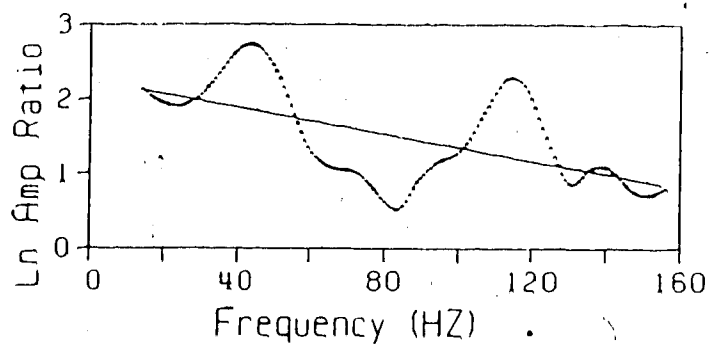
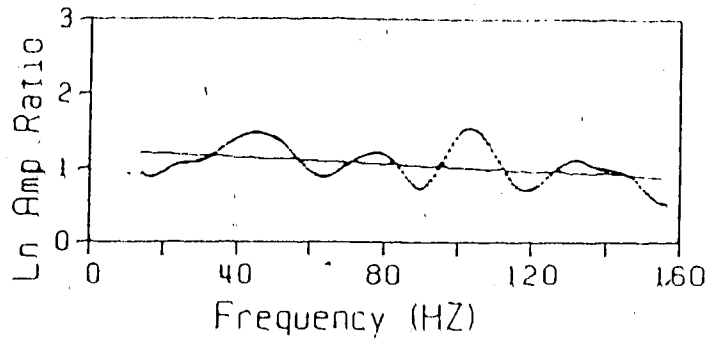
- Seeman, B., and Horowicz, L., 1983, Vertical seismic profiling: separation of upgoing and downgoing acoustic waves in a stratified medium, *Geophysics*, 48, 555-568.
- Sheriff, R. E., and Geldart, L. P., 1982, *Exploration Seismology, Volume 1, History, Theory, and Data Acquisition*, Cambridge University Press.
- Simaan, M., (editor), 1984, *Advances In Geophysical Data Processing; Vertical Seismic Profiles*, JAI Press Inc., Greenwich, Connecticut, USA.
- Spencer, J. W., 1981, Stress relaxations at low frequencies in fluid-saturated rocks: Attenuation and modulus dispersion, *Journal of Geophysical Research*, 86, 1803-1812.
- Spencer, T. W., Sonnad, J. R., and Butler, T. M., 1982, Seismic Q - stratigraphy or dissipation, *Geophysics*, 47, 16-24.
- Stainsby, S. D., Worthington, M. H., 1985, Q estimation from vertical seismic profile data and anomalous variations in the central North Sea, *Geophysics*, 50, 615-626.
- Stewart, R. R., Huddleston, P. D., and Kan, T. K., 1984, Seismic versus sonic velocities: a vertical seismic profiling study, *Geophysics*, 49, 1153-1168.
- Toksoz, M. N., Stewart, R. R., (editors), 1984, *Vertical Seismic Profiling, Part B: Advanced Concepts*, Geophysical Press, London-Amsterdam.
- Treitel, S., and Robinson, E. A., 1966, Seismic wave propagation in layered media in terms of communication theory, *Geophysics*, 31, 17-32.

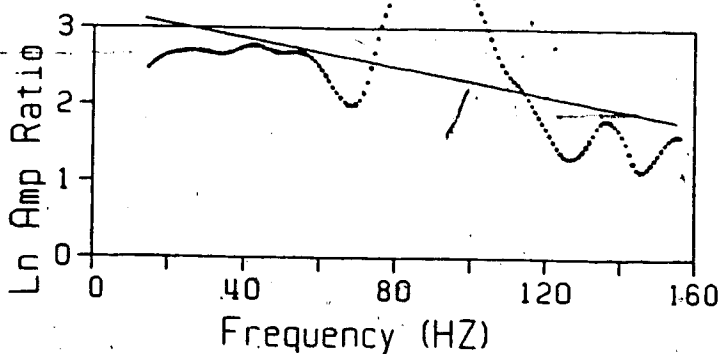
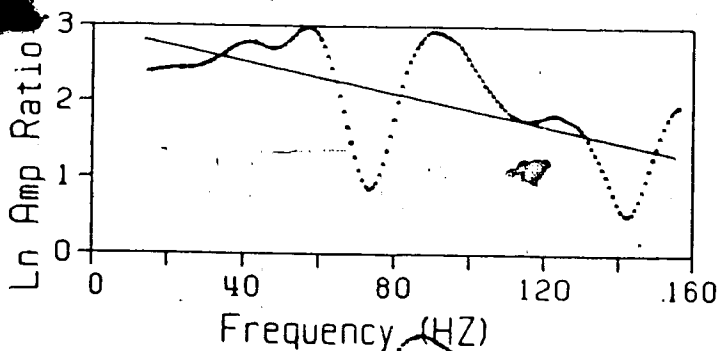
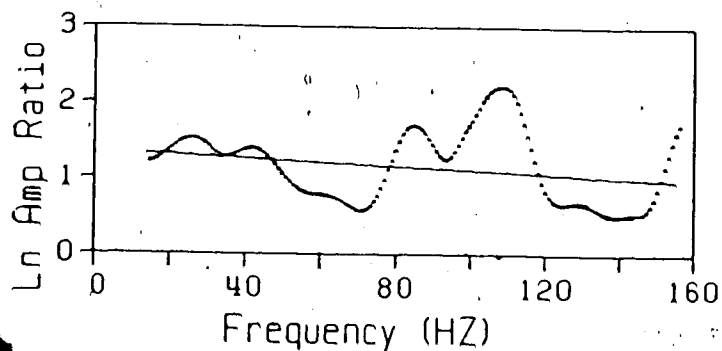
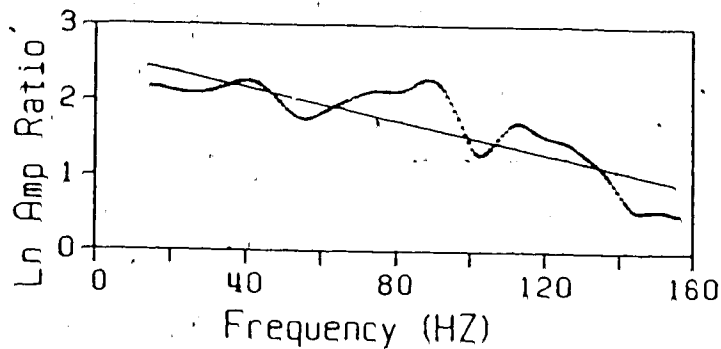
- Waters, K. H., 1978, *Reflection Seismology, a Tool for Energy Resource Exploration*, John Wiley and Sons.
- Winkler, K. W., and Nur, A., 1979, Pore fluids and seismic attenuation in rocks, *Geophysical Research Letters*, 1-4.
- Winkler, K. W., and Nur, A., 1982, Seismic attenuation: effects of pore fluids and frictional sliding, *Geophysics*, 47, 1-15.
- White, J. E., 1965, *Seismic Waves: Radiation, Transmission, and Attenuation*, McGraw-Hill.
- Winkler, K. W., 1986, Estimates of velocity dispersion between seismic and ultrasonic frequencies, *Geophysics*, 51, 183-189.
- Yale, D. P., 1985, Recent advances in rock physics, *Geophysics*, 50, 2480-2491.
- Zener, C., 1948, *Elasticity and Anelasticity of Metals*, University of Chicago Press, Chicago, Ill.

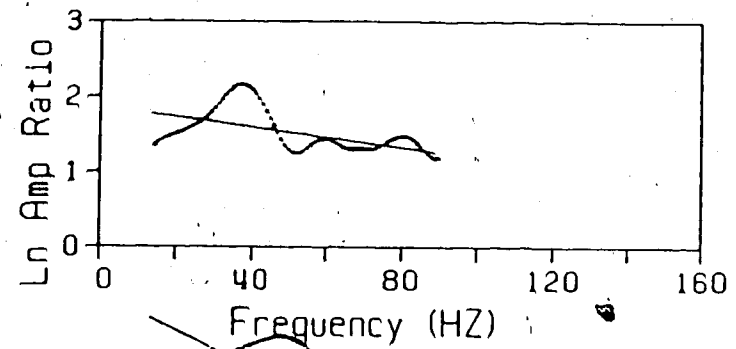
Appendix A : Log Plots

Aquaflex Source

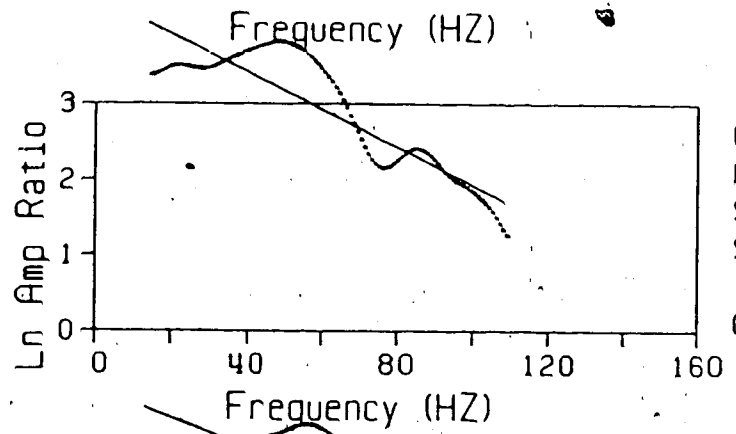




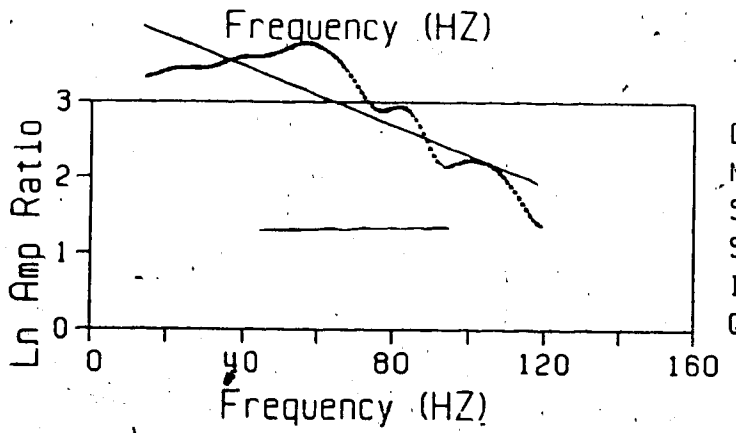




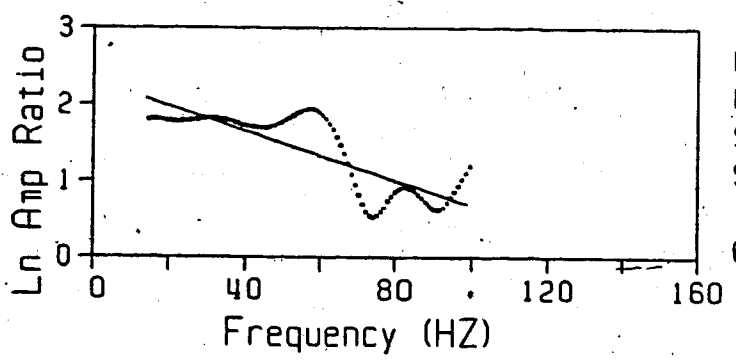
DEPTHS: 1450. - 1750. M
MID-DEPTH: 1600.0 M
SLOPE: -0.006793
SLOPE STD: 0.0012049
INT. VEL.: 3488.0
Q-VALUE: 39.8



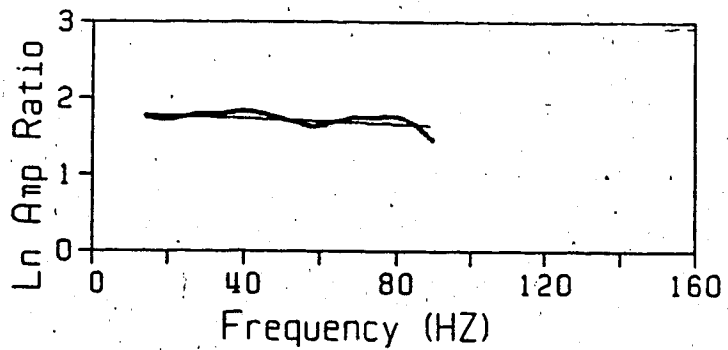
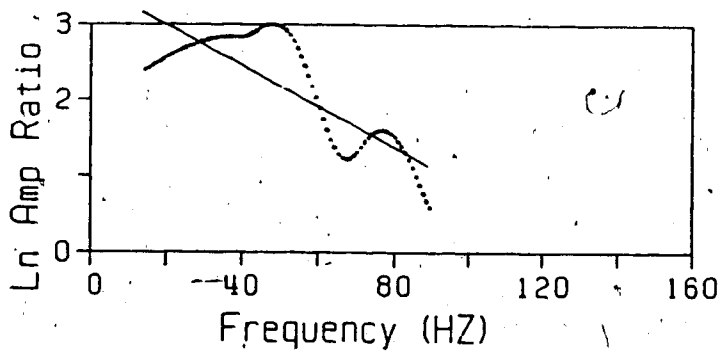
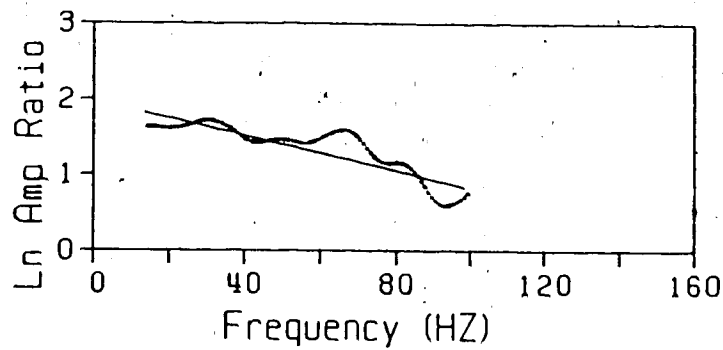
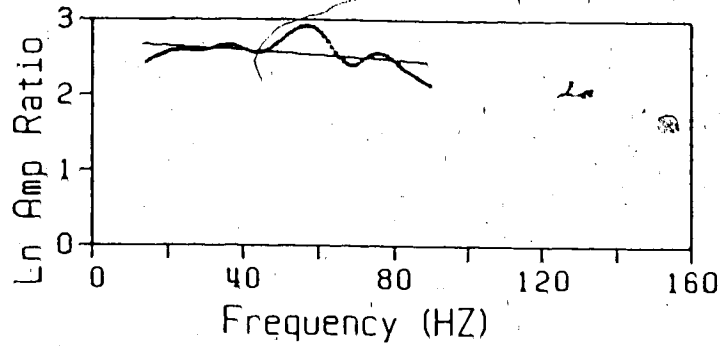
DEPTHS: 1540. - 1780. M
MID-DEPTH: 1660.0 M
SLOPE: -0.024817
SLOPE STD: 0.0013094
INT. VEL.: 3586.0
Q-VALUE: 8.5

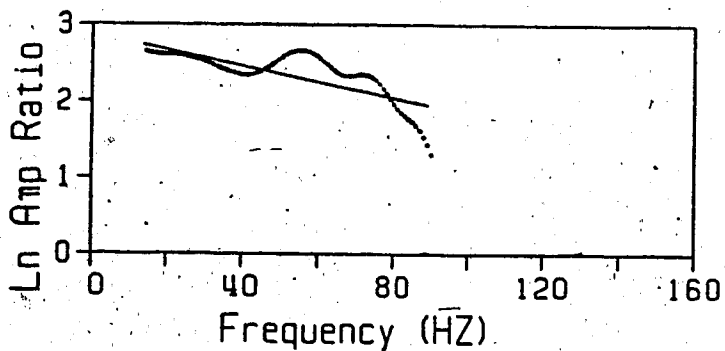
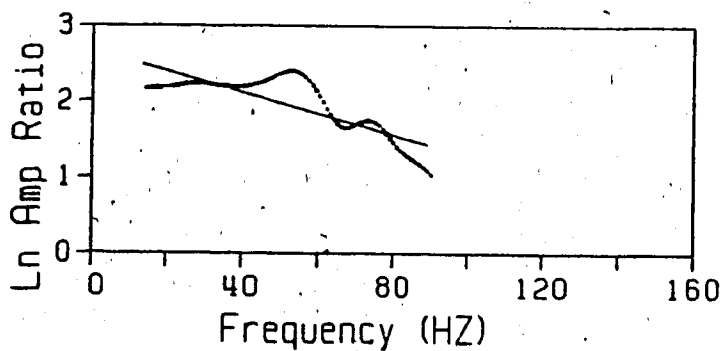
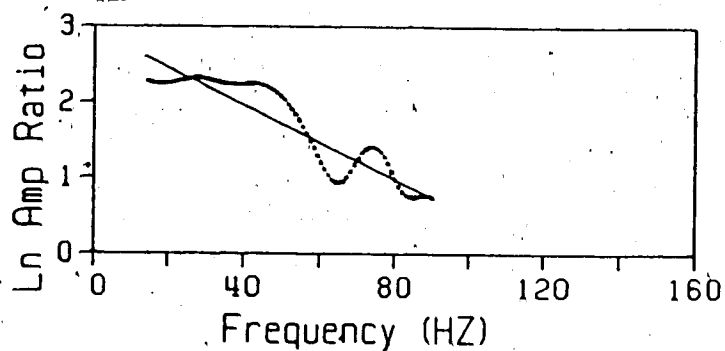
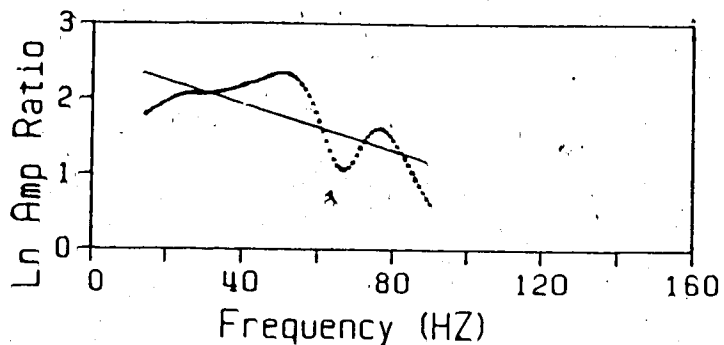


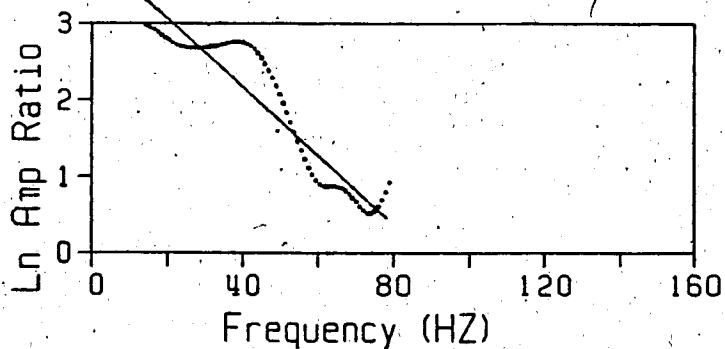
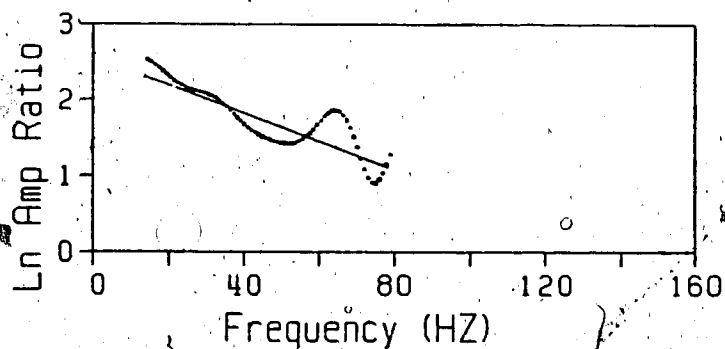
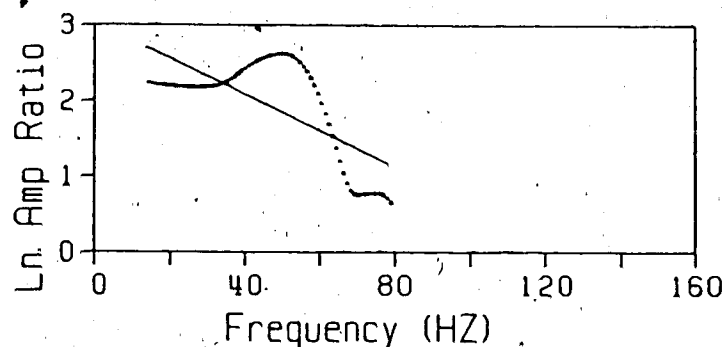
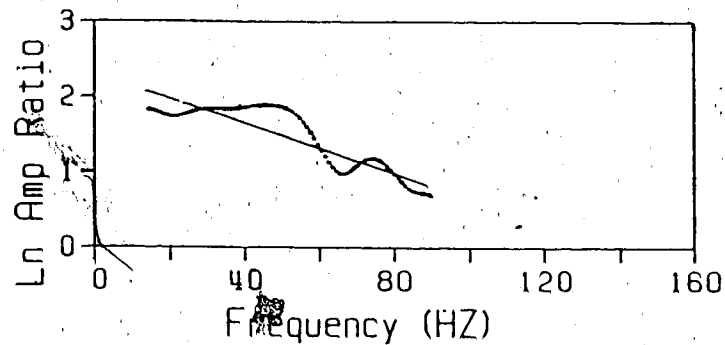
DEPTHS: 1540. - 1870. M
MID-DEPTH: 1705.0 M
SLOPE: -0.019601
SLOPE STD: 0.0010998
INT. VEL.: 3675.0
Q-VALUE: 14.4

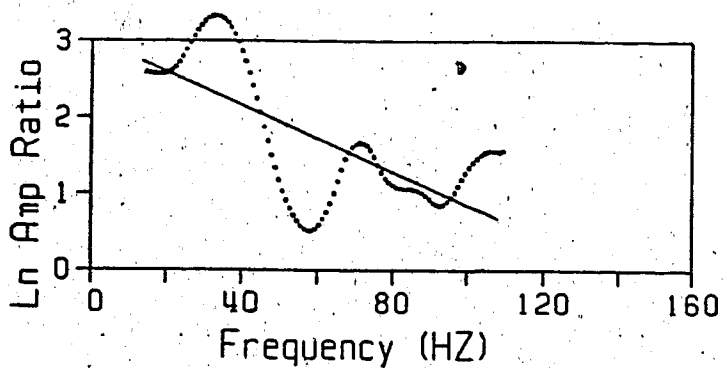
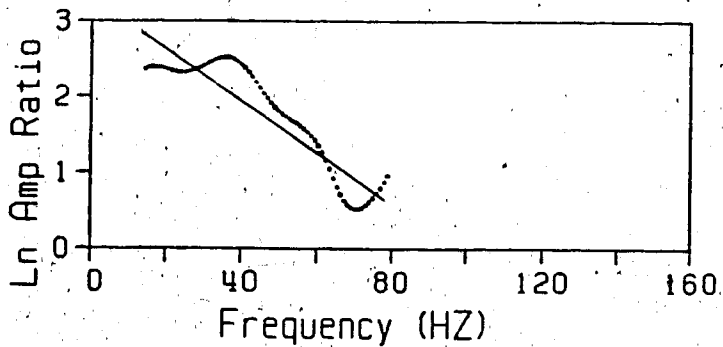
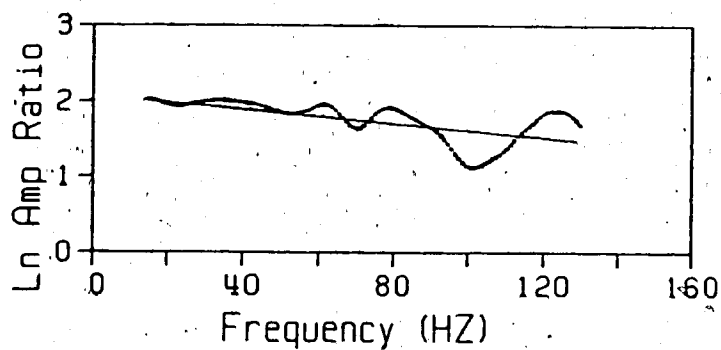
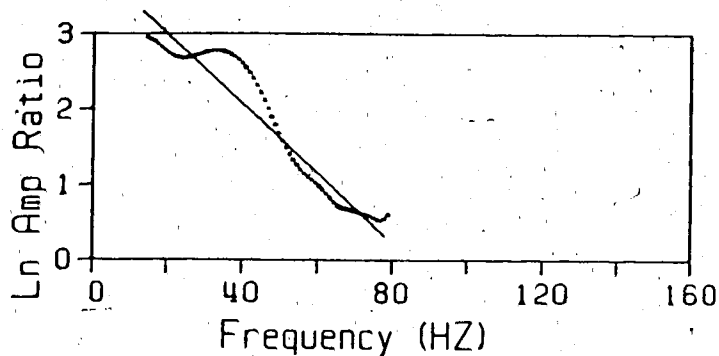


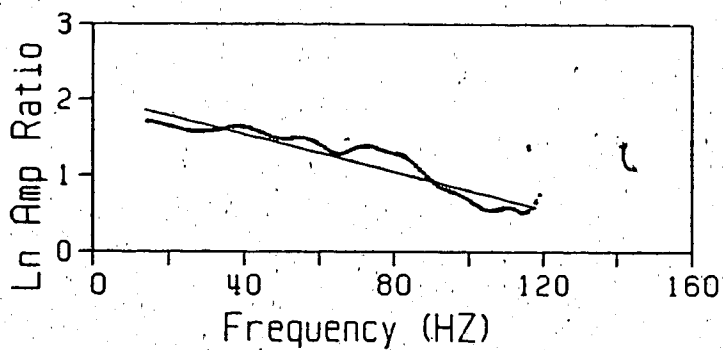
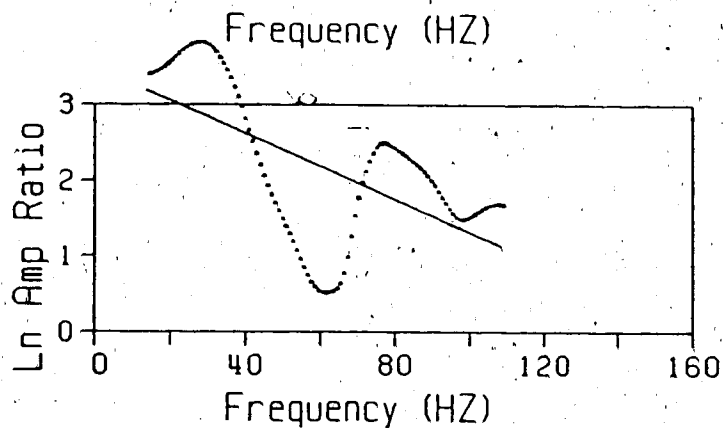
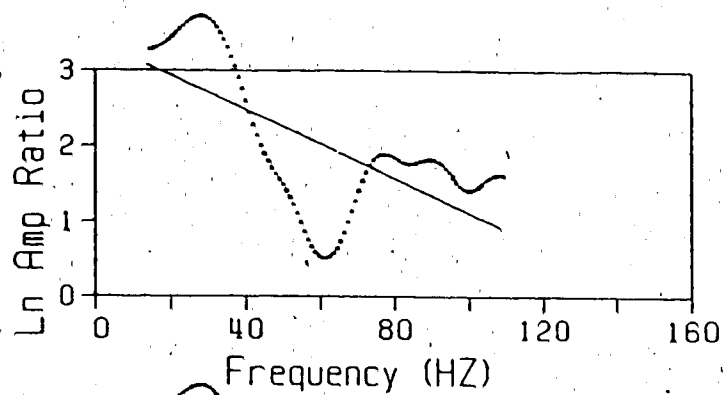
DEPTHS: 1570. - 1840. M
MID-DEPTH: 1705.0 M
SLOPE: -0.016342
SLOPE STD: 0.0012430
INT. VEL.: 3675.4
Q-VALUE: 14.1



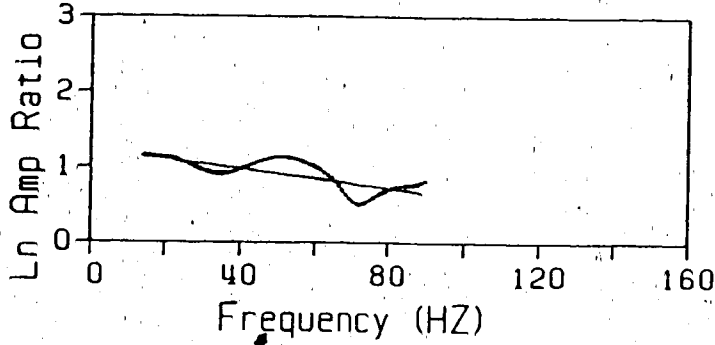




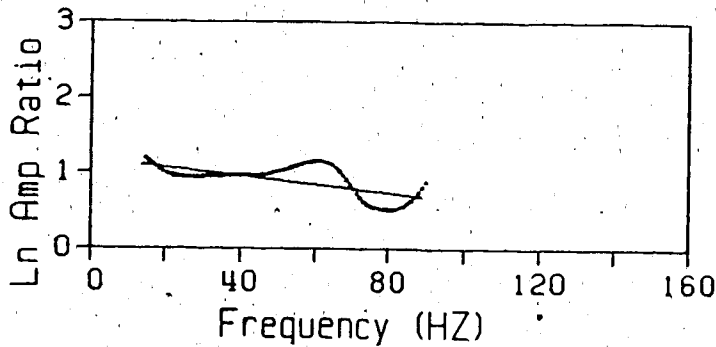




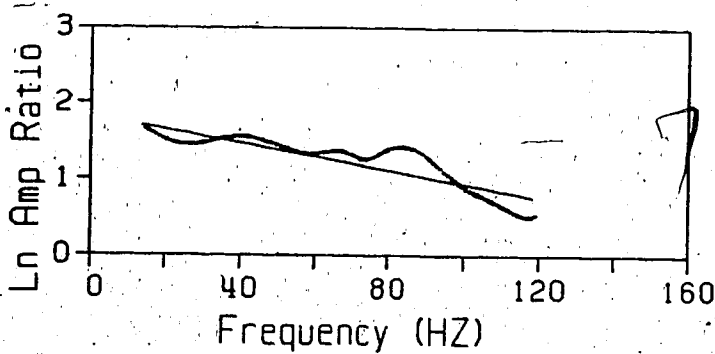
Geogel Source



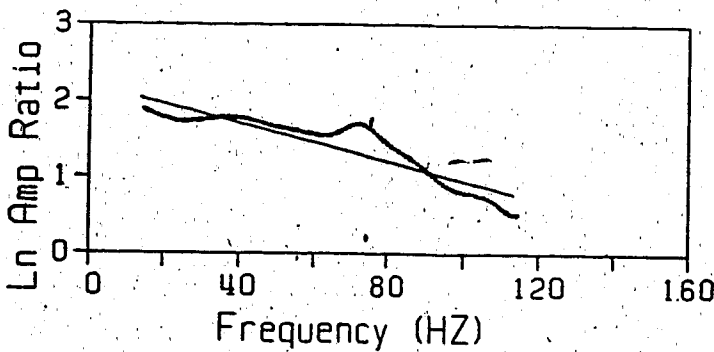
DEPTHS: 2290. - 2530. M
 MID-DEPTH: 2410.0 M
 SLOPE: -0.006398
 SLOPE STD: 0.0006770
 INT. VEL.: 4276.4
 Q-VALUE: 27.6



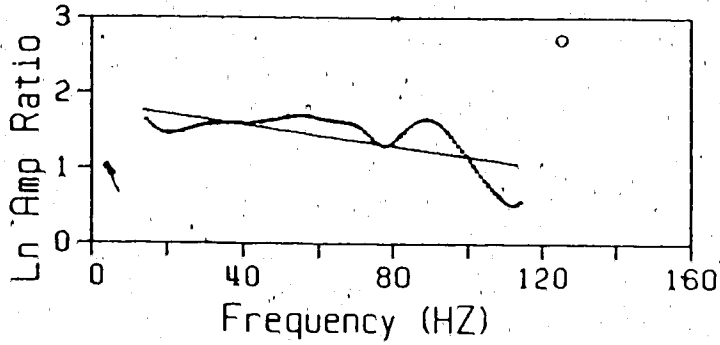
DEPTHS: 2290. - 2560. M
 MID-DEPTH: 2425.0 M
 SLOPE: -0.005499
 SLOPE STD: 0.0007948
 INT. VEL.: 4280.9
 Q-VALUE: 36.0



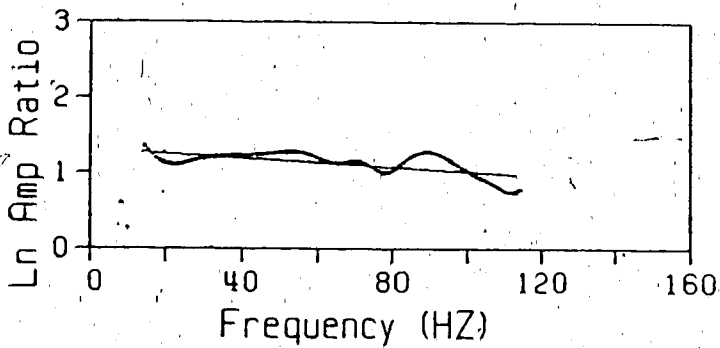
DEPTHS: 2380. - 2620. M
 MID-DEPTH: 2500.0 M
 SLOPE: -0.008995
 SLOPE STD: 0.0005062
 INT. VEL.: 4258.1
 Q-VALUE: 19.7



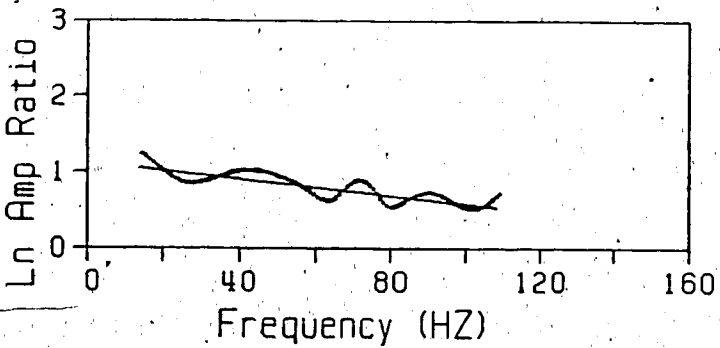
DEPTHS: 2380. - 2645. M
 MID-DEPTH: 2512.5 M
 SLOPE: -0.012648
 SLOPE STD: 0.0005955
 INT. VEL.: 4278.6
 Q-VALUE: 15.4



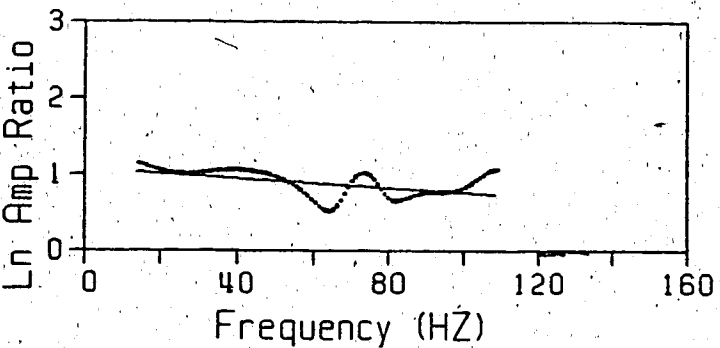
DEPTHS: 2380. - 2680. M
 MID-DEPTH: 2530.0 M
 SLOPE: -0.007005
 SLOPE STD: 0.0008262
 INT. VEL.: 4409.0
 Q-VALUE: 30.5



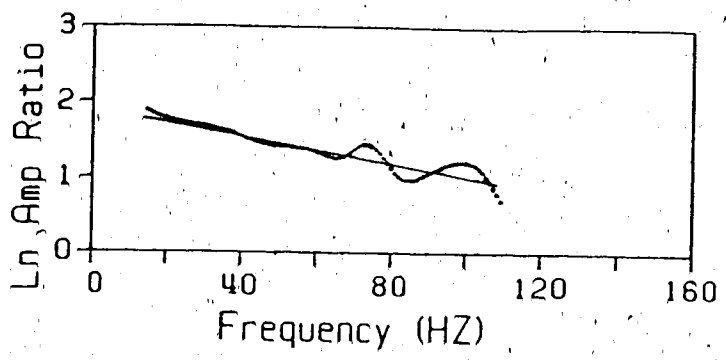
DEPTHS: 2440. - 2680. M
 MID-DEPTH: 2560.0 M
 SLOPE: -0.002982
 SLOPE STD: 0.0003781
 INT. VEL.: 4387.6
 Q-VALUE: 57.6



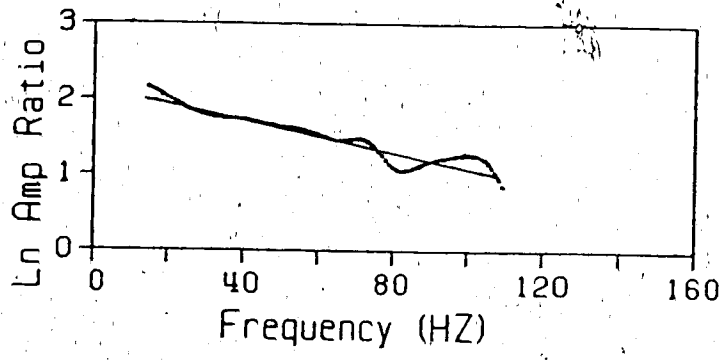
DEPTHS: 2440. - 2712. M
 MID-DEPTH: 2576.0 M
 SLOPE: -0.005419
 SLOPE STD: 0.0003500
 INT. VEL.: 4423.7
 Q-VALUE: 35.6



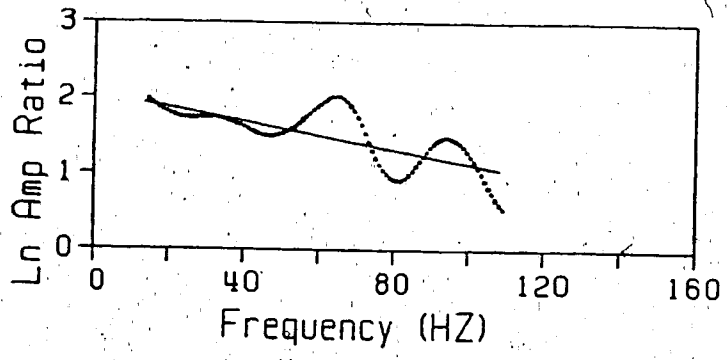
DEPTHS: 2470. - 2712. M
 MID-DEPTH: 2591.0 M
 SLOPE: -0.003022
 SLOPE STD: 0.0005178
 INT. VEL.: 4425.0
 Q-VALUE: 56.9



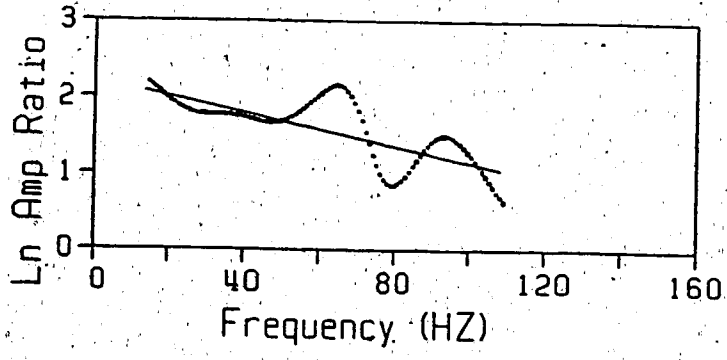
DEPTHS: 2470. - 2740. M
MID-DEPTH: 2605.0 M
SLOPE: -0.008906
SLOPE STD: 0.0003527
INT. VEL.: 4419.2
Q-VALUE: 21.6



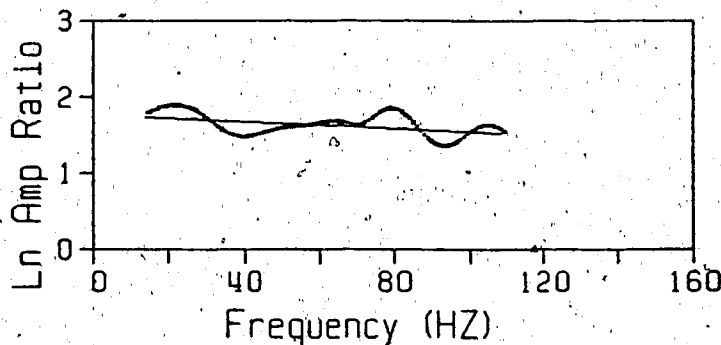
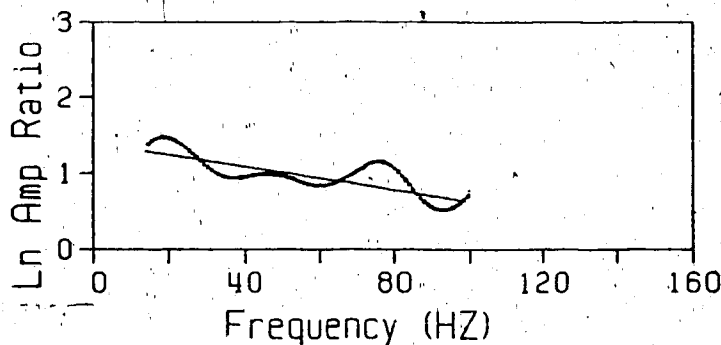
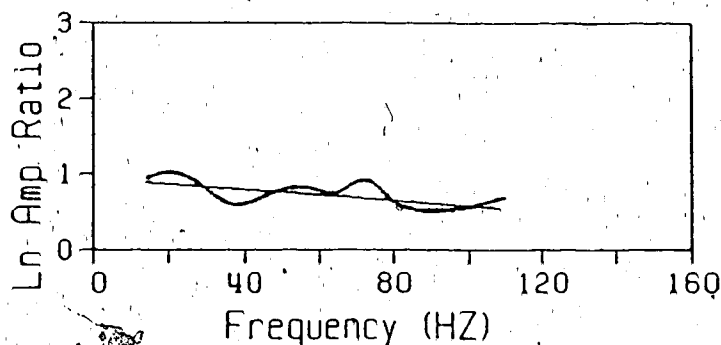
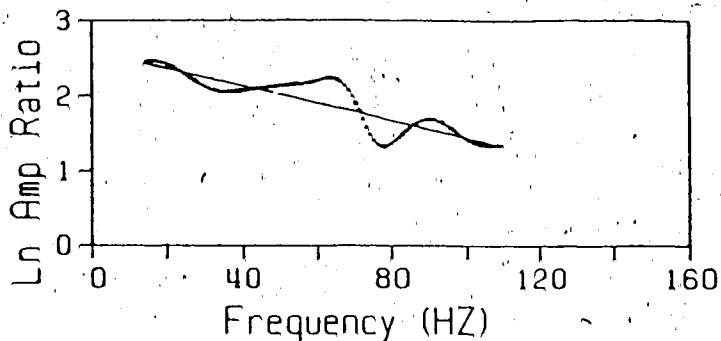
DEPTHS: 2470. - 2770. M
MID-DEPTH: 2620.0 M
SLOPE: -0.010484
SLOPE STD: 0.0003347
INT. VEL.: 4398.5
Q-VALUE: 20.4

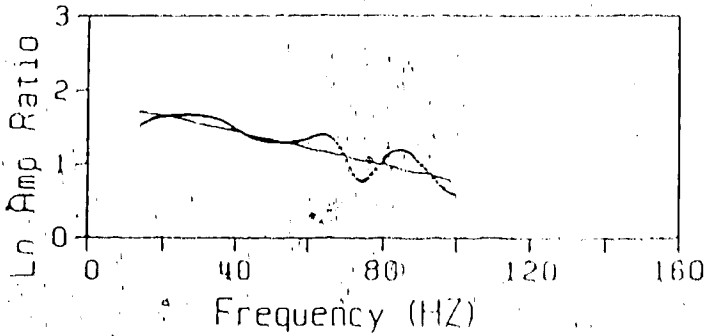


DEPTHS: 2530. - 2740. M
MID-DEPTH: 2635.0 M
SLOPE: -0.009285
SLOPE STD: 0.0009144
INT. VEL.: 4478.8
Q-VALUE: 15.9

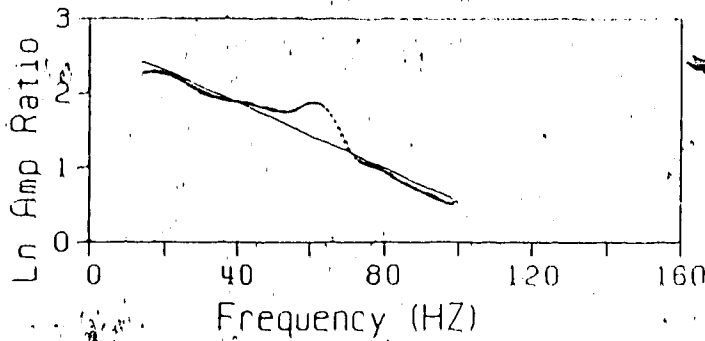


DEPTHS: 2530. - 2770. M
MID-DEPTH: 2650.0 M
SLOPE: -0.010832
SLOPE STD: 0.0010144
INT. VEL.: 4445.5
Q-VALUE: 15.7

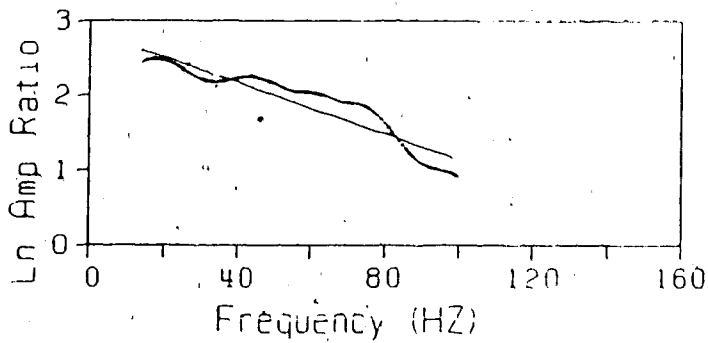




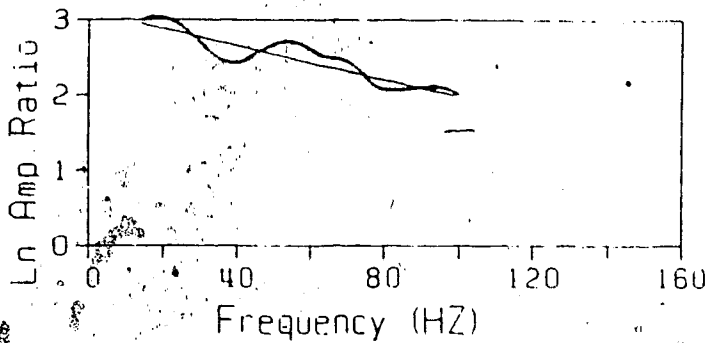
DEPTHS: 3206. - 3450. M
 MID-DEPTH: 3328.0 M
 SLOPE: -0.011013
 SLOPE STD: 0.0005684
 INT. VEL.: 3785.2
 Q-VALUE: 18.4



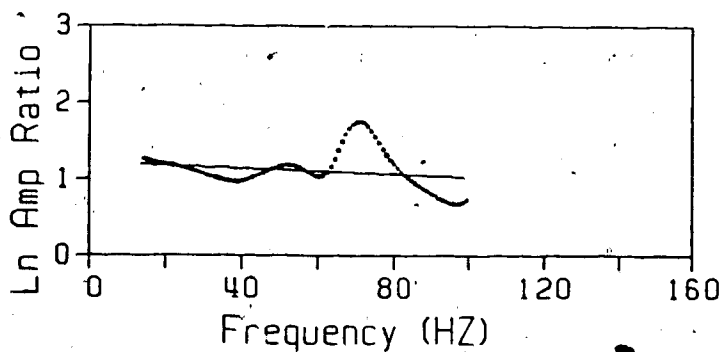
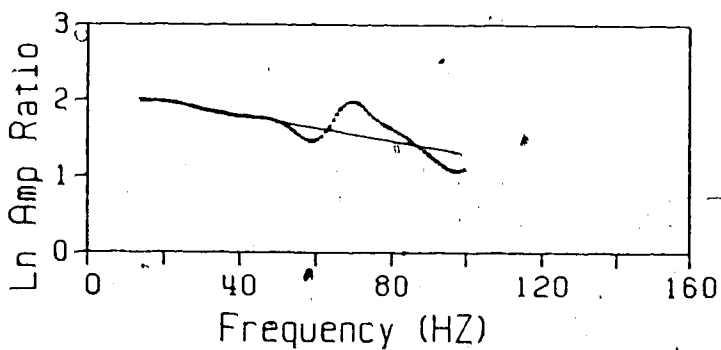
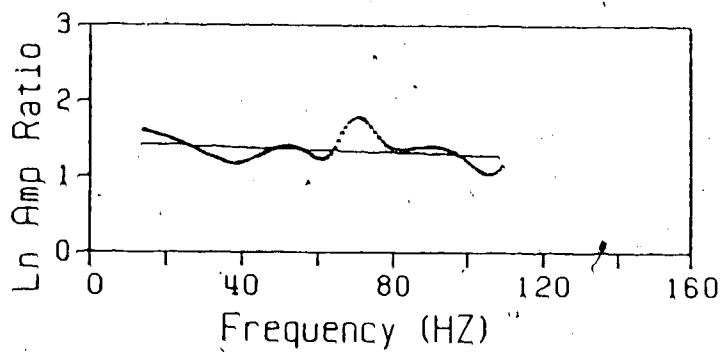
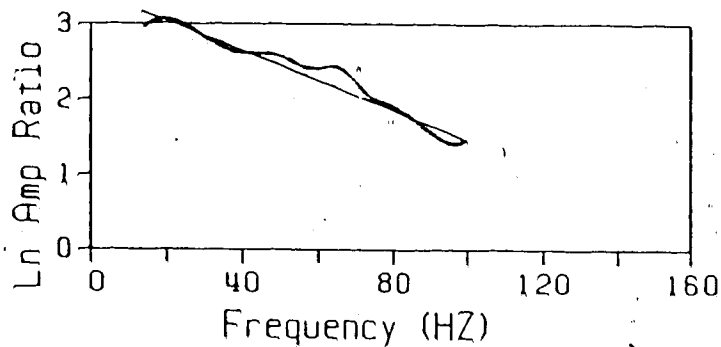
DEPTHS: 3815. - 4032. M
 MID-DEPTH: 3923.5 M
 SLOPE: -0.021794
 SLOPE STD: 0.0007235
 INT. VEL.: 4718.0
 Q-VALUE: 6.6

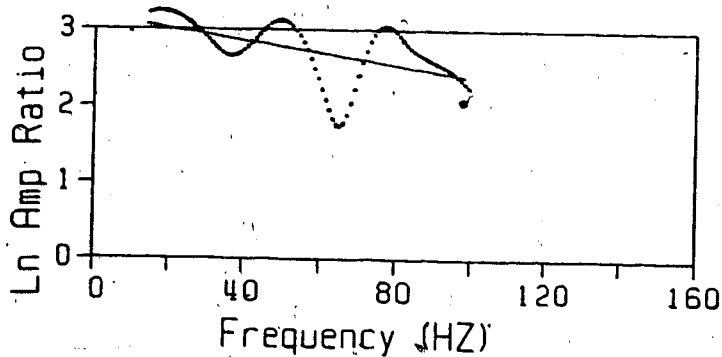
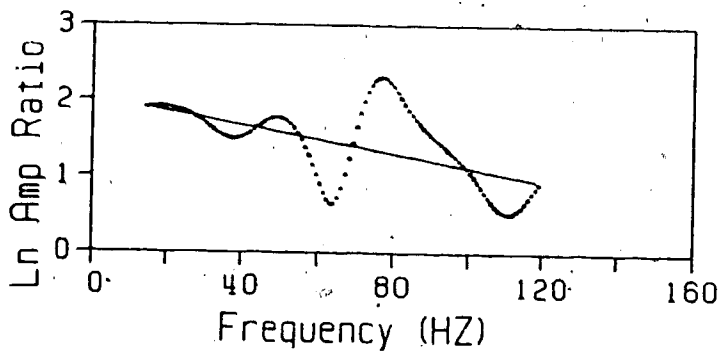
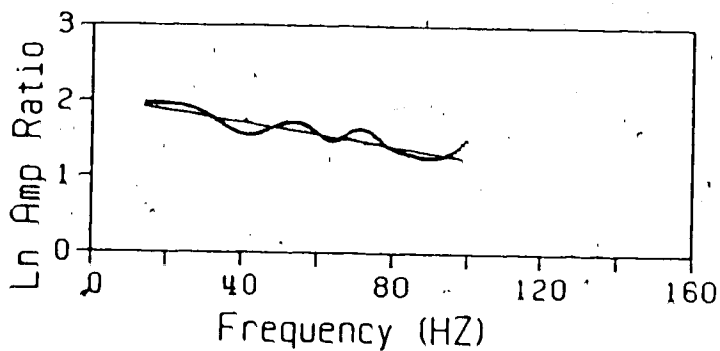
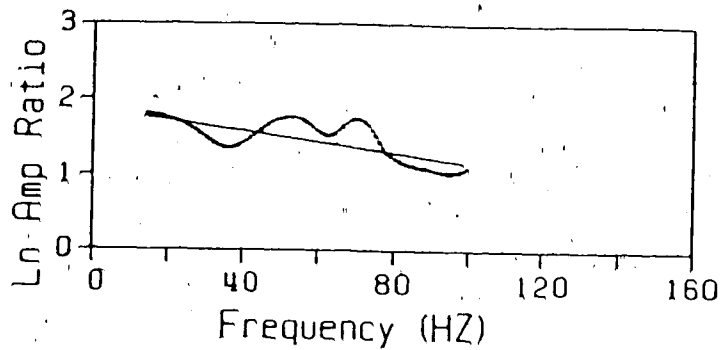


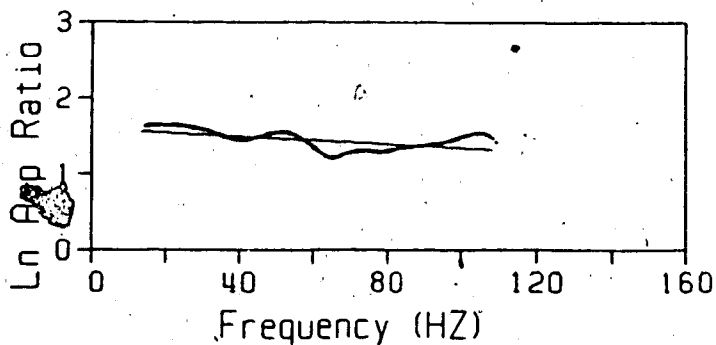
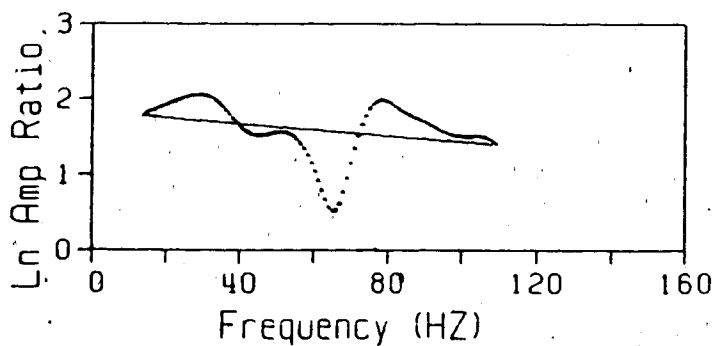
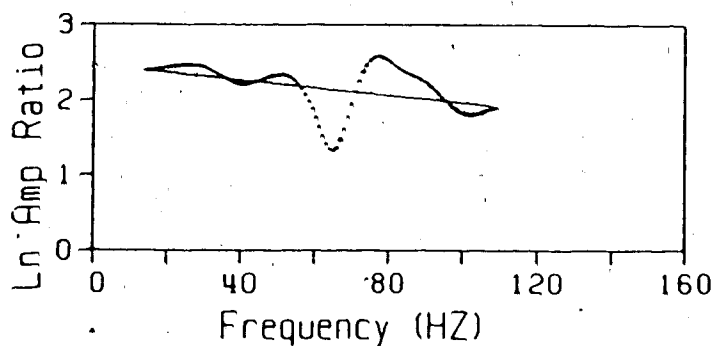
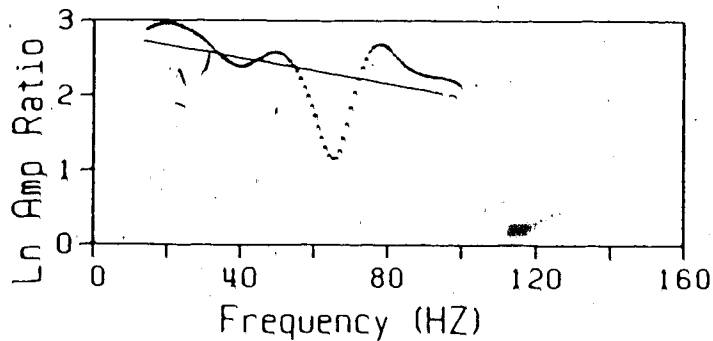
DEPTHS: 3815. - 4040. M
 MID-DEPTH: 3927.5 M
 SLOPE: -0.017108
 SLOPE STD: 0.0007242
 INT. VEL.: 4697.0
 Q-VALUE: 8.8

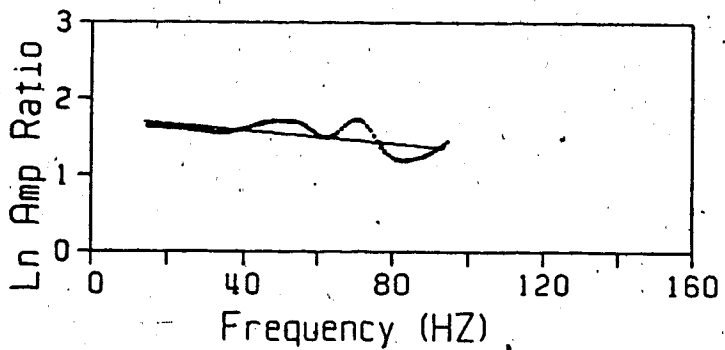
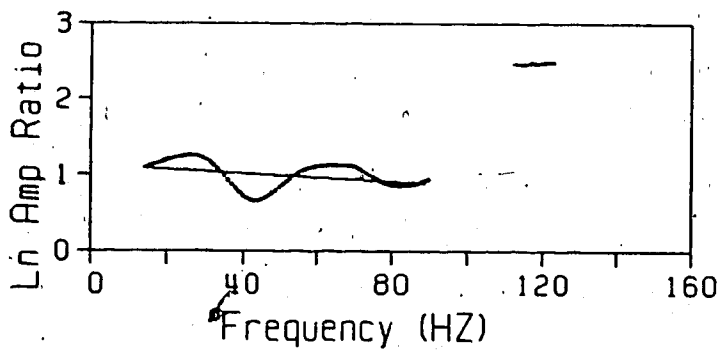
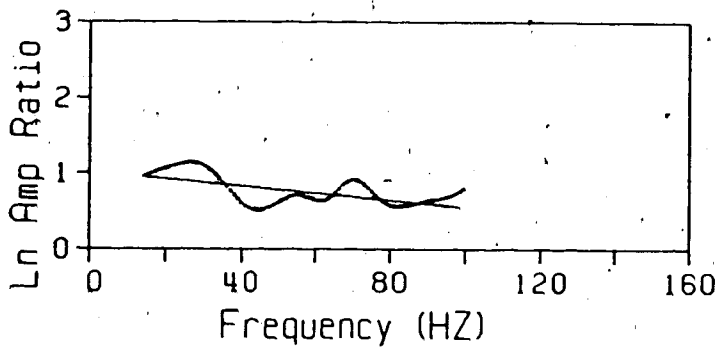
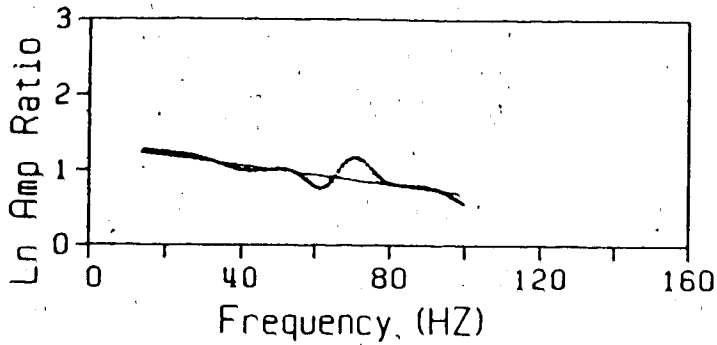


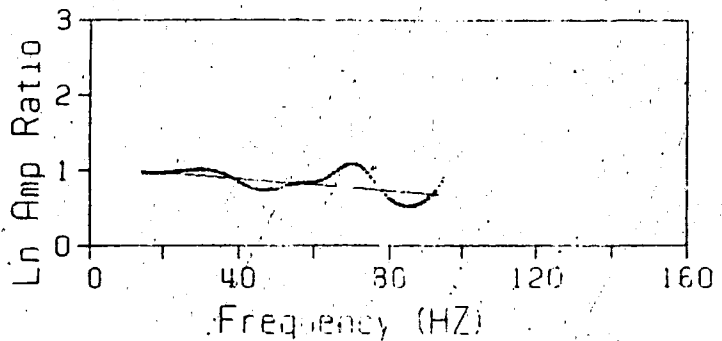
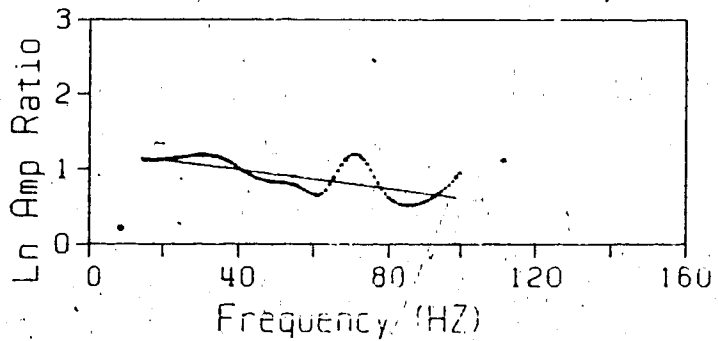
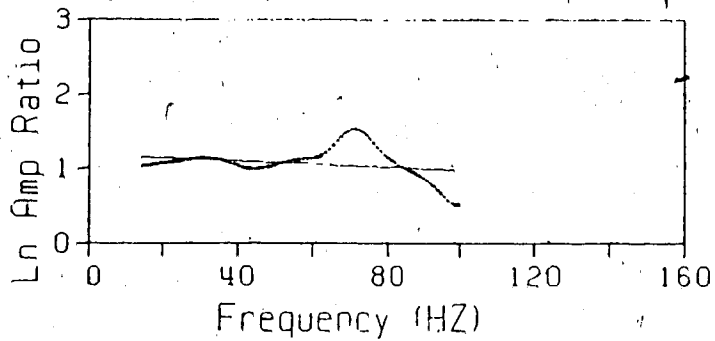
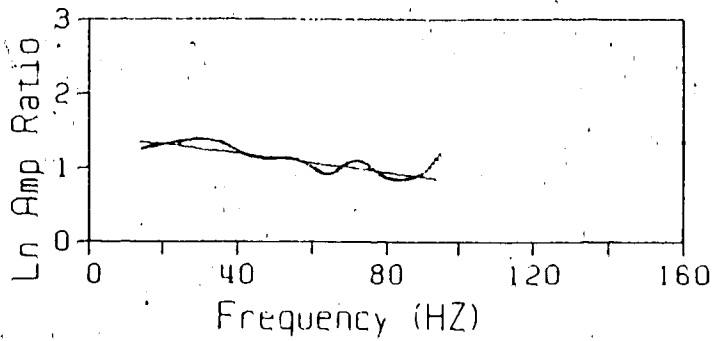
DEPTHS: 3815. - 4070. M
 MID-DEPTH: 3942.5 M
 SLOPE: -0.011262
 SLOPE STD: 0.0005608
 INT. VEL.: 4769.1
 Q-VALUE: 14.9

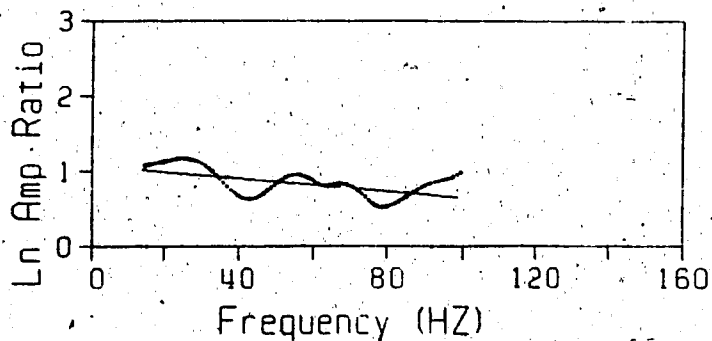
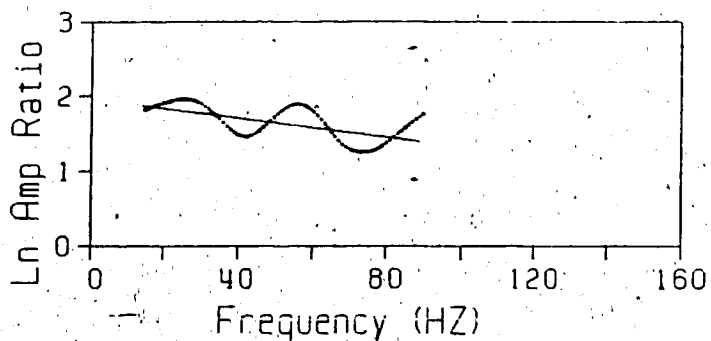
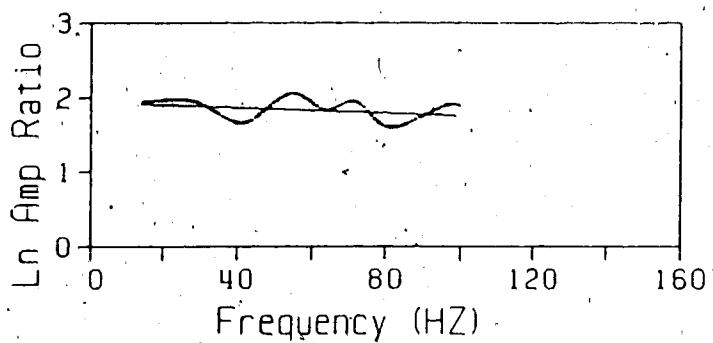
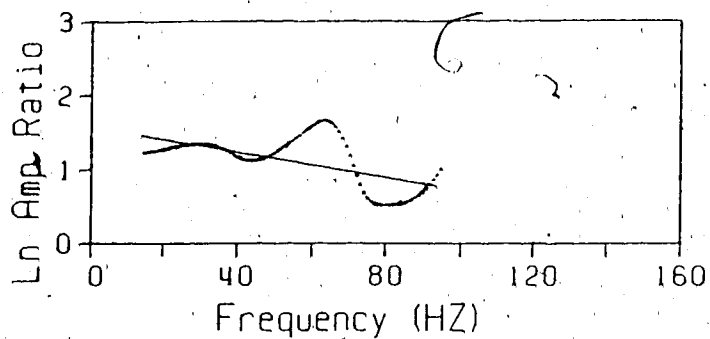


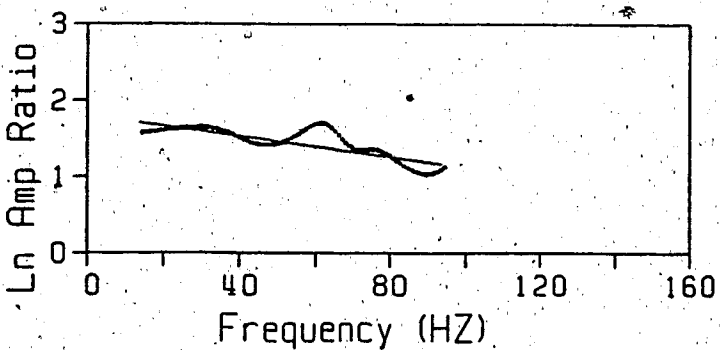
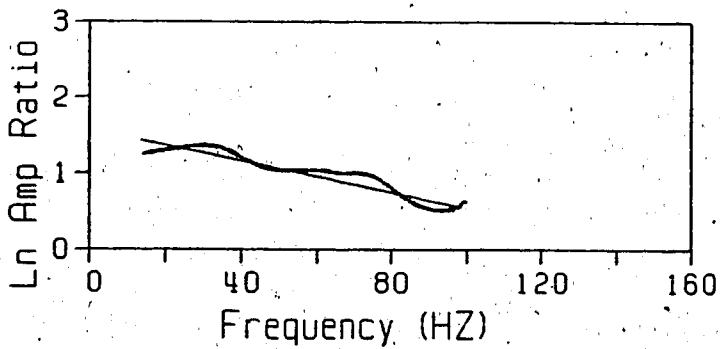
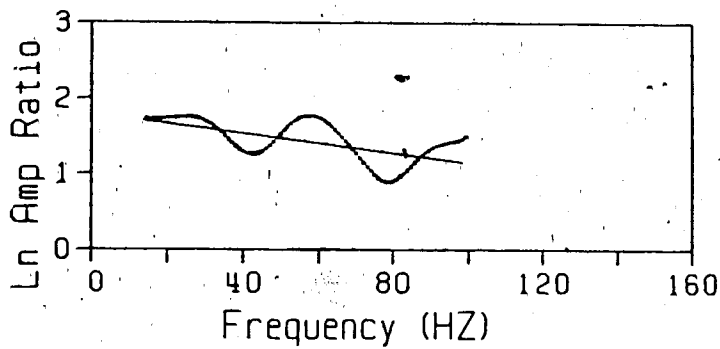
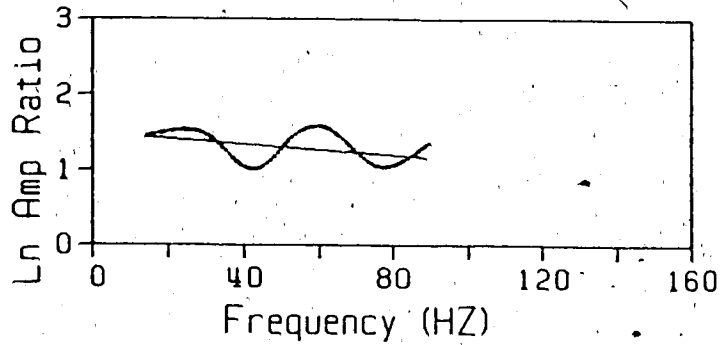


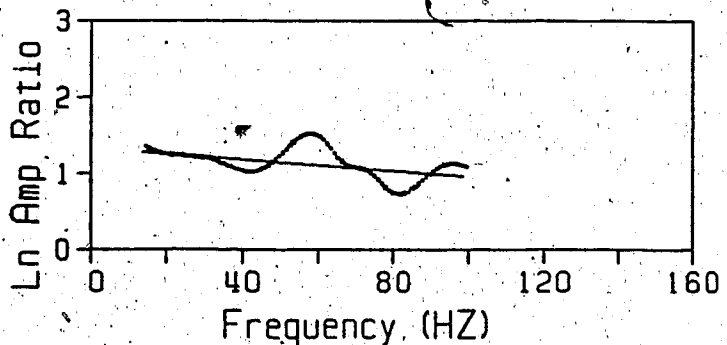
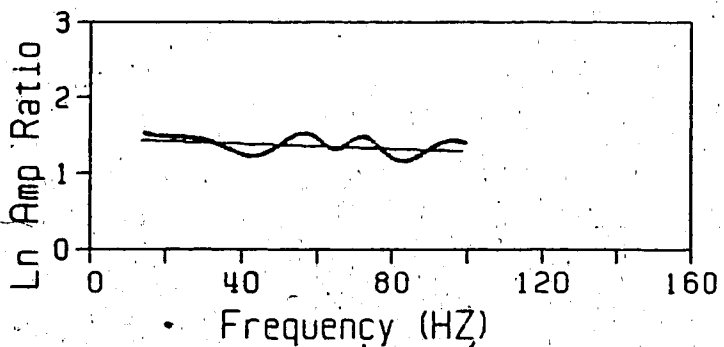
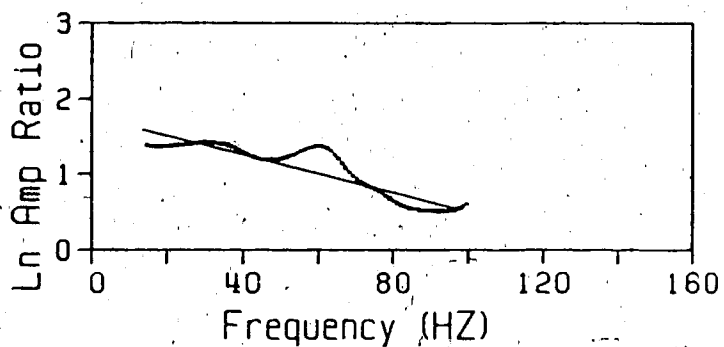
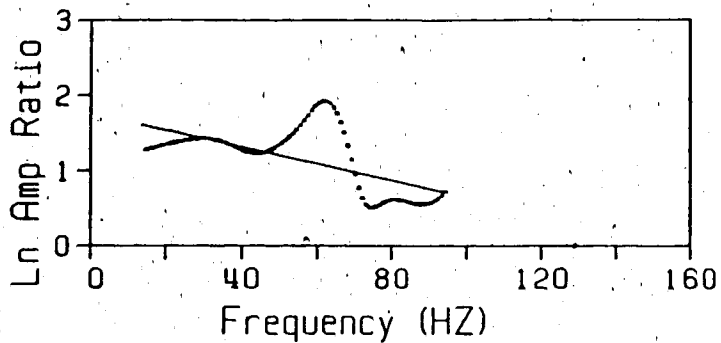


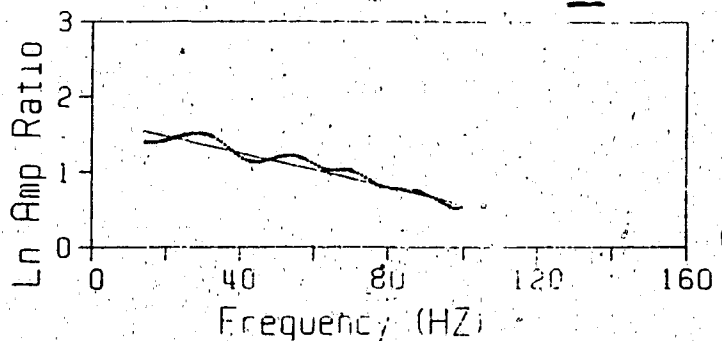
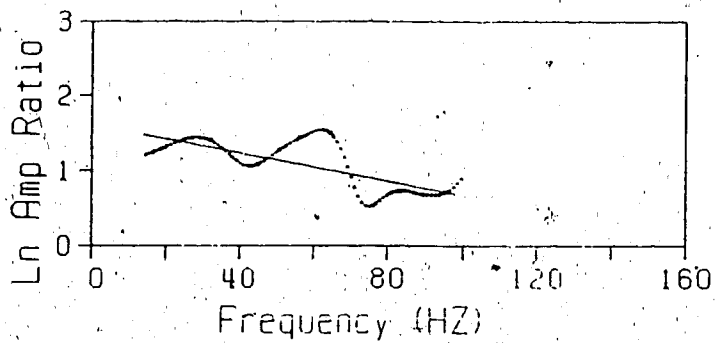
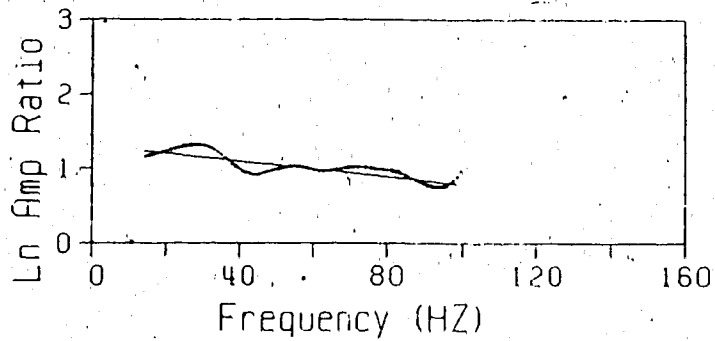
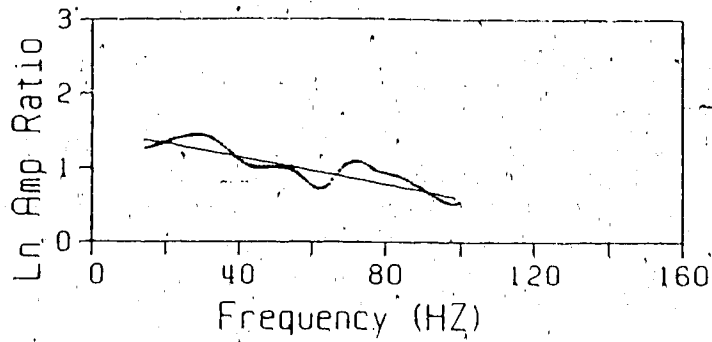


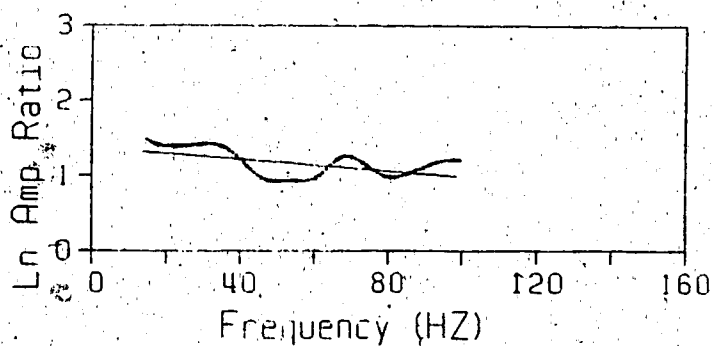
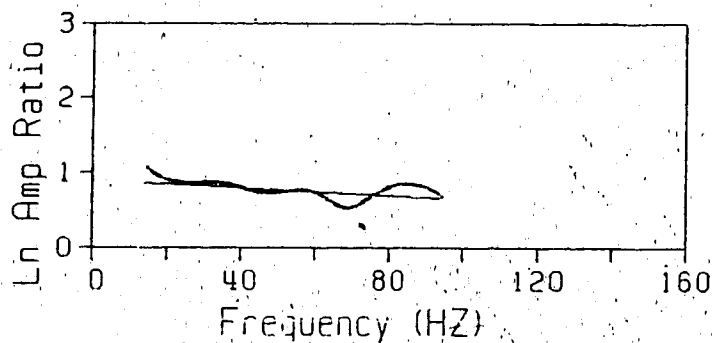
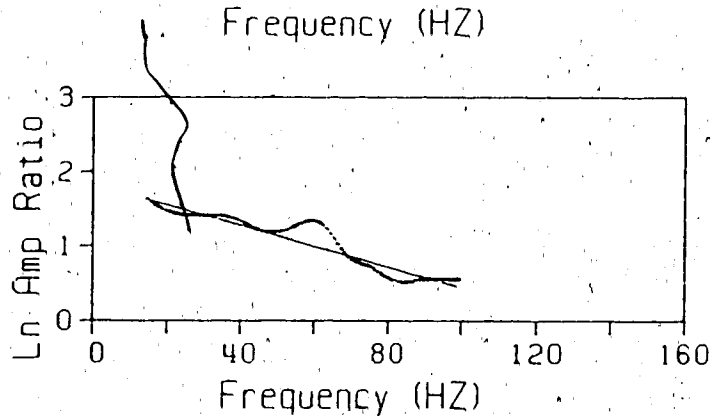
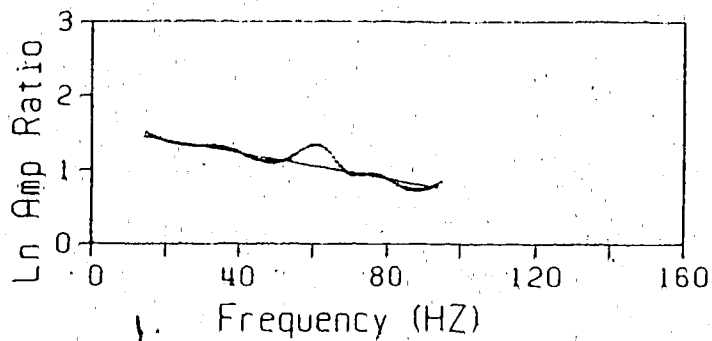


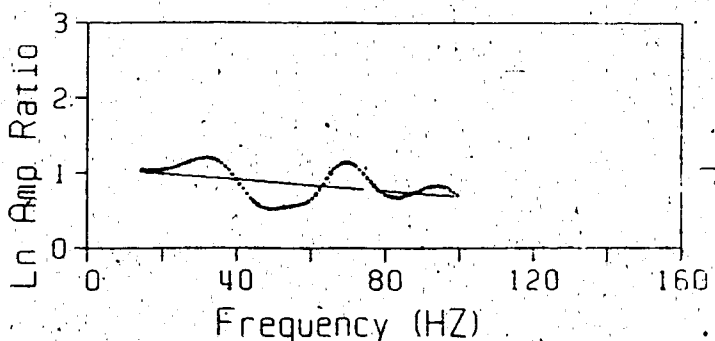
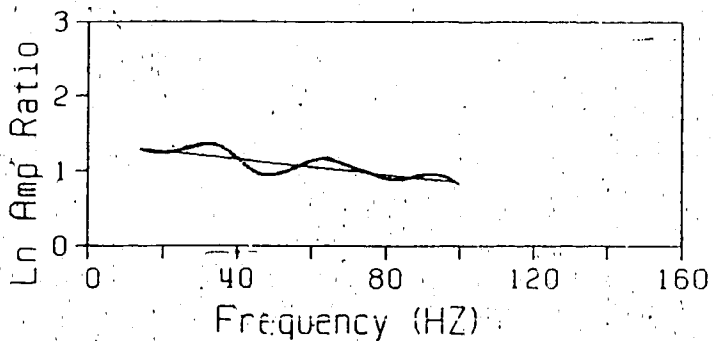
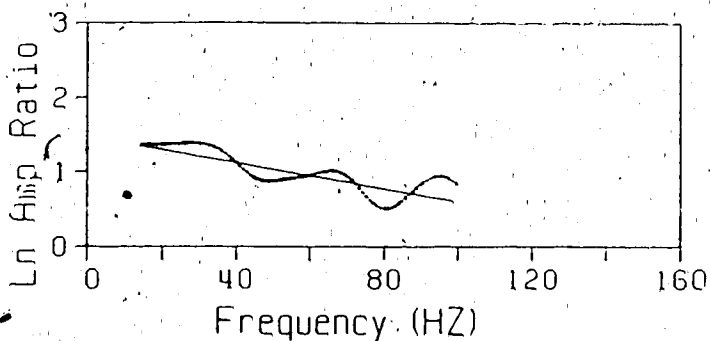
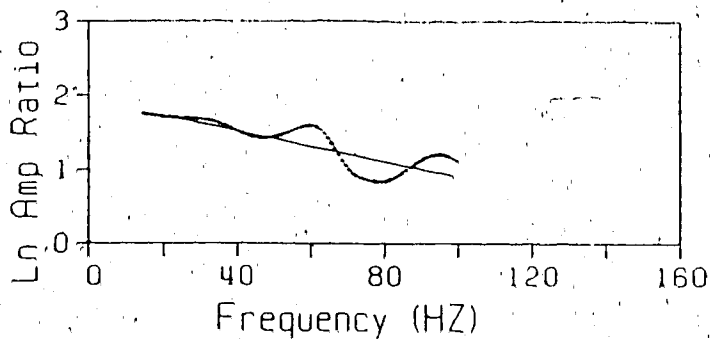


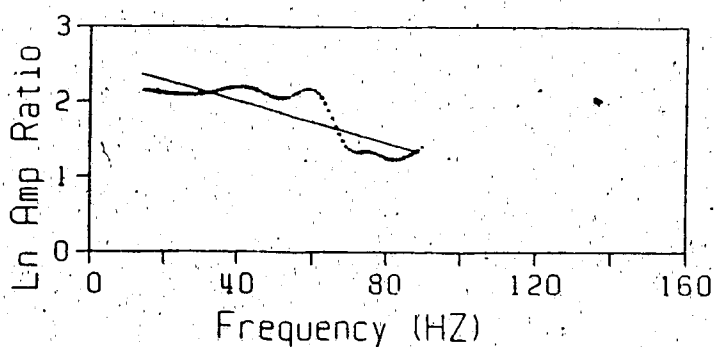
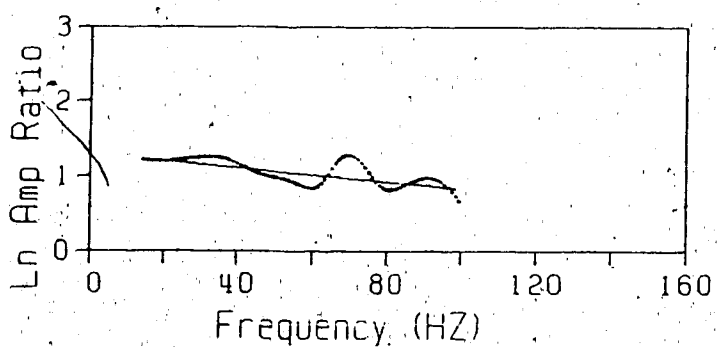
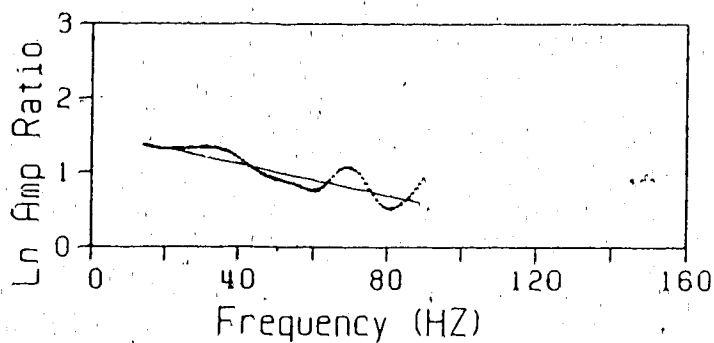
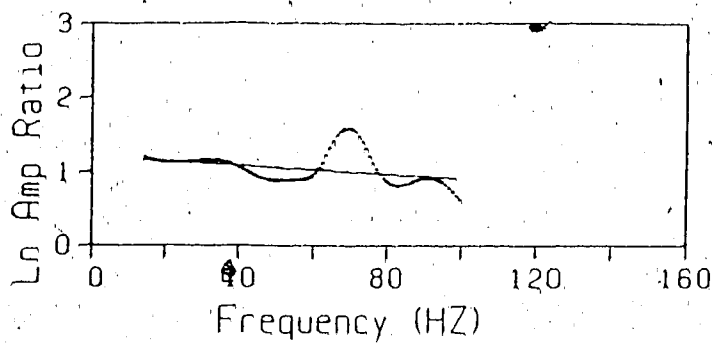


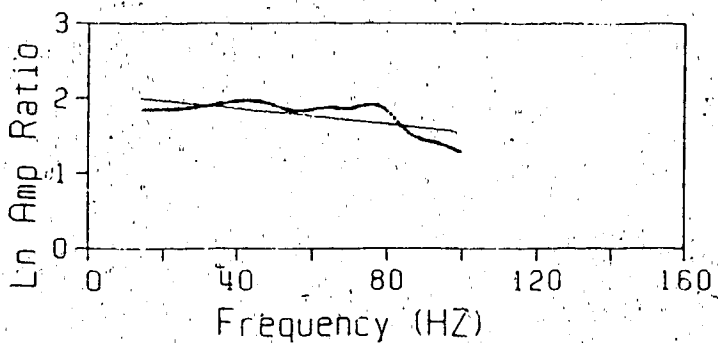
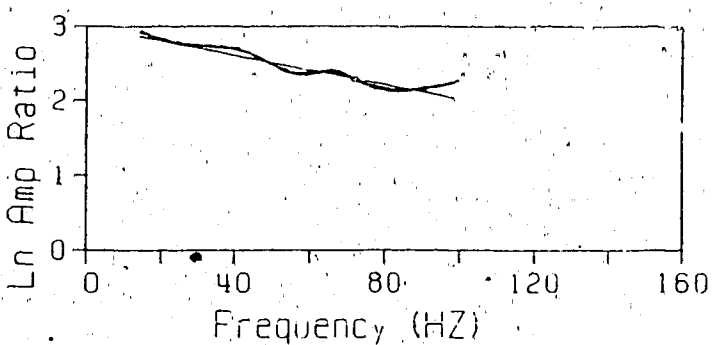
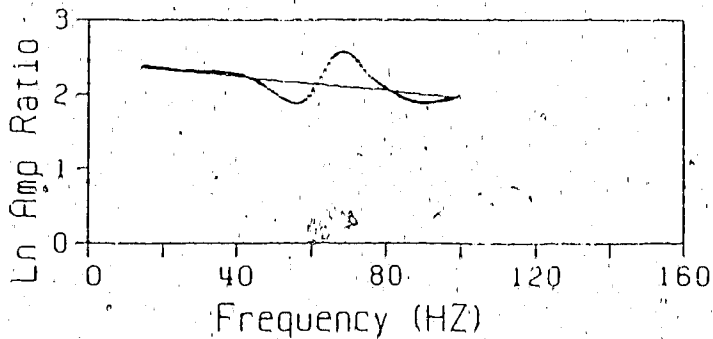
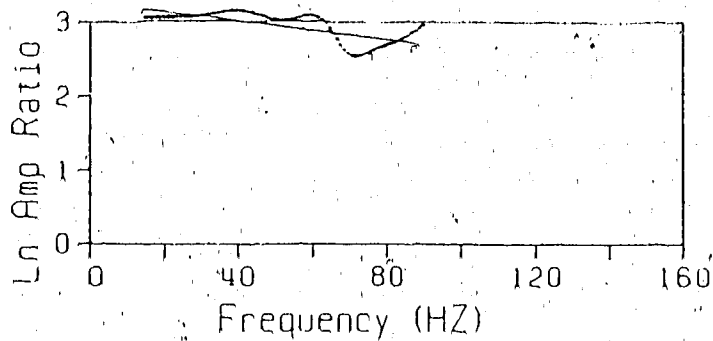


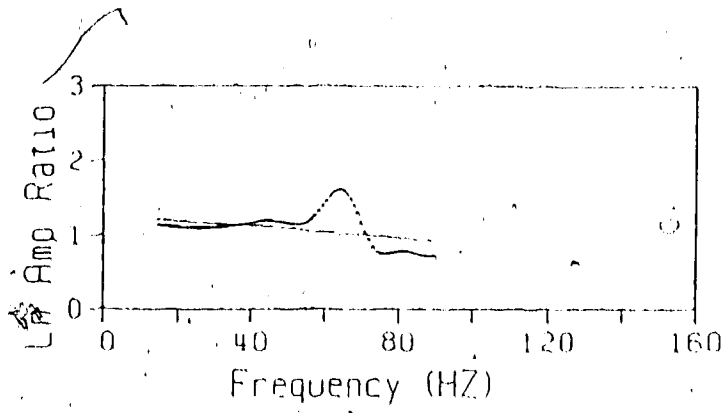












DEPTHS: 5195. - 5440. M
MID-DEPTH: 5317.5 M
SLOPE: -0.003720
SLOPE STD: 0.0011411
INT. VEL.: 6201.4
Q-VALUE: 33.4

Appendix B : Listing of Programs

```

C           PROGRAM GEN.DENSTIES
C WRITTEN BY NICK KEEHN NOVEMBER 1985.
C THIS PROGRAM GENERATES A DENSITY PROFILE
C GIVEN AN INTERVAL VELOCITY (4 DIGIT INTEGER,M/S) PROFILE
C AND A REFLECTIVITY COEFFICIENT PROFILE (REAL).
C FROM A VELOCITY OF LAYER I, A VELOCITY AND DENSITY OF
C OF LAYER I-1, AND A REFLECTIVITY COEFFICIENT OF THE
C INTERVENING LAYER, IT CALCULATES THE DENSITY OF THE
C LAYER I. IT PROCEEDS ONE LAYER AT A TIME UNTIL THE
C END OF EITHER THE VELOCITY OR THE REFLECTIVITY DATA
C RUNS OUT.
C IT ASSUMES A DENSITY FOR THE FIRST LAYER OF 1 (THIS
C CAN BE SET TO ANYTHING DESIRED)
C
C
C INPUT: FILE 1 - INTERVAL VELOCITIES EVERY ONE
C              UNIT OF TIME. ONE VALUE PER
C              RECORD IN FIRST 5 COLUMNS.
C           FILE 2 - REFLECTIVITY COEF.S FOR EACH
C              INTERFACE. ONE VALUE PER
C              RECORD IN FIRST 5 COLUMNS.
C OUTPUT:FILE 3 - RELATIVE INTERVAL DENSITIES (NO UNITS).
C              ONE VALUE PER RECORD IN FIRST 5 COLUMNS.
C
C
C           VARIABLES: RHO = RELATIVE DENSITIES
C                      R   = REFLECTIVITY COEFFICIENTS
C                      VEL = INTERVAL VELOCITIES
C
C INITIALIZE RHO1 AND VEL1
C           RHO1=1.0
C           READ(1,10,END=999) VEL1
10          FORMAT(F4.0)
C           WRITE(3,5) RHO1
5           FORMAT(F7.5)
C
C START LOOPING
100         READ(1,10,END=999) VEL2
C           READ(2,11,END=998) R
11          FORMAT(F11.0)
C           WRITE OUT VARIABLES TO THE SCREEN TO CHECK DATA
C           WRITE(20,20) VEL1,VEL2,R
C20         FORMAT(1X,F6.1,2X,F6.1,2X,F7.5)
C           RHO2 = (R*RHO1*VEL1+RHO1*VEL1)/(VEL2*(1.0-R))
C           WRITE(3,5) RHO2
C           - RESET RHO1 AND VEL1

```

```
        VEL1 = VEL2  
        RHO1 = RHO2  
GOTO 100  
998   CONTINUE  
999   CONTINUE  
C998  WRITE(20,30)  
C30   FORMAT('END OF REFLECTIVITY DATA')  
C999  WRITE(20,40)  
C40   FORMAT('END OF VELOCITY DATA')  
  
STOP  
END
```

C PROGRAM GEN.MODEL
 C WRITTEN BY NICK KEEHN NOVEMBER 1985
 C THIS PROGRAM USES THE OUTPUT FROM LOGSMOOTH2 (ITS FILE
 C #2, WHICH CONTAINS TIME DURATIONS (DURATN) AND INTERVAL
 C VELOCITIES (VELMOD), TO GENERATE AN EARTH MODEL CONTAINING
 C LAYER THICKNESSES (METERS), INTERVAL VELOCITIES (VELMOD),
 C AND INTERVAL DENSITIES (DENMOD). IT AVERAGES
 C (WEIGHTED ACCORDING TO LAYER THICKNESSES, THKLOG)
 C THE DENSITIES OF THE FULL DENSITY LOG WITHIN A DEPTH
 C INTERVAL OF THICKNESS, THKMOD.
 C INPUT FILES: FILE 1- VELOCITY MODEL FROM LOGSMOOTH2
 C (TIME DURATION AND VELOCITY MODEL)
 C 2- DENSITY LOG (FULL LOG)
 C 3- VELOCITY LOG (FULL LOG)
 C OUTPUT FILES:FILE 4- EARTHMODEL (TO BE USED BY Z1 OR Z2)
 C
 C VARIABLE LIST :
 C AGREE = DISCREPANCY BETWEEN MY MODEL
 C DEPTHS AND PANARCTIC'S
 C DEPTHS SUB K.B.
 C MY SHERARD MODEL STARTS AT THE SURFACE OF THE
 C GROUND SO MY DEPTHS ARE METERS BELOW THE SURFACE,
 C BUT PANARCTICS DEPTHS ARE METERS SUB K.B.
 C DENMOD = RELATIVE DENSITY OF A LAYER IN THE
 C MODEL (UNITLESS)
 C DENLOG = RELATIVE DENSITY OF A LAYER IN THE
 C FULL LOG (UNITLESS)
 C DENSTY = REL. DENSITY OF THE MATERIAL BETWEEN
 C THE SURFACE AND THE FIRST LAYER
 C (UNITLESS)
 C DEPTH = DEPTH FROM K.B. TO THE TOP OF A
 C LAYER IN THE MODEL (METERS)
 C DURMOD = TIME SPENT IN A LAYER IN THE MODEL
 C (TRAVELTIME, DURATION, UNITS=MSEC)
 C DURLOG = TIME SPENT IN A LAYER IN THE FULL
 C LOG (1 MSEC)
 C GRDELV = METERS TO SURFACE ABOVE DATUM
 C KBELV = METERS TO K.B. ABOVE DATUM
 C STARTD = DEPTH SUB K.B. TO FIRST LAYER
 C SUMDEN = SUM OF THE DENSITIES IN THE LOG
 C OVER THE DEPTH INTERVAL THKMOD.
 C THICK = THICKNESS OF MATERIAL BETWEEN
 C DATUM AND TOP OF FIRST LAYER
 C THKMOD = THICKNESS (DISTANCE) OF A LAYER
 C IN THE MODEL (METERS)
 C THKLOG = THICKNESS (DISTANCE) OF A LAYER
 C IN THE FULL VELOCITY LOG (METERS)
 C VEL1 = WEIGHTED AVERAGE-VELOCITY OF THE
 C MATERIAL BETWEEN THE SURFACE & THE
 C DATUM AND THE DATUM AND THE FIRST
 C LAYER (METERS/SECOND)
 C VELDAT = VELOCITY OF THE MATERIAL BETWEEN
 C THE DATUM AND THE FIRST LAYER
 C (METERS/SECOND)

```

C          VELELV = VELOCITY OF THE MATERIAL BETWEEN
C          THE DATUM AND THE SURFACE
C          (METERS/SECOND)
C          VELMOD = VELOCITY OF A LAYER IN THE MODEL
C          (METERS/SECOND)
C          VELLOG = VELOCITY OF A LAYER IN THE FULL LOG
C          (METERS/SECOND)
C INITIALIZE VARIABLES:
      GRDELV = 62.0
      KBELV  = 72.0
      STARTD = 399.9
      VELDAT = 2253.0
      VELELV = 2300.0
      DURLOG = .001

C INITIAL CALCULATIONS
      AGREE = KBELV - GRDELV
      THICK = STARTD - KBELV
      VEL1  = (GRDELV*VELELV + THICK*VELDAT)/(GRDELV+THICK)
      VELMOD = VEL1
      THKMOD = GRDELV + THICK
      DENSTY = 1.0
      DENMOD = DENSTY

C          DUE TO RESTRICTIONS PLACED BY Z1
C          VELMOD MUST BE CONVERTED TO AN INTEGER
C          (IE. THERE IS NOT ENOUGH SPACE FOR THE
C          DECIMAL POINT)
      IVELMD = INT(VELMOD+.5)
      DEPTH  = THKMOD
      TFSTAR = THKMOD/FLOAT(IVELMD)
      IF (THKMOD.GE.100.0) WRITE(4,128) THKMOD,IVELMD,
&                                     DENMOD,DEPTH,TFSTAR
      IF ((THKMOD.GE.10.0).AND.(THKMOD.LT.100.0))
&       WRITE(4,129) THKMOD,IVELMD,DENMOD,DEPTH,TFSTAR
      IF (THKMOD.LT.10.0) WRITE(4,130) THKMOD,IVELMD,
&                                     DENMOD,DEPTH,TFSTAR
128  FORMAT(5X,F5.1,15,F5.2,5X,F6.1,5X,F6.4)
129  FORMAT(5X,F5.2,15,F5.2,5X,F6.1,5X,F6.4)
130  FORMAT(5X,F5.3,15,F5.2,5X,F6.1,5X,F6.4)

C START LOOPING THROUGH THE DATA:
1000 READ(1,100,END=999) DURMOD,VELMOD
100   FORMAT(F5.0,1X,F6.0)
      THKMOD = DURMOD*VELMOD*.001
      IDUR   = INT(DURMOD)
      SUMDEN = 0.0
      DO 10 I=1,IDUR
          READ(2,110) DENLOG
110   FORMAT(F7.0)
          READ(3,120) VELLOG
120   FORMAT(F4.0)
      THKLOG = VELLOG*DURLOG

```

```

          SUMDEN = SUMDEN + DENLOG*THKLOG
10      CONTINUE
C      THKMOD IS THE SUM OF THE THKLOG'S FOR A LAYER
C      IN THE MODEL
          DENMOD = SUMDEN/THKMOD
          DEPTH = THKMOD + DEPTH

C      WRITE OUT THE RESULTS FOR THE LAYER OF THE MODEL
C      JUST ANALYSED.
C      DUE TO RESTRICTIONS PLACED BY Z1
C      VELMOD MUST BE CONVERTED TO AN INTEGER
C      (IE. THERE IS NOT ENOUGH SPACE FOR THE
C      DECIMAL POINT)

          IVELMD = INT(VELMOD+.5)
          TFSTAR = TFSTAR + THKMOD/FLOAT(IVELMD)

C      ERROR CONDITION FOR IVELMD THERE IS NO ROOM FOR
C      NUMBERS GREATER THAN 4 DIGITS
          IF (IVELMD.GT.9999) GO TO 990
          IF (THKMOD.GE.100.0) WRITE(4,128) THKMOD,IVELMD,
&                                         DENMOD,DEPTH,TFSTAR
          IF ((THKMOD.GE.10.0).AND.(THKMOD.LT.100.0))
&             WRITE(4,129) THKMOD,IVELMD,DENMOD,DEPTH,TFSTAR
          IF (THKMOD.LT.10.0) WRITE(4,130) THKMOD,IVELMD,
&                                         DENMOD,DEPTH,TFSTAR

          GO TO 1000
990     WRITE(4,18) 'ERROR: VELOCITY BECAME UNREASONABLE'
18      FORMAT(A35)
          STOP

C      LAST LINE OF MODEL DATA MUST HAVE A THICKNESS OF 99999
C      METERS FOR THE PROGRAMS Z1 AND Z2 WRITTEN BY DAVE GANLEY.
999     WRITE(4,131) 99999,IVELMD,DENMOD
131     FORMAT(5X,15,15,F5.2)

C      WRITE(4,151) 'KB IS ',AGREE,' METERS ABOVE THE SURFACE'
C151    FORMAT(A6,F4.1,A25)

          STOP
          END

```



```

C          PROGRAM INVQ.RUN.WTA
C WRITTEN BY NICK KEEHN 1986.
C THIS PROGRAM CALCULATES A WEIGHTED RUNNING AVERAGE
C OF Q DATA. THREE WEIGHTS ARE ALLOWED FOR:
C          1.  1/RESIDUAL*1/(STD OF SLOPE OF LOG OF
C              RATIO PLOT)
C          2.  1/(STD OF SLOPE ONLY)
C          3.  NO WIGHTING IE. WEIGHT = 1

```

```

DIMENSION DEPTH(200),INVQ(200),SLSTD(200),RES(200)
DIMENSION Q(200),IHOLD(200)
DIMENSION WT(200),WTEDIQ(200)
CHARACTER*50 TITLE
REAL INVQ
WLEN = 200.0

```

```
I=1
```

```

C READ IN THE ENTIRE SET OF DATA
  READ(1,34) TITLE
  WRITE(2,34) TITLE
 34  FORMAT(A50)
100  READ (1,*,END=999) DEPTH(I), Q(I), SLSTD(I)
      INVQ(I)=1.0/Q(I)
      I=I+1
      GOTO 100

999  CONTINUE

```

```

C PERFORM THE RUNNING AVERAGE
  NDEPTH = I-1

```

```

DO 300 J=1,NDEPTH
  SUMWTQ = 0.0
  SUMSTD = 0.0
  SUMWTS = 0.0
  II = 0
  SUMDEP = 0.0
  SUMIQ = 0.0
  P = 0.0
  DO 200 I=1,NDEPTH
    IF(DEPTH(I).LT.(DEPTH(J)-WLEN/2.0)) GOTO 250
    IF(DEPTH(I).GT.(DEPTH(J)+WLEN/2.0)) GOTO 250
    II = II + 1
    IHOLD(II) = I
    P = P+1.0
    SUMDEP = SUMDEP + DEPTH(I)
    SUMIQ = SUMIQ + INVQ(I)
 250  CONTINUE
200  CONTINUE

  IP = INT(P)
  AVEDEP = SUMDEP/P
  AVEIQ = SUMIQ/P

```

```
DO 600 L=1,IP
RES(L) = ABS(AVEIQ - INVQ(IHOLD(L)))
C      WT(L) = 1.0/RES(L) * 1.0/SLSTD(IHOLD(L))
C      WT(L) = 1.0/SLSTD(IHOLD(L))
      WT(L) = 1.0
      WTEDIQ(L) = INVQ(IHOLD(L)) * WT(L)
      SUMWTQ = SUMWTQ + WTEDIQ(L)
      SUMWTS = SUMWTS + WT(L)
600   CONTINUE
      AVEWTQ = SUMWTQ/SUMWTS
      WRITE(2,400) DEPTH(J), AVEWTQ
300   CONTINUE
400   FORMAT(F6.1,5X,F6.5)

STOP
END
```

C PROGRAM PLOT.LOG
 C WRITTEN BY NICK KEEHN NOVEMBER 1985,
 C THIS PROGRAM PRODUCES A LOG PLOT GIVEN THE THICKNESSES OR
 C DURATIONS OF EACH LAYER (ANY NUMBER OF LAYERS) AND ITS
 C CORRESPONDING LOG VALUE.
 C NOTE: EVERY LAYER WILL ALWAYS BE PRESENT REGARDLESS OF
 C VERTICAL SCALE OR HORIZONTAL SCALE USED. THE MORE
 C CONDENSED THE PLOT THE MORE THE THICKER LAYERS ARE
 C CONDENSED. IN THE EXTREME ALL LAYERS WILL APPEAR
 C TO BE THE SAME THICKNESS.

C INPUT FILES : FILE 1-CONTAINES THICKNESSES AND
 C LOG VALUES WITH 1 PAIR PER
 C RECORD. (FREE FORMATED)
 C OUTPUT FILES: FILE 2-CONTAINES A DEPTH (OR TIME)
 C VS LOG-VALUE (INTERVAL VELOCITY)
 C LINE PRINTER PROFILE.
 C 7-CONTAINES A VELOCITY PROFILE
 C SUITABLE FOR AN ESPP VERSION
 C OF FILE #2 (FORMATED DATA 10F12.1)

C VERSCL = VERTICAL (TIME OR DEPTH) SCALING FACTOR
 C (=1 FOR NO CONTRACTION)
 C LATSCL = LATERAL (INTERVAL VELOCITY) SCALING FACTOR
 C (=1 FOR NO CONTRACTION)
 C VUNITS = UNITS OF THE VERTICAL AXIS (MSEC, METERS ETC.)
 C VORGIN = STARTING VALUE OF VUNITS
 C HUNITS = UNITS OF THE HORIZONTAL AXIS (METERS/SEC ETC.)
 C OPTION = 2 ==> LINE PRINTER PLOT
 C 1 ==> ESP PLOT

DIMENSION PLOT(6000)
 REAL LOGVAL,VERSCL,VORGIN
 INTEGER LATSCL,OPTION
 CHARACTER*1 STRING(1:100),TITLE*60,VUNITS*6
 CHARACTER*1 HUNITS*10
 CHARACTER*100 JUNK1
 CHARACTER DOT
 DATA (STRING(I),I=1,100)/100*' '/
 DATA (PLOT(II),II=1,6000)/6000*0/
 DUMMY = 0.0

C READ ONE LINE OF TITLE FROM EARTH.MODEL AND THROW AWAY
 READ(1,8) JUNK1
 8 FORMAT(A100)

C SET UP TITLES AND RUN PARAMETERS
 TITLE = 'SHERARD: FILTER= , %CHANGE= %, IDC=
 C VERSCL = .01 WORKS WELL FOR LINE PRINTER PLOTS BUT = 1.0
 C SHOULD BE USED FOR ESP PLOTS TO GET FULL RESOLUTION,
 C THE ACTUAL SIZE OF THE PLOT CAN BE CHANGED WITH
 C ESPP COMMANDS
 C HOFSET = HORIZONTAL OFFSET OF THE ESPP PROFILE.
 C THIS JUST SUBTRACTS OFF ##### METERS/SECOND

C FROM EACH INTERVAL VELOCITY SO IT LOOKS BETTER
C

```

OPTION = 1
HOFSET = 0000.
VERSCL = 1.0
IF (OPTION.EQ.1) VERSCL = 1.00
LATSCL = 1
VORGIN = 0.0
VUNITS = 'METERS'
HUNITS = 'M/S'
IF (OPTION.EQ.1) GOTO 432
WRITE(2,6) 'VERT SCALE: ',VERSCL,'HORIZ SCALE: ',
& LATSCL,TITLE
6  FORMAT(A12,F4.2,3X,A13,I1,5X,A60)
WRITE(2,7) VUNITS,HUNITS.
7  FORMAT(A6,3X,A10)

432 CONTINUE

```

C INITIALIZE VARIABLES

```

DOT = '.'
COUNT = 0.0 + VORGIN
II=0

```

C START LOOPING DOWN THE HOLE

```

5  READ(1,*,END=999) THKNS,LOGVAL
   IF (THKNS.EQ.99999.0) GOTO 999
   ITHKNS = INT(THKNS*VERSCL+0.5)
   IF ((THKNS*VERSCL).LT.0.5) ITHKNS=1.
   NBLANK = INT(LOGVAL/100.0+0.5)
   NBLANK = LATSCL*NBLANK-20
   IF (OPTION.EQ.2) STRING(NBLANK)='|'

```

C PRINTOUT A LAYER OF THE EARTH

```

DUMMY = DUMMY+THKNS
DO 100 I=1,ITHKNS
C   COUNT=COUNT+1.0
C   DUMMY=DUMMY+THKNS
C   II = II+1
   PLOT(II) = LOGVAL - HOFSET
   IF ((OPTION.EQ.2).AND.(I.NE.ITHKNS))
&   WRITE(2,11) LOGVAL,DOT,(STRING(J),J=1,100)
   IF ((OPTION.EQ.2).AND.(I.EQ.ITHKNS))
&   WRITE(2,10) DUMMY,LOGVAL,DOT,(STRING(J),J=1,100)
11  FORMAT(10X,F6.1,4X,A1,100A1)
10  FORMAT(F7.1,3X,F6.1,4X,A1,100A1)
100 CONTINUE

```

```

   IF (OPTION.EQ.2) STRING(NBLANK)='|'
   --GOTO 5
999 CONTINUE
IF (OPTION.EQ.1) WRITE (3,337)

```

```
      &      '# POINTS IN ESPP LOG = ', II  
337  FORMAT (A38,I4)  
      IF (OPTION.EQ.1) WRITE (7,447) (PLOT(I),I=1,II)  
447  FORMAT(254F8.0,254F8.0,254F8.0,254F8.0,  
$      254F8.0,254F8.0,254F8.0,254F8.0,  
$      254F8.0,254F8.0,254F8.0,254F8.0,  
$      254F8.0,254F8.0,254F8.0,254F8.0)  
      STOP  
      END
```

```

C          PROGRAM SONIC2.PGRM
C WRITTEN BY NICK KEEHN (FORTRAN77)
C DATE: AUG 1985
C   ATSD      ADJUSTED TIME SUB DATUM (SECONDS)
C   AVEVEL    AVERAGE VELOCITY (M/S)
C   DSKB      DEPTH SUB K.B. (METERS)      FILE 1
C   INTVL1    INTERVAL VEL. OF A DEPTH INTERVAL
C   INTVL2    INTERVAL VEL. OF LAYER BELOW THE LAYER
C             ASSOCIATED WITH INTVL1
C   KBEL      K.B. ELEVATION (METERS)
C   RCOEF     REFLECTION COEFFICIENT
C   UNAIT     UNADJUSTED INTEGRATED TIME (SECONDS)
C
C           SONIC2.PGRM >> FORTRAN77 PROGRAM
C   FILE 1    SONIC2.INPUT >> INPUT DATA: KBEL,DSKB,ATSD
C             >> INTERVAL VELOCITIES
C   FILE 9    SONIC2.OUT >> OUTPUT FILE
C
C   REAL ATSD,DSKB,KBEL,UNAIT,RCOEF,DT
C   REAL INTVL1,INTVL2,AVEVEL
C   INTEGER COUNT
C
C START PROGRAM WITH INITIAL VALUES
COUNT = 0
DT = .001
READ(1,*,END=9999) KBEL,DSKB,ATSD
UNAIT = 0.0
AVEVEL = (DSKB - KBEL) / ATSD
READ(2,*,END=9999) RHO1
READ(1,*,END=9999) INTVL1
COUNT = COUNT+1
C
C SET UP OUTPUT FILE TITLE LINES(FILE 9)
WRITE(9,1010) 'KBel = ',KBEL,'meters'
1010 FORMAT(A7,F5.0,A8)
WRITE(9,*) ' '
WRITE(9,1011) 'Depth','Adj.','Unadj.','Avge.',
&'Int.','Refl.'
1011 FORMAT(A6,2X,A6,2X,A6,2X,A6,2X,A6,2X,A6)
WRITE(9,1011) 'Sub','Time','Integ.','Vel.',
&'Vel.','Coef.'
WRITE(9,1011) 'K.B.','Sub','Time','(m/s)',
&'(m/s)','approx'
WRITE(9,1011) '(m)','Datum'
WRITE(9,*) ' '
WRITE(9,*) ' '
C
C WRITE OUT THE INITIAL VALUES
WRITE(9,1020) DSKB,ATSD,UNAIT,INT(AVEVEL)
1020 FORMAT (F6.1,2X,F6.4,2X,F6.4,2X,I6,10X,F7.5)

```

```

C START LOOPING THROUGH THE DATA
5000   DSKB = DSKB + INTVL1*DT
      ATSD = ATSD + DT
      UNAIT = 0.0
      AVEVEL = (DSKB - KBEL) / ATSD
      READ(2,*,END=9000) RHO2
      READ(1,*,END=9000) INTVL2
      COUNT = COUNT+1
      RCOEF = (RHO2*INTVL2 - RHO1*INTVL1) /
&         (RHO2*INTVL2 + RHO1*INTVL1)

      WRITE(9,1030) INT(INTVL1)
1030   FORMAT(32X,I6)
      WRITE(9,1020) DSKB,ATSD,UNAIT,INT(AVEVEL),RCOEF

      INTVL1 = INTVL2
      RHO1   = RHO2

      GO TO 5000

9000   WRITE(9,1040)'TOTAL # OF INTERVAL VELOCITIES READ = ',
&         COUNT
1040   FORMAT(A40,I4)
      GO TO 10000
9999   WRITE(9,*)'THERE IS NO INTERVAL VELOCITY DATA PRESENT'

10000  CONTINUE
      STOP
      END

```

```

C          PROGRAM SPECTRL.ANAL
C  WRITTEN BY NICK KEEHN (1986).
C  RECNUM = RECORD NUMBER TO BE ANALYSED
C  ILAHZ  = CALCULATE THE SPECTRUM FOR THE FIRST ILAHZ HZ
C  IWSTRT = WINDOW START, IN # OF DATA POINTS (NOT MSECS)
C  IWLEN  = WINDOW LENGTH, IN # OF DATA POINTS (NOT MSECS)
C  ZROPAD = PAD THE WINDOW AT THE END WITH ZEROS
C          THIS MUST BE A POWER OF 2, SO THAT THE TOTAL
C          NUMBER OF POINTS IN THE SERIES IS ZROPAD
C  IMAG   = THE IMAGINARY PART OF THE FOURIER SPECTRUM.
C  B      = INPUT RECORD, B(1) AND B(2) ARE HEADER
C          INFORMATION
C  NPTS   = NUMBER OF DATA POINTS IN RECORD INCLUDING HEADER
C          THE ENTIRE NPTS DATA POINTS IS READ IN. THE
C          HEADER IS SKIPPED AND THE SPECIFIC WINDOW POINTS
C          IS ASSIGNED TO TRACE(I).
C          THE TRACE(I) IS THEN INCREASED IN LENGTH TO ZROPAD
C          A COSINE BELL IS THEN APPLIED TO THE DATA AT
C          BOTH ENDS OF THE WINDOW DATA.
C  IFORMT = 1 BINARY DISK INPUT OF RECORD
C          (NOT INCORPORATED YET)
C          = 2 REAL DISK INPUT OF RECORD
C  HEADER = HEADER LENGTH (NUMBER OF DATA VALUES)

```

```

      DIMENSION B(5000),TRACE(5000),AMPLTD(2500),PHASE(2500)
      DIMENSION IMAG(5000)
      DIMENSION X(520),Y(520)
      INTEGER RECNUM,IWSTRT,IWLEN,ZROPAD,IFORMT,HEADER,NPTS
      REAL IMAG

```

```

      CALL PLOTS
      CALL PLOT(-12.0,2:0,-3)

```

```

      IORGIN = 0
      KK = 0

```

```

100 READ (5,*,END=999) RECNUM,IWSTRT,IWLEN,ZROPAD,IFORMT,
&      HEADER,NPTS,DT,ILAHZ
      DF=1.0/(ZROPAD*DT)
      WRITE(2,*)RECNUM,IWSTRT,IWLEN,ZROPAD,IFORMT,HEADER,
&      NPTS,DT,ILAHZ,DF

```

```

87   KK = KK + 1
      IF (IFORMT.EQ.2) READ(4,37) (B(K),K=1,NPTS)
      IF (IFORMT.EQ.1) READ (4) (B(K),K=1,NPTS)
      IF (KK.LT.RECNUM) GOTO 87

```

```

37   FORMAT(254F8.0,254F8.0,254F8.0,254F8.0,
$     254F8.0,254F8.0,254F8.0,254F8.0,
$     254F8.0,254F8.0,254F8.0,254F8.0,
$     254F8.0,254F8.0,254F8.0,254F8.0)
      TRSQN=B(1)
      DEPTH=B(2)
      WRITE(2,*) 'TRSQN AND DEPTH = ',TRSQN,DEPTH
      M = IWSTRT + HEADER - 1

```



```

SUM = 0.0

DO 2 I=1,IWLEN
  M=M+1
  TRACE(I) = B(M)
  SUM = SUM + TRACE(I)
2 CONTINUE

C REMOVE DC BIAS FROM THE WINDOW
AVE = SUM/(FLOAT(IWLEN))
DO 33 I=1,IWLEN
  TRACE(I) = TRACE(I) - AVE
33 CONTINUE

C PAD WITH ZEROS UPTO ZROPAD
WINLP1 = IWLEN + 1
DO 5 I=WINLP1,ZROPAD
  TRACE(I) = 0.0
5 CONTINUE

DO 16 I=1,5000
  IMAG(I) = 0.0
16 CONTINUE

C TAPER THE DATA WITH A COSINE BELL AND FOURIER TRANSFORM.
C THE TRACE NOW IS THE TIME DOMAIN DATA
CALL TAPER(TRACE,IWLEN,10)

CALL MYFFT(TRACE,IMAG,ZROPAD,1)

C TRACE IS NOW THE REAL PART OF THE SPECTRUM

MPTS = ZROPAD / 2.0

DO 479 J=1,MPTS
  PHASE(J)=ATAN2(IMAG(J),TRACE(J))
  AMPLTD(J)=SQRT(ABS(TRACE(J))**2.0+ABS(IMAG(J))**2.0)
  & /ZROPAD
479 CONTINUE

C WRITE OUT THE SPECTRUM WITH DEPTH AND TRSQN
C WRITE(8) TRSQN,DEPTH,(AMPLTD(I),I=1,MPTS)
C WRITE(8,43) TRSQN,DEPTH,(AMPLTD(I),I=1,MPTS)
C WRITE(8,43) TRSQN,DEPTH,(PHASE(I),I=1,MPTS)
C 43 FORMAT(10F8.1)

C PLOT THE SPECTRUM
IORGIN = IORGIN + 1
XORGIN = 0.0
IF (IORGIN.EQ.4) IORGIN = 1
IF (IORGIN.EQ.1) YORGIN = 14.0
IF (IORGIN.EQ.1) XORGIN = 14.0
IF (IORGIN.NE.1) YORGIN = -7.0
C MOVE THE ORIGIN

```

```

      CALL PLOT(XORGIN,YORGIN,-3)
      CALL PLOT3(AMPLTD,DF,ILAHZ,TRSQN,DEPTH,IWSTRT,IWLEN)
C   GO BACK FOR ANOTHER SPECTRUM
      GO TO 100

999  CALL PLOT(0.0,0.0,999)
      STOP
      END
PROCESS SC(AXIS2,SYMBOL)
      SUBROUTINE PLOT3(Y,DF,ILAHZ,TRSQN,DEPTH,IWSTRT,IWLEN)
      DIMENSION X(516),Y(516)
      WSTRT = FLOAT(IWSTRT)
      WLEN  = FLOAT(IWLEN)

      ILAPTS = INT(FLOAT(ILAHZ)/DF)
      ILAP1 = ILAPTS+1
      DO 9 I=1,ILAP1
          X(I) = (I-1)*DF
9      CONTINUE

C   DO THE NEXT TWO LINES IN THE CALLING ROUTINE IF MORE
C   THAN ONE PLOT IS TO BE MADE
C       CALL PLOTS
C       CALL PLOT(2.0,2.0,-3)

C   AUTOMATIC SCALING
C       CALL SCALE(X,7.0,ILAPTS,1)
C       CALL SCALE(Y,7.0,ILAPTS,1)

C   MANUAL SCALING
C       X(ILAPTS+1) = LOWEST VALUE ON X AXIS
C       X(ILAPTS+2) = # OF POINTS PER CENTIMETER ALONG X AXIS
C       Y(ILAPTS+1) = LOWEST VALUE ON Y AXIS
C       Y(ILAPTS+2) = # OF POINTS PER CENTIMETER ALONG Y AXIS
          X(ILAPTS+1) = 0.0
          X(ILAPTS+2) = 20.0
          Y(ILAPTS+1) = 0.0
          Y(ILAPTS+2) = 8.0

C   SET UP AND LABEL AXES
      CALL AXIS2(0.0,0.0,'      Frequency (HZ)',-18,8.0,0.0,
$           X(ILAPTS+1),X(ILAPTS+2),1.0)
      CALL AXIS2(0.0,0.0,' Amplitude',10,5.0,90.0,
$           Y(ILAPTS+1),Y(ILAPTS+2),-1.0)

C   DRAW BOX AROUND PLOT
      CALL PLOT(8.0,0.0,3)
      CALL PLOT(8.0,5.0,2)
      CALL PLOT(0.0,5.0,2)

```

```
C DOCUMENT THE PLOT
  CALL SYMBOL(8.5,4.5,.25,'TRSQN =',0.0,7)
  CALL NUMBER(10.4,4.5,.25,TRSQN,0.0,-1)
  CALL SYMBOL(8.5,4.0,.25,'DEPTH =',0.0,7)
  CALL NUMBER(10.4,4.0,.25,DEPTH,0.0,-1)
  CALL SYMBOL(8.5,3.5,.25,'WSTRT =',0.0,7)
  CALL NUMBER(10.4,3.5,.25,WSTRT,0.0,-1)
  CALL SYMBOL(8.5,3.0,.25,'WLEN =',0.0,7)
  CALL NUMBER(10.4,3.0,.25,WLEN,0.0,-1)

C PLOT THE DATA
  CALL LINE(X,Y,ILAPTS,1,0,4)

C DO THE NEXT LINE IN THE MAIN PROGRAM
C CALL PLOT(0.0,0.0,999)
  RETURN
  END
```

```

SUBROUTINE MYFFT(FR,FI,N,ISIGN)
C WRITTEN BY NICK KEEHN (1986).
C N IS THE NUMBER OF DATA POINTS=2**M
C FR IS THE REAL DATA SET
C FI IS THE IMAGINARY PART OF DATA SET(=0.0 IF ONLY REAL)
C
C      ISIGN = +1, APPLY FFT
C      -1, APPLY IFFT

REAL FR(N),FI(N),GR,GI,ER,EI,EU,EZ,PI
DATA PI/3.141592654/

C FIRST COMPUTE M

M = 0
KD = N
1 KD = KD/2
M = M+1
IF(KD .GE. 2) GOTO 1
ND2 = N/2
NM1 = N-1
L = 1

C SHUFFLE INPUT DATA IN BINARY DIGIT REVERSE ORDER

DO 4 K=1,NM1
  IF(K .GE. L) GOTO 2
  GR = FR(L)
  GI = FI(L)
  FR(L) = FR(K)
  FI(L) = FI(K)
  FR(K) = GR
  FI(K) = GI
2
  NND2 = ND2
3
  IF(NND2 .GE. L) GOTO 4
  L = L - NND2
  NND2 = NND2/2
  GOTO 3
4
  L = L+NND2

SIGN = -FLOAT(ISIGN)*PI

C FIRST ARRANGE ACCOUNTING OF M STAGE

DO 6 J=1,M
  NJ = 2**J
  NJD2 = NJ/2
  EU = 1.0
  EZ = 0.0
  ER = COS(SIGN/NJD2)
  EI = SIN(SIGN/NJD2)

C COMPUTE FOURIER TRANSFORM IN EACH M STAGE

```

```
DO 6 IT=1,NJD2
  DO 5 IW=IT,N,NJ
    IWJ = IW+NJD2
    GR = FR(IWJ)*EU - FI(IWJ)*EZ
    GI = FI(IWJ)*EU + FR(IWJ)*EZ
    FR(IWJ) = FR(IW) - GR
    FI(IWJ) = FI(IW) - GI
    FR(IW) = FR(IW) + GR
    FI(IW) = FI(IW) + GI
  5   SEU = EU
    EU = SEU*ER - EZ*EI
  6   EZ = EZ*ER + SEU*EI

  IF(ISIGN .EQ. 1) RETURN

  RN = FLOAT(N)

  DO 7 I=1,N
  7   FR(I) = FR(I)/RN

  DO 8 I=1,N
  8   FI(I) = FI(I)/RN

  RETURN
  END
```

```

C          PROGRAM LSR4F.CALL
C WRITTEN BY NICK KEEHN, JULY 1985.
C THIS PROGRAM WAS WITTEN AS A CALLING PROGRAM FOR
C D.C. GANLEY'S LSR4F SUBROUTINE.

      DIMENSION X1(8192),X2(8192),X3(8192),X4(8192)
C      DIMENSION X11(8192),Y11(8192)
      DIMENSION Y1(8192),Y2(8192),Y3(8192),Y4(8192)
      DIMENSION RAT(512),DIF(512)

      DATA RLN2/.693147181/
      COMMON /LSRCOM/ L2NY,DT,DF,IWL,IC,IWT,ISM,FSWID

C      DT IS IN MILLISECONDS
      READ (15,1) NX,DT
1  FORMAT(5X,15,F5.0)

C      MAXIMUM VALUE OF MPTS=1000./(2.*DT*DF) = NY/2

      READ (5,3) MPTS,NY,IWL,IC,IWT,ISM,FSWID,NX12
C      FOR PANARCTIC DATA NX12 = 4000
C      FOR Z2 DATA NX12 = NX
C      NX12 = NX

      3  FORMAT(5X,6I5,F5.0,15)

      DF = 1000.0/(DT*NY)

C      CHANGE MPTS FROM NO. OF HERTZ TO NO. OF POINTS
      MPTS = INT(FLOAT(MPTS)/DF)
      REALNY = NY
      L2NY = ALOG(REALNY)/RLN2

      WRITE (6,37)NX,NX12,DT,MPTS,NY,IWL,IC,IWT,ISM,FSWID,
&      DF,L2NY
37  FORMAT(5X,2I5,F5.1,6I5,F5.1,F10.7,15)

C      CALL LSR4F(X1,X2,X3,X4,Y1,Y2,Y3,Y4,RAT,DIF,NX,NX12,
&      NY,MPTS,X11,Y11)
C      CALL LSR4F(X1,X2,X3,X4,Y1,Y2,Y3,Y4,RAT,DIF,NX,NX12,
&      NY,MPTS)

      STOP
      END

```

SUBROUTINE LSR4F(X1,X2,X3,X4,Y1,Y2,Y3,Y4,RAT,DIF,
& NX,NX12,NY,MPTS)

C

SUBROUTINE BY DAVE GANLEY OCT 24, 1977.

C

C CHANGES MADE BY NICK KEEHN (1986).

C FOR CHANGES MADE TO THIS PROGRAM FROM GANLEYS VERSION

C SCAN THIS FILE FOR "CHANGE".

CHANGE: INCLUDE X11 AND Y11 (THE STACKED SPECTRA)

C SUBROUTINE LSR4F(X1,X2,X3,X4,Y1,Y2,Y3,Y4,RAT,DIF,

C & NX,NX12,NY,MPTS,X11,Y11)

C THIS SUBROUTINE WILL CALCULATE THE NATURAL LOGARITHM OF
C THE SPECTRAL RATIO AND/OR THE PHASE DIFFERENCE FOR ANY
C NUMBER OF PAIRS OF SEISMIC TRACES. THE SPECTRAL RATIO
C (PHASE DIFFERENCE) IS CORRECTED BY DIVIDING BY THE RATIO
C (SUBTRACTING THE PHASE DIFFERENCE) OF 2 OTHER TRACES ON
C A SECOND INPUT TAPE. DIFFERENT TIME WINDOWS CAN BE USED
C FOR EACH TRACE. THE RESULTS ARE OUTPUT IN GRAPHICAL FORM
C ON THE LINE PRINTER AND INTO A SEQUENTIAL FILE ON LOGICAL
C UNIT 3.

C

C A FAST FOURIER TRANSFORM IS USED TO CALCULATE THE SPECTRA.
C THE DATA CAN BE WEIGHTED WITH A COSINE TAPER AT THE ENDS
C AND THE SPECTRA CAN BE SMOOTHED. THIS SMOOTHING CAN BE
C APPLIED TO THE COMPLEX FOURIER COEFFICIENTS OR TO THE
C AMPLITUDE AND PHASE.

C

C INPUTS ARE:

CHANGE X3,X4 = ARRAYS OF LENGTH NX

C X1,X2 = ARRAYS OF LENGTH NX12

C Y1,Y2 = ARRAYS OF LENGTH NY

C NX = NUMBER OF DATA POINTS IN A BLOCK ON TAPE

C NY = NUMBER OF POINTS TO USE IN FFT AND MUST BE A
C POWER OF 2

C MPTS = DO THE CALCULATION FOR THE FIRST MPTS
C FREQUENCY VALUES

C

C OUTPUTS ARE:

C RAT = NATURAL LOG OF SPECTRAL RATIO (LENGTH IS MPTS)

C DIF = PHASE DIFFERENCE (LENGTH IS MPTS)

C

C SUBROUTINES CALLED:

C 1. FFTR2

C 2. MR1DFT

C 3. AMPPHZ

C 4. SW2RBO

C 5. GRAF

C 6. TAPER

CHANGE: 7. RUNAVE

C

DIMENSION X1(NX12),X2(NX12),X3(NX),X4(NX)

CHANGE: THE NEXT LINE IS USED WHEN STACKING SPECTRA

C DIMENSION X11(NX12),Y11(NY)
 DIMENSION Y1(NY),Y2(NY),Y3(NY),Y4(NY)
 DIMENSION RAT(MPTS),DIF(MPTS)

CHANGE: INCLUDE THE FOLLOWING DIMENSION STATEMENT

DIMENSION RATIO(200)

DATA IBLOCK/1/

COMMON /LSRCOM/ L2NY,DT,DF,IWL,IC,IWT,ISM,FSWID

C++++

C L2NY = SUCH THAT NY=2**L2NY
 C DT = SAMPLE INTERVAL IN MILLISECONDS (SAME FOR BOTH TAPES)
 C DF = SPACING BETWEEN FREQUENCY VALUES IN HERTZ
 C IWL = TIME WINDOW LENGTH IN SAMPLES (SAME FOR ALL WINDOWS)
 C IC = 1 CALCULATE LOG OF SPECTRAL RATIO & PHASE DIFFERENCE
 C = 2 CALCULATE LOG OF SPECTRAL RATIO ONLY
 C = 3 CALCULATE PHASE DIFFERENCE ONLY
 C IWT = NUMBER OF POINTS AT EACH END OF DATA TO WEIGHT WITH
 C COSINE TAPER
 C ISM = 1 MEANS DO NOT SMOOTH SPECTRAL ESTIMATE
 C = 2 MEANS SMOOTH AMPLITUDE AND PHASE SPECTRA
 C = 3 MEANS TO SMOOTH COMPLEX FOURIER COEFFICIENTS
 C FSWID = WIDTH OF WINDOW TO USE FOR SMOOTHING (IN HERTZ)

C++++

CHANGE: NEW CONSTANTS REQUIRED FOR WRITING

C OUT SMOOTHED AMPLITUDES AND PHASES

NYD2P1 = NY/2+1

NYD2P2 = NY/2+2

IWLP1=IWL+1

MY=NY/2

MYP1=MY+1

MYP2=MY+2

MYM1=MY-1

MPTS1=MPTS-1

IRL=0

IR1L=0

IR2L=0

JRL=0

JR1L=0

JR2L=0

10 READ (5,1,END=99) IR1,IWS1,IR2,IWS2,JR1,JWS1,

.JR2,JWS2,DELT,IP1,IP2,JP1,JP2

1 FORMAT (5X,8I5,F5.0,4I1)

C****

C IR1 = NUMBER OF THE BLOCK ON TAPE 1 CONTAINING TRACE 1
 C IWS1 = WINDOW START FOR TRACE 1 IN MILLISECONDS
 C IP1 = 1 MEANS TO PLOT TRACE 1 DATA WINDOW ON LINE PRINTER
 C IR2, IWS2, IP2 = SAME AS ABOVE FOR TRACE 2 (ON TAPE 1)
 C JR1 = NUMBER OF THE BLOCK ON TAPE 2 CONTAINING TRACE 3
 C JWS1 = WINDOW START FOR TRACE 3 IN MILLISECONDS
 C JP1 = 1 MEANS TO PLOT TRACE 3 DATA WINDOW ON LINE PRINTER
 C JR2, JWS2, JP2 = SAME AS ABOVE FOR TRACE 4 (ON TAPE 2)

C DELT = ACTUAL TIME DIFFERENCE (MSEC) BETWEEN ARRIVALS FOR
 C THE TWO CORRECTION TRACES (3 AND 4). THIS IS USED TO REMOVE
 C A LINEAR TREND FROM THE PHASE DIFFERENCE WHICH IS
 C CAUSED BY THE FACT THAT THE TIME DIFFERENCE BETWEEN
 C TRACES 3 AND 4 MUST BE A MULTIPLE OF THE SAMPLE
 C INTERVAL WHEN IT SHOULD BE DELT. IF DELT=0.0 THIS
 C CORRECTION IS IGNORED.

C IR2 MUST BE GREATER THAN IR1 AND JR2 GREATER THAN JR1
 C IT IS ASSUMED THAT FOR A GIVEN IR1 OR IR2 THE SAME JR1
 C OR JR2 WILL CORRESPOND TO IT FOR ALL CALCULATIONS AND
 C THAT A DIFFERENT IR1 OR IR2 WILL HAVE A DIFFERENT JR1
 C OR JR2. THERE CAN BE A DIFFERENT NUMBER OF TRACES ON
 C TAPE 1 AND TAPE 2 SO THAT IR1 AND IR2 DO NOT EQUAL
 C JR1 OR JR2.

C THE RATIO IS (TRACE 2 / TRACE 1) * (TRACE 3 / TRACE 4)
 C THE DIFFERENCE IS (TRACE 2 - TRACE 1) - (TRACE 4 - TRACE 3)

C IF THE SAME TRACE IS USED ON TWO CONSECUTIVE CARDS THE
 C WINDOW MUST BE THE SAME

C****

IF (IR2.LE.IR1) GO TO 92
 IF (JR2.LE.JR1) GO TO 93

C

C CALCULATE WINDOW STARTING POINTS

C

T1=(IWL-1)*DT
 WRITE(6,2)T1,IR1,IWS1,IR2,IWS2,JR1,JWS1,JR2,JWS2,DELT
 2 FORMAT (' WINDOW LENGTH IS ',F7.2,' MSEC',2(/,6X,
 &'TAPE 1 RECORD ',
 .I3,' WINDOW START IS ',I5,' MSEC'),2(/,6X,
 &'TAPE 2 RECORD ',I3,' WI
 .NDOW START IS ',I5,' MSEC'),
 &/' PHASE WILL BE CORRECTED TO ACTUAL T
 .IME DIFFERENCE OF ',F7.2,
 &' MSEC BETWEEN CORRECTION TRACES.')

IWS1=IWS1/DT+1.5
 IWS2=IWS2/DT+1.5
 JWS1=JWS1/DT+1.5
 JWS2=JWS2/DT+1.5

C

C-----C

C

LOCATE AND READ THE FOUR INPUT RECORDS AND
 CALCULATE AMPLITUDE AND/OR PHASE SPECTRA

C

IF (IR1.EQ.IR1L) GO TO 22
 IF (IR1.NE.IR2L) GO TO 31

C

C

NEW TRACE 1 IS TRACE 2 FROM LAST CALCULATION
 NEW TRACE 3 IS THUS TRACE 4 FROM LAST CALCULATION

C

DO 21 I=1,NY
 Y1(I)=Y2(I)

```

21      Y3(I)=Y4(I)
CHANGE:THE FOLLOWING LINES HAVE BEEN ADDED TO SWAP
C      DEPTHS AS WELL
        DEPTH1 = DEPTH2
        DEPTH3 = DEPTH4
        IR1L=IR1
        IWS1L=IWS2L
        JR1L=JR1
        JWS1L=JWS2L
C
C      READ A NEW TRACE 2 IF TRACE 1 WAS USED ON LAST
C      CALCULATION ALSO READ THE NEW TRACE 4
C
22 IWS1=IWS1L
   JWS1=JWS1L
   NSKIP=IR2-IRL-1
   IF (NSKIP.NE.0) CALL SKIP(0,NSKIP,1,&91,&91,&91)
CHANGE: THE FOLLOWING LINE HAS BEEN REPLACED BY,
   READ (1) TRSQN,DEPTH2, X2
COMMENT      READ (1) X2
   IRL=IR2
   IR2L=IR2
   IWS2L=IWS2
   J=IWS2

CHANGE : REMOVE DC-BIAS FROM THE WAVELETS (Y'S)
C      BEFORE ADDING THE ZEROS AND COSINE-BELLING.
        SUMY2 = 0.0

        DO 24 I=1,IWL
          Y2(I)=X2(J)
          SUMY2 = SUMY2 + Y2(I)
24      J=J+1
        AVEY2 = SUMY2/FLOAT(IWL)
        DO 1024 I=1,IWL
          Y2(I) = Y2(I) - AVEY2
1024 CONTINUE

        NSKIP=JR2-JRL-1
        IF (NSKIP.NE.0) CALL SKIP(0,NSKIP,2,&91,&91,&91)

CHANGE: THE FOLLOWING LINE HAS BEEN REPLACED BY,
        READ (2) TRSQN,DEPTH4, X4
COMMENT      IF (DEPTH4.NE.DEPTH2) STOP 11
COMMENT      READ (2) X4
        JRL=JR2
        JR2L=JR2
        JWS2L=JWS2
        J=JWS2

CHANGE : REMOVE DC-BIAS FROM THE WAVELETS (Y'S)
C      BEFORE ADDING THE ZEROS AND COSINE-BELLING.
        SUMY4 = 0.0

```

```

DO 25 I=1,IWL
Y4(I)=X4(J)
SUMY4 = SUMY4 + Y4(I)
25 J=J+1
AVEY4 = SUMY4/FLOAT(IWL)
DO 1025 I=1,IWL
Y4(I) = Y4(I) - AVEY4
1025 CONTINUE

IF (IWL.EQ.NY) GO TO 27
DO 26 I=IWL,1,NY
Y2(I)=0.0
26 Y4(I)=0.0

C
C CALCULATE SPECTRA FOR NEW TRACES 2 AND 4
C
27 IF (IWT.EQ.0) GO TO 28
CALL TAPER(Y2,IWL,IWT)
CALL TAPER(Y4,IWL,IWT)
CHANGE: WRITE OUT THE RESULTING PULSE AND THE ZEROS
C WRITE (14) TRSQN,DEPTH2, (Y2(I),I=1,NY)
C WRITE (14) TRSQN,DEPTH4, (Y4(I),I=1,NY)

28 CALL FFTR2(L2NY,Y2,Y4)
GO TO (29,29),ISM
CALL DANIEL(Y2,NY,FSWID,DT)
CALL DANIEL(Y4,NY,FSWID,DT)
29 CALL AMPPHZ(L2NY,Y2,IC,PDC2,PFN2)
CALL AMPPHZ(L2NY,Y4,IC,PDC4,PFN4)
GO TO (60,30,60),ISM
30 CALL UNWRAP(Y2(MYP2),MYM1)
CALL UNWRAP(Y4(MYP2),MYM1)
CALL DANIEL(Y2,NY,FSWID,DT)
CALL DANIEL(Y4,NY,FSWID,DT)
GO TO 60

C
C NEW TRACES 1 AND 2 (AND THUS 3 AND 4) ARE TO BE READ
C
31 IF (IR2.EQ.IR2L) GO TO 50
NSKIP=IR1-IRL-1
IF (NSKIP.NE.0) CALL SKIP(0,NSKIP,1,&91,&91,&91)

CHANGE: THE FOLLOWING LINE HAS BEEN REPLACED BY,
READ (1) TRSQN1,DEPTH1, X1
COMMENT READ (1) X1
IRL=IR1
IR1L=IR1
IWS1L=IWS1
J=IWS1

CHANGE : REMOVE DC-BIAS FROM THE WAVELETS (Y'S)
C BEFORE ADDING THE ZEROS AND COSINE-BELLING.
SUMY1 = 0.0

```

```

      DO 33 I=1,IWL
      Y1(I)=X1(J)
      SUMY1 = SUMY1 + Y1(I)
33     J=J+1
      AVEY1 = SUMY1/FLOAT(IWL)
      DO 1033 I=1,IWL
      Y1(I) = Y1(I) - AVEY1
1033  CONTINUE

C *****START*****TEST*****
C THIS READS IN ANOTHER TRACE TO BE AMPL. SPECT. STACKED
C WITH Y1. TO IMPLEMENT SCAN LSR4F AND LSR4F CALL FOR
C Y11 AND X11
C   CALL SKIP(0,1,1,&91,&91,&91)
C
C   READ (1) TRSQ11,DEPT11, X11
C   J=293
C
CHANGE : REMOVE DC-BIAS FROM THE WAVELETS (Y'S)
C   BEFORE ADDING THE ZEROS AND COSINE-BELLING.
C   SUMY11= 0.0
C
C   DO 133 I=1,IWL
C   Y11(I)=X11(J)
C   SUMY11 = SUMY11 + Y11(I)
C 133  J=J+1
C   AVEY11 = SUMY11/FLOAT(IWL)
C   DO 1133 I=1,IWL
C   Y11(I) = Y11(I) - AVEY11
C1133 CONTINUE
C
C *****END*****

      NSKIP=JR1-JRL-1
      IF (NSKIP.NE.0) CALL SKIP(0,NSKIP,2,&91,&91,&91)

CHANGE: THE FOLLOWING LINE HAS BEEN REPLACED BY,
      READ (2) TRSQ3,DEPTH3, X3
COMMENT   IF (DEPTH3.NE.DEPTH1) STOP 22
COMMENT   READ (2) X3
      JRL=JR1
      JRL=JR1
      JWS1L=JWS1
      J=JWS1

CHANGE.: REMOVE DC-BIAS FROM THE WAVELETS (Y'S)
C   BEFORE ADDING THE ZEROS AND COSINE-BELLING.
      SUMY3 = 0.0

      DO 35 I=1,IWL
      Y3(I)=X3(J)
      SUMY3 = SUMY3 + Y3(I)

```

```

35      J=J+1
      AVEY3 = SUMY3/FLOAT(IWL)
      DO 1035 I=1,IWL
          Y3(I) = Y3(I) - AVEY3
1035  CONTINUE

```

```

      NSKIP=IR2-IRL-1
      IF (NSKIP.NE.0) CALL SKIP(0,NSKIP,1,&91,&91,&91)
CHANGE: THE FOLLOWING LINE HAS BEEN REPLACED BY,
      READ (1) TRSQN2,DEPTH2, X2
COMMENT      READ (1) X2
      IRL=IR2
      IR2L=IR2
      IWS2L=IWS2
      J=IWS2

```

```

CHANGE : REMOVE DC-BIAS FROM THE WAVELETS (Y'S)
C      BEFORE ADDING THE ZEROS AND COSINE-BELLING.
      SUMY2 = 0.0

```

```

      DO 37 I=1,IWL
          Y2(I)=X2(J)
          SUMY2 = SUMY2 + Y2(I)
37      J=J+1
      AVEY2 = SUMY2/FLOAT(IWL)
      DO 1037 I=1,IWL
          Y2(I) = Y2(I) - AVEY2
1037  CONTINUE

```

```

      NSKIP=JR2-JRL-1
      IF (NSKIP.NE.0) CALL SKIP(0,NSKIP,2,&91,&91,&91)
CHANGE: THE FOLLOWING LINE HAS BEEN REPLACED BY,
      READ (2) TRSQN4,DEPTH4, X4
COMMENT      IF (DEPTH4.NE.DEPTH2) STOP 33
COMMENT      READ (2) X4
      JRL=JR2
      JR2L=JR2
      JWS2L=JWS2
      J=JWS2

```

```

CHANGE : REMOVE DC-BIAS FROM THE WAVELETS (Y'S)
C      BEFORE ADDING THE ZEROS AND COSINE-BELLING.
      SUMY4 = 0.0

```

```

      DO 39 I=1,IWL
          Y4(I)=X4(J)
          SUMY4 = SUMY4 + Y4(I)
39      J=J+1
      AVEY4 = SUMY4/FLOAT(IWL)
      DO 1039 I=1,IWL
          Y4(I) = Y4(I) - AVEY4
1039  CONTINUE

```

```

      IF (IWL.EQ.NY) GO TO 46

```

```

DO 41 I=FWLP1,NY
Y1(I)=0.0
CHANGE:
C      Y11(I)=0.0
      Y2(I)=0.0
      Y3(I)=0.0
      Y4(I)=0.0
41
C
C      CALCULATE SPECTRA FOR 4 NEW TRACES
C
46 IF (IWT.EQ.0) GO TO 47
CALL TAPER(Y1,IWL,IWT)
CHANGE:
C      CALL TAPER(Y11,IWL,IWT)
      CALL TAPER(Y2,IWL,IWT)
      CALL TAPER(Y3,IWL,IWT)
      CALL TAPER(Y4,IWL,IWT)
CHANGE: WRITE OUT THE RESULTING PULSE AND THE ZEROS
C      WRITE (14) TRSQN1,DEPTH1, (Y1(I),I=1,NY)
CC     WRITE (14) TRSQ11,DEPT11, (Y11(I),I=1,NY)
C      WRITE (14) TRSQN2,DEPTH2, (Y2(I),I=1,NY)
C      WRITE (14) TRSQN3,DEPTH3, (Y3(I),I=1,NY)
C      WRITE (14) TRSQN4,DEPTH4, (Y4(I),I=1,NY)

47 CALL FFTR2(L2NY,Y1,Y2)
      CALL FFTR2(L2NY,Y3,Y4)
CHANGE:
C      CALL FFTR1(L2NY,Y11)

      GO TO (48,48),ISM
      CALL DANIEL(Y1,NY,FSWID,DT)
CHANGE:
C      CALL DANIEL(Y11,NY,FSWID,DT)
      CALL DANIEL(Y2,NY,FSWID,DT)
      CALL DANIEL(Y3,NY,FSWID,DT)
      CALL DANIEL(Y4,NY,FSWID,DT)
48 CALL AMPPHZ(L2NY,Y1,IC,PDC1,PFN1)
CHANGE:
C      CALL AMPPHZ(L2NY,Y11,IC,PDC11,PFN11)
      CALL AMPPHZ(L2NY,Y2,IC,PDC2,PFN2)
      CALL AMPPHZ(L2NY,Y3,IC,PDC3,PFN3)
      CALL AMPPHZ(L2NY,Y4,IC,PDC4,PFN4)

CHANGE: STACK THE AMPLITUDE SPECTRA OF Y1 AND Y11
C      WRITE(22,6754) (Y1(I),I=1,MPTS)
C      WRITE(22,6754) (Y11(I),I=1,MPTS)
C6754 FORMAT (12F5.1)
C      DO 4246 I=1,MPTS
C          Y1(I) = Y1(I) + Y11(I)
C4246 CONTINUE
CCCC THE STACKED SPECTRUM IS NOW IN Y1
C      WRITE(22,6754) (Y1(I),I=1,MPTS)

```

```

      GO TO (60,49,60),ISM
    49 CALL UNWRAP(Y1(MYP2),MYM1)
CHANGE:
C    CALL UNWRAP(Y11(MYP2),MYM1)
      CALL UNWRAP(Y2(MYP2),MYM1)
      CALL UNWRAP(Y3(MYP2),MYM1)
      CALL UNWRAP(Y4(MYP2),MYM1)
      CALL DANIEL(Y1,NY,FSWID,DT)
CHANGE:
C    CALL DANIEL(Y11,NY,FSWID,DT)
      CALL DANIEL(Y2,NY,FSWID,DT)
      CALL DANIEL(Y3,NY,FSWID,DT)
      CALL DANIEL(Y4,NY,FSWID,DT)
      GO TO 60
C
C READ A NEW TRACE 1 IF TRACE 2 WAS USED ON LAST CALCULATION
C ALSO READ THE NEW TRACE 3
C
    50 IWS2=IWS2L
      NSKIP=IR1-IRL-1
      IF (NSKIP.NE.0) CALL SKIP(0,NSKIP,1,&91,&91,&91)
CHANGE: THE FOLLOWING LINE HAS BEEN REPLACED BY,
      READ (1) TRSQN,DEPTH1, X1
COMMENT      READ (1) X1
      IRL=IR1
      IR1L=IR1
      IWS1L=IWS1
      J=IWS1

CHANGE : REMOVE DC-BIAS FROM THE WAVELETS (Y'S)
C      BEFORE ADDING THE ZEROS AND COSINE-BELLING.
      SUMY1 = 0.0

      DO 52 I=1,IWL
        Y1(I)=X1(J)
        SUMY1 = SUMY1 + Y1(I)
    52      J=J+1
      AVEY1 = SUMY1/FLOAT(IWL)
      DO 1052 I=1,IWL
        Y1(I) = Y1(I) - AVEY1
    1052 CONTINUE

      NSKIP=JR1-JRL-1
      IF (NSKIP.NE.0) CALL SKIP(0,NSKIP,2,&91,&91,&91)
CHANGE: THE FOLLOWING LINE HAS BEEN REPLACED BY,
      READ (2) TRSQN,DEPTH3, X3
COMMENT      IF (DEPTH3.NE.DEPTH1) STOP 44
COMMENT DEPTH1 AND DEPTH2 DO NOT ALWAYS EXIST
COMMENT      READ (2) X3
      JRL=JR1
      JR1L=JR1
      JWS1L=JWS1
      J=JWS1

```

CHANGE : REMOVE DC-BIAS FROM THE WAVELETS (Y'S)
 C BEFORE ADDING THE ZEROS AND COSINE-BELLING.
 SUMY3 = 0.0

```

      DO 54 I=1,IWL
      Y3(I)=X3(J)
      SUMY3 = SUMY3 + Y3(I)
54    J=J+1
      AVEY3 = SUMY3/FLOAT(IWL)
      DO 1054 I=1,IWL
      Y3(I) = Y3(I) - AVEY3
1054 CONTINUE

```

```

      IF (IWL.EQ.NY) GO TO 56
      DO 55 I=IWLP1,NY
      Y1(I)=0.0
55    Y3(I)=0.0

```

C
 C
 C

CALCULATE SPECTRA OF NEW TRACES 1 AND 3

```

56 IF (IWT.EQ.0) GO TO 57
      CALL TAPER(Y1,IWL,IWT)

```

CHANGE: LINE 298 (SR4F2980) IS IN ERROR! IT HAS BEEN
 C REPLACED WITH:
 CALL TAPER(Y3,IWL,IWT)
 COMMENT CALL TAPER(Y2,IWL,IWT)

CHANGE: WRITE OUT THE RESULTING PULSE AND THE ZEROS
 C WRITE (14) TRSQN,DEPTH1, (Y1(I),I=1,NY)
 C WRITE (14) TRSQN,DEPTH3, (Y3(I),I=1,NY)

```

57 CALL FFTR2(L2NY,Y1,Y3)
      GO TO (58,58),ISM
      CALL DANIEL(Y1,NY,FSWID,DT)
      CALL DANIEL(Y3,NY,FSWID,DT)
58 CALL AMPPHZ(L2NY,Y1,IC,PDC1,PFN1)
      CALL AMPPHZ(L2NY,Y3,IC,PDC3,PFN3)
      GO TO (60,59,60),ISM
59 CALL UNWRAP(Y1(MYP2),MYM1)
      CALL UNWRAP(Y3(MYP2),MYM1)
      CALL DANIEL(Y1,NY,FSWID,DT)
      CALL DANIEL(Y3,NY,FSWID,DT)

```

C
 C-----C
 C
 C

C CALCULATE NATURAL LOGARITHM OF RATIO OF AMPLITUDE SPECTRA

CHANGE: WRITE OUT THE RESULTING SMOOTHED
 C AMPLITUDES AND PHASES (PHASES ARE QUESTIONABLE)
 60 CONTINUE


```

C      WRITE (16) (Y1(I),I=1,NYD2P1)
C      WRITE (17) (Y1(I),I=NYD2P2,NY)
C      WRITE (16) (Y2(I),I=1,NYD2P1)
C      WRITE (17) (Y2(I),I=NYD2P2,NY)
C      WRITE (16) (Y3(I),I=1,NYD2P1)
C      WRITE (17) (Y3(I),I=NYD2P2,NY)
C      WRITE (16) (Y4(I),I=1,NYD2P1)
C      WRITE (17) (Y4(I),I=NYD2P2,NY)

COMMENT 60 GO TO (61,61,65),IC
        GO TO (61,61,65),IC
        61 RMIN=0.0
CHANGE:
        DO 62 I=1,MPTS
C      THIS IS A PROVISION WHEREBY GANLEY CORRECTION
C      MAY NOT BE IMPLEMENTED...
C      RATIO(I) = Y2(I)/Y1(I)*Y3(I)/Y4(I)
        RATIO(I) = Y2(I)/Y1(I)
        62 CONTINUE
C      SMOOTH THE RATIO WITH A 9 POINT RUNNING AVERAGE
        CALL RUNAVE(RATIO,MPTS,9)
C      RATIO(I) NOW CONTAINS THE SMOOTHED RATIOS

        DO 63 I=1,MPTS
CHANGE:  RAT(I)=ALOG(Y2(I)/Y1(I)*Y3(I)/Y4(I)).
        RAT(I)=ALOG(RATIO(I))

        IF (RAT(I).LT.RMIN) RMIN=RAT(I)
        63 CONTINUE
        DO 64 I=1,MPTS
        64 RAT(I)=RAT(I)-RMIN + 0.5

C
C      CALCULATE PHASE DIFFERENCE
C
        GO TO (65,70),IC
        65 DO 66 I=2,MPTS
            J=I+MY
        66 DIF(I)=Y2(J)-Y1(J)+Y3(J)-Y4(J)
            DIF(1)=PDC2-PDC1+PDC3-PDC4
            IF (MPTS.EQ.MYP1) DIF(MPTS)=PFN2-PFN1+PFN3-PFN4
            PFACT=((JWS2-JWS1)*DT-DELT)*0.36*DF
            IF (DELT.EQ.0.0) PFACT=0.0
            IF (PFACT.EQ.0.0) GO TO 68
            DO 67 I=2,MPTS
                PCOR=PFACT*(I-1)
        67 DIF(I)=DIF(I)+PCOR
        68 IF (ISM.EQ.2) GO TO 70
            DO 69 I=1,MPTS
                IF (DIF(I).LE.-540.0) DIF(I)=DIF(I)+720.0
                IF (DIF(I).GT.540.0) DIF(I)=DIF(I)-720.0
                IF (DIF(I).LE.-180.0) DIF(I)=DIF(I)+360.0
                IF (DIF(I).GT.180.0) DIF(I)=DIF(I)-360.0
        69 CONTINUE

```

```

-----C
C   PLOT INPUT TRACES IF REQUESTED AND
C   PLOT RATIOS AND/OR DIFFERENCES
C   OUTPUT RATIOS AND DIFFERENCES TO LOGICAL UNIT 3
C
3   FORMAT ('1PLOT OF BLOCK ',15,' TAPE 1')
4   FORMAT ('1PLOT OF BLOCK ',15,' TAPE 2')
5   FORMAT ('1CORRECTED RATIO/DIFFERENCE OF BLOCK ',13,
.   ' TO BLOCK ',13,' IS BLOCK ',13,' ON TAPE')
C
70  IF (IP1.NE.1) GO TO 72
    WRITE (6,3) IR1
    T1=(IWS1-1)*DT
C   CALL GRAF(T1,DT,X1(IWS1),IWL,3)
72  IF (IP2.NE.1) GO TO 74
    WRITE (6,3) IR2
    T1=(IWS2-1)*DT
C   CALL GRAF(T1,DT,X2(IWS2),IWL,3)
74  IF (JP1.NE.1) GO TO 76
    WRITE (6,4) JR1
    T1=(JWS1-1)*DT
C   CALL GRAF(T1,DT,X3(JWS1),IWL,3)
76  IF (JP2.NE.1) GO TO 80
    WRITE (6,4) JR2
    T1=(JWS2-1)*DT
C   CALL GRAF(T1,DT,X4(JWS2),IWL,3)
80  GO TO (81,81,83),IC
81  WRITE (6,5) IR2,IR1,IBLOCK
CHANGE: THE FOLLOWING WRITE STATEMENT IS REPLACED BY:
    WRITE (3) DEPTH1,DEPTH2, RAT
COMMENT   WRITE (3) RAT
    IBLOCK=IBLOCK+1
C   CALL GRAF(0.0,DF,RAT,MPTS,1)
83  GO TO (85,10,85),IC
85  WRITE (6,5) IR2,IR1,IBLOCK
CHANGE: THE FOLLOWING WRITE STATEMENT IS REPLACED BY:
    WRITE (3) DEPTH3,DEPTH4, DIF
COMMENT   WRITE (3) DIF
    IBLOCK=IBLOCK+1
C   CALL GRAF(0.0,DF,DIF,MPTS,2)
    GO TO 10
C
-----C
C   ERROR MESSAGES
C
91  WRITE (6,96)
    RETURN
92  WRITE (6,97) IR1,IR2
    RETURN
93  WRITE (6,98) JR1,JR2
    RETURN
96  FORMAT ('-BAD RETURN FROM SKIP IN LSR2F')
97  FORMAT ('-IR2 MUST BE GREATER THAN IR1 ',15,5X,15)
98  FORMAT ('-JR2 MUST BE GREATER THAN JR1 ',15,5X,15)

```

99 RETURN
END

```

C
C          PROGRAM LSRANP
C
C          PROGRAM BY DAVE GANLEY, NOVEMBER 14, 1977.
C
C          CHANGES MADE BY NICK KEEHN (1986)
C          SCAN THIS FILE FOR "CHANGE" TO FIND ALL CHANGES MADE
C          TO THE ORIGINAL GANLEY PROGRAM.
C
C          THIS PROGRAM WILL DO A LEAST-SQUARES FIT OF A STRAIGHT
C          LINE TO DATA WHICH HAS BEEN OUTPUT BY MY SPECTRAL RATIO
C          PROGRAM FOR THE PURPOSE OF ESTIMATING Q.  IT CAN ALSO
C          OUTPUT DISPERSION CURVE CORRESPONDING TO THE PHASE
C          DIFFERENCE WHICH WAS OUTPUT BY THE SPECTRAL RATIO PROGRAM
C          AND PRODUCE LINE PRINTER GRAPHS AND CALCOMP PLOTS.
C
C          SUBROUTINES CALLED:
C             1. SLOPE
C             2. GRAF
C             3. UNWRAP
C             4. CALCOMP PLOTTER ROUTINES
C
C          DIMENSION X(257),Y(260),C(103),F(103)
CHANGE: BQPROF AND JUNK1 ARE NEW VARIABLES
C          INTEGER BQPROF
C          REAL INTVEL, NINES
C          DATA PI/3.141593/,IBL/0/
CHANGE: TO ALLOW FOR Q TO BE CALCULATED THE FOLLOWING
C          IS INCLUDED
C          HOLDD = 0.0
C          IORGIN = 0
C
CHANGE      READ (5,1) N,DF,FN,ICALC
C          READ(7,37) DT,N,DF
C          37  FORMAT (15X,F5.0,15,30X,F10.0)
C          READ(5,38) ICALC,BQPROF
C          38  FORMAT (25X,15,15)
C          IF (BQPROF.NE.0) WRITE (11,192)
C          192  FORMAT (' THICKNESS Q-VALUE')
C
C          FN = 1000./(2.0*DT)
C
COMMENT      WRITE(2,36) DT,N,DF,ICALC
COMMENT      36  FORMAT(F5.1,15,F10.8,15)
C
C****
CHANGE: BQPROF = 0 =>NO BLOCK Q PROFILE IS GENERATED
C          = 1 =>GENERATES A BLOCKED Q PROFILE
C          A Q PROFILE CAN BE GENERATED ONLY IF ANALYSED DEPTH
C          INTERVALS DO NOT OVERLAP AND ARE IN ORDER DOWN THE
C          HOLE WITH THE MOST SHALLOW INTERVAL FIRST.
C          IF AN INTERVENING INTERVAL IS MISSING THEN ZEROS
C          ARE INSERTED AND ARE PLOTTED AS SUCH.
C
C          N = NUMBER OF POINTS IN A RECORD ON TAPE (LOGICAL UNIT 1)

```

```

C      N CANNOT EXCEED 257
C      DF = FREQUENCY INTERVAL (HZ) BETWEEN INPUT POINTS
C      FN = NYQUIST FREQUENCY FOR THIS DATA
C      ICALC = 1 MEANS THAT CALCOMP PLOTS ARE TO BE MADE
C****
1  FORMAT (5X,I5,F10.0,F5.0,I5)*
   IF (N.GT.257) GO TO 91
C
      DO 9 I=1,N
9    X(I)=(I-1)*DF
      IF (ICALC.NE.1) GO TO 10
      CALL PLOTS
      CALL PLOT(-15.0,2.0,-3)
CHANGE: READ IN ISAHZ AND ILAHZ
10  READ (5,2,END=99) IB,ISAHZ,ILAHZ,IQPC,ISP,ILP,
   &      DELZ,DELT,FZERO,PSTAT,ICPC,ICPL,IQPL
      ISA = INT(FLOAT(ISAHZ)/DF)
      ILA = INT(FLOAT(ILAHZ)/DF)

C 10  READ (5,2,END=99) IB,ISA,ILA,IQPC,ISP,ILP,DELZ,DELT
C      .FZERO,PSTAT,IC,PC,ICPL,IQPL
C****
C  IB = NUMBER OF BLOCK CONTAINING LOG SPECTRAL RATIO DATA
C      THIS REFERS TO LOGICAL UNIT 1
C  ISA = FIRST POINT TO USE IN ANALYSIS OF AMPLITUDE DATA
C      (CLOSEST POINT TO THE DESIRED FREQUENCY OF ISAHZ)
C  ILA = LAST POINT TO USE IN ANALYSIS OF AMPLITUDE DATA
C      (CLOSEST POINT TO THE DESIRED FREQUENCY OF ILAHZ)
C  ISAHZ = STARTING FREQUENCY OF ANALYSIS (IN HZ)
C  ILAHZ = LAST FREQUENCY OF ANALYSIS (HZ)
C  IQPC = 1 MEANS PLOT AMPLITUDE DATA AND REGRESSION LINE
C      ON CALCOMP
C  ISP = FIRST POINT TO USE IN ANALYSIS OF PHASE DATA
C      = 0 OR BLANK MEANS DO NOT CALCULATE DISPERSION CURVE
C  IF A DISPERSION CURVE IS TO BE CALCULATED THEN THE PHASE
C  CURVE MUST BE IN THE BLOCK IMMEDIATELY BEHIND THAT
C  CONTAINING THE AMPLITUDE DATA ON LOGICAL UNIT 1.
C  ILP = LAST POINT TO USE IN ANALYSIS OF PHASE DATA
C  DELZ = DISTANCE BETWEEN RECEIVERS FOR THIS PHASE DIFFERENCE
C  DELT = TIME DIFFERENCE BETWEEN WINDOWS FOR THIS PHASE
C      DIFFERENCE
C  FZERO = LOWEST FREQUENCY AT WHICH PHASE CURVE CROSSES ZERO
C      AT THIS FREQUENCY THE PHASE VELOCITY IS DELZ/DELT.
C      THIS IS USED IN PLOTTING THE DISPERSION CURVE.
C  PSTAT = REMOVE A PHASE OF PSTAT*FREQUENCY DEGREES FROM
C      THE PHASE CURVE BEFORE ANALYSIS.
C  ICPC = 1 MEANS TO PLOT DISPERSION DATA AND THEORETICAL
C      DISPERSION CURVE ON CALCOMP PLOTTER.
C  ICPL = 1 MEANS TO PLOT DISPERSION CURVE ON LINE PRINTER
C  IQPL = 1 MEANS TO PLOT Q VERSUS FREQUENCY CURVE ON LINE
C      PRINTER
C  IORGIN = DUMMY COUNTER; THE ORIGIN OF THE NEXT PLOT IS
C      DETERMINED BY THIS VARIABLE
C

```

C XORGIN = X ORIGIN OF THE PLOT OF THE LOG OF AMPL RATIO
 C YORGIN = Y ORIGIN OF THE PLOT OF THE LOG OF AMPL RATIO
 C
 C DEPAVE = AVERAGE DEPTH, OR MIDDEPTH OF DEPTH1 AND DEPTH2.
 C THE DEPTH AT WHICH THE Q VALUE IS APPLIED

C****

2 FORMAT (5X,6I5,4F5.0,3I5)
 IF (ISA.EQ.0) ISA=1
 IF (ILA.EQ.0) ILA=N
 IF (ISA.GE.ILA) GO TO 93
 IF (FZERO.EQ.0.0) FZERO=FN

C
 C CALCULATE SLOPE OF LOG SPECTRAL RATIO PLOT
 C

NSKIP=IB-IBL-1
 IF (NSKIP.NE.0) CALL SKIP(0,NSKIP,1,&95,&95,&95)
 CHANGE: THE FOLLOWING READ STATEMENT IS REPLACED BY

READ (1) DEPTH1,DEPTH2, (Y(I),I=1,N)
 COMMENT READ (1) (Y(I),I=1,N)

IBL=IB
 MA=ILA-ISA+1
 CALL SLOPE(X(ISA),Y(ISA),MA,S,SD,YI,YID)
 CHANGE: THE FOLLOWING WRITE STATEMENT IS ADDED TO GIVE A
 C DEPTH REFERENCE

WRITE (6,24) DEPTH1,DEPTH2
 24 FORMAT ('1PANARCTIC DEPTHS ',F6.1,' TO ',
 & F6.1,' METERS')
 WRITE (6,3) IB,ISA,ILA,S,SD,YI,YID
 3 FORMAT ('BLOCK ',I3,' POINTS ',I3,' TO ',I3,'/,6X,
 & 'SLOPE = ',E10.4
 .,5X,' STD DEV = ',E10.4,'/,6X,' INTERCEPT = ',E10.4,
 .5X,' STD DEV = ',E10.4)

C*****
 CHANGE: THE FOLLOWING IS INCLUDED TO CALCULATE Q

CALL INTVL(DEPTH1,DEPTH2,INTVEL)
 $Q = (-PI * (DEPTH2 - DEPTH1)) / (INTVEL * S)$
 DEPAVE = (DEPTH2+DEPTH1)/2.0
 DEPSEP = DEPTH2-DEPTH1
 IF (BQPROF.EQ.0) GOTO 194

IF (HOLDD.EQ.DEPTH1) GOTO 193
 THKNES = DEPTH1 - HOLDD
 ZERO = 0.0
 WRITE (11,191) THKNES, ZERO
 193 THKNES = DEPTH2 - DEPTH1
 WRITE (11,191) THKNES,Q
 191 FORMAT(5X,F6.0,F6.1,2X,F9.7,2X,3F6.0)

194 CONTINUE
 IF (BQPROF.EQ.0) WRITE (11,191) DEPAVE,Q,SD,DEPTH1,
 & DEPTH2,DEPSEP
 WRITE (6,190) INTVEL, Q
 190 FORMAT ('INTERVAL VELOCITY = ',F6.1,'/, 'Q VALUE = ',

```

& F5.1)
195 WRITE (6,195)
    FORMAT (' ')

    HOLDD = DEPTH2

C*****

    IF (IQPC.NE.1) GO TO 25
C
C MAKE CALCOMP PLOT OF AMPLITUDE DATA
C
CHANGE DO MY OWN PLOTTING TO GET FIXED AXES
    IORGIN = IORGIN + 1
    XORGIN = 0.0
    IF (IORGIN.EQ.5) IORGIN = 1
    IF (IORGIN.EQ.1) YORGIN = 15.0
    IF (IORGIN.EQ.1) XORGIN = 17.0
    IF (IORGIN.NE.1) YORGIN = -5.0
C MOVE THE ORIGIN
    CALL PLOT(XORGIN,YORGIN,-3)
    CALL PLOT1(X,Y,ISA,ILA,DEPTH1,DEPTH2,YI,S,SD,INTVEL,
& Q,DEPAVE)

C IT1=X(ISA)/10.0
C IT1=10*IT1
C IT2=X(ILA)/10.0+1.0
C IT2=IT2*10
C IT3=IT2-IT1+1
C T=1.0
C IF (IT3.GT.101) T=2.0
C IF (IT3.GT.201) T=4.0
C 13 IF (IT3.GT.401) STOP 13
C IT3=IT3/T+.8
C DO 15 I=1,IT3
C F(I)=(I-1)*T+IT1
C C(I)=-(YI+F(I)*S)
C IF (C(I).GT.0.0) C(I)=0.0
C 15 CONTINUE
C F(IT3+1)=F(1)
C F(IT3+2)=10.*T
C FLEN=(F(IT3)-F(1))/F(IT3+2)
C Y(ILA+1)=-C(1)
C CALL SCALE(Y(ISA),7.0,MA+1,1)
C C(IT3+1)=-Y(ILA+2)-7.0*Y(ILA+3)
C C(IT3+2)=Y(ILA+3)
C CALL AXIS2(0.0,0.0,' LN OF AMPLITUDE',-16,7.0,
C 0.0,-C(IT3+1),-C(IT3+2),1.0)
C CALL AXIS2(7.0,0.0,'FREQUENCY (HZ)',-14,FLEN,
C 90.0,F(IT3+1),F(IT3+2),1.0)
C CALL PLOT(7.0,FLEN,3)
C CALL PLOT(0.0,FLEN,2)
C CALL PLOT(0.0,0.0,2)
C CALL SYMBOL(-1.0,0.0,0.20,'BLOCK',90.0,5)

```

```

C      T=IB+.05
C      CALL NUMBER(-1.0,1.2,0.20,T,90.0,-1)
C      T=(C(1)-C(IT3+1))/C(IT3+2)
C      CALL PLOT(T,0.0,3)
C      CALL LINE(C,F,IT3,1,0)
C      DO 19 I=ISA,ILA
C      XP=(Y(I)+C(IT3+1))/(-C(IT3+2))
C      YP=(X(I)-F(IT3+1))/F(IT3+2)
C 19    CALL SYMBOL(XP,YP,0.10,1,90.0,-1)
C      IF (ICPC.NE.1.OR.ISP.EQ.0) GO TO 22
C      CALL PLOT(0.0,15.0,-3)
C      GO TO 25
C 22    CALL PLOT(10.0,0.0,-3)
C 25    IF (ISP.EQ.0) GO TO 10
C
C      CALCULATE DISPERSION CURVE
C
C      IF (ILP.EQ.0) ILP=ILA
C      IF (ISP.GE.ILP) GO TO 93
CHANGE: THE FOLLOWING READ STATEMENT IS REPLACED BY
      READ (1) DEPTH1,DEPTH2, (Y(I),I=1,N)
COMMENT      READ (1) (Y(I),I=1,N)
      IBL=IBL+1
CHANGE: THE FOLLOWING WRITE STATEMENT IS ADDED TO GIVE A
C      DEPTH REFERENCE
      WRITE (6,24) DEPTH1,DEPTH2
      WRITE (6,4)
      4 FORMAT ('-FREQUENCY',5X,'PHASE VELOCITY')
C
C IN CALCULATING THE DISPERSION CURVE FROM THE PHASE
C SPECTRUM I AM USING ROUTINE UNWRAP TO UNWRAP THE PHASE
C CURVE IF IT IS LIMITED TO THE PRINCIPAL BAND BETWEEN
C -180 AND 180.
C I AM ALSO REMOVING ANY LINEAR TREND BY SUBTRACTING
C PSTAT*FREQUENCY DEGREES FROM THE PHASE CURVE.
C
      CALL UNWRAP(Y,N)
      DELT=DELT-PSTAT/360.0
      DO 29 I=ISP,ILP
      PHZ=Y(I)-X(I)*PSTAT
      Y(I)=DELT/(DELT-PHZ/(360.0*X(I)))
29    WRITE (6,5) X(I),Y(I)
      5 FORMAT ('',E12,6,5X,E10.4)
      IF (ICPC.NE.1) GO TO 40
C
C      MAKE CALCOMP PLOT OF DISPERSION CURVE
C
      MP=ILP-ISP+1
      IT1=X(ISP)/10.0
      IT1=10*IT1
      IT2=X(ILP)/10.0+1.0
      IT2=IT2*10
      IT3=IT2-IT1+1
      T=1.0

```



```

IF (IT3.GT.101) T=2.0
IF (IT3.GT.201) T=4.0
32 IF (IT3.GT.401) STOP 32
IT3=IT3/T+.8
QR=-PI*DELT/S
CR=DELT/DELT
F(1)=IT1
C(1)=-CR/(1.0+ALOG(FZERO*1000.0)/(PI*QR))
IF (F(1).NE.0.0) C(1)=-CR/(1.0-ALOG(F(1)/FZERO)/
& (PI*QR))
DO 35 I=2,IT3
F(I)=(I-1)*T+IT1
35 C(I)=-CR/(1.0-ALOG(F(I)/FZERO)/(PI*QR))
F(IT3+1)=F(1)
F(IT3+2)=10.*T
FLEN=(F(IT3)-F(1))/F(IT3+2)
Y(ILP+1)=-C(IT3)
CALL SCALE(Y(ISP),3.0,MP+1,1)
C(IT3+1)=-Y(ILP+2)-3.0*Y(ILP+3)
C(IT3+2)=Y(ILP+3)
IF (C(1).GT.(C(IT3+1)+7.0*C(IT3+2)))
& C(1)=C(IT3+1)+7.0*C(IT3+2)
CALL AXIS2(0.0,0.0,'VELOCITY',-8,7.0,0.0)
& -C(IT3+1),-C(IT3+2),1.0)
CALL AXIS2(7.0,0.0,'FREQUENCY (HZ)',-14,
& FLEN,90.0,F(IT3+1),F(IT3+2),1.0)
CALL PLOT(7.0,FLEN,3)
CALL PLOT(0.0,FLEN,2)
CALL PLOT(0.0,0.0,2)
CALL SYMBOL(-1.0,0.0,0.20,'BLOCK',90.0,5)
T=IBL+.05
CALL NUMBER(-1.0,1.2,0.20,T,90.0,-1)
T=(C(1)-C(IT3+1))/C(IT3+2)
CALL PLOT(T,0.0,3)
CALL LINE(C,F,IT3,1,0)
DO 39 I=ISP,ILP
XP=(Y(I)+C(IT3+1))/(-C(IT3+2))
YP=(X(I)-F(IT3+1))/F(IT3+2)
39 CALL SYMBOL(XP,YP,0.10,4,90.0,-1)
IF (IQPC.EQ.1) CALL PLOT(0.0,-15.0,-3)
CALL PLOT(-10.0,0.0,-3)
C
C PLOT DISPERSION CURVE ON LINE PRINTER
C
40 IF (ICPL.NE.1) GO TO 42
F1=DF*(ISP-1)
MP=ILP-ISP+1
DELT=DELT+PSTAT/360.0
WRITE (6,6) IBL,DELT,DELT,FZERO,PSTAT
6 FORMAT ('1DISPERSION CURVE FOR BLOCK ',I3,/,6X,
& 'DELZ = ',F10.4,5X,
& 'DELT = ',F10.4,5X,'FZERO = ',F6.1,5X,'PSTAT = ',
& F10.4)
CALL GRAF(F1,DF,Y(ISP),MP,1)

```

C
C
C

PLOT Q VERSUS FREQUENCY CURVE ON LINE PRINTER

```

42 IF (IQPL.NE.1) GO TO 10
   IF (ISA.LT.ISP) ISA=ISP
   IF (ILA.GT.ILP) ILA=ILP
   MA=ILA-ISA+1
      DO 44 I=ISA,ILA
44   Y(I)=-PI*DELZ/(Y(I)*S)
      F1=DF*(ISA-1)
      WRITE (6,7) IB
7   FORMAT ('1Q VERSUS FREQUENCY CURVE FOR BLOCK ',I3)
   CALL GRAF(F1,DF,Y(ISA),MA,1)
   GO TO 10
91  WRITE (6,92)
92  FORMAT ('1N CANNOT EXCEED 257')
   GO TO 99
93  WRITE (6,94)
94  FORMAT ('1ISA (ISP) MUST BE LESS THAN ILA (ILP)')
   GO TO 99
95  WRITE (6,96)
96  FORMAT ('1BAD RETURN FROM SKIP')
99  IF (ICALC.EQ.1) CALL PLOT(0.0,0.0,999)

```

CHANGE: PLOT.LOG REQUIRES THE LAST THICKNESS IN Q.MODEL
 C TO BE 99999 FOR TERMINATION OF THE PROGRAM, THIS
 C IS THE SAME AS IN THE CASE OF EARTHMODEL.
 NINES = 99999.0
 IF (BQPROF.NE.0) WRITE (11,191) NINES, ZERO

```

STOP
END
SUBROUTINE SLOPE(X,Y,N,S,SD,B,BD)

```

C
C
C

SUBROUTINE BY DAVE GANLEY, NOV 14, 1977.

C THIS SUBROUTINE WILL CALCULATE THE LEAST SQUARES ESTIMATE
 C OF THE EQUATION OF A STRAIGHT LINE THROUGH N DATA POINTS.

C
C
C

INPUTS:

C X = ARRAY OF X COORDINATES OF THE POINTS
 C Y = ARRAY OF Y COORDINATES OF THE POINTS
 C N = NUMBER OF INPUT POINTS (N MUST BE AT LEAST 3)

C
C
C

OUTPUTS:

C S = LEAST SQUARES ESTIMATE OF THE SLOPE
 C SD = ESTIMATE OF THE STANDARD DEVIATION OF THE SLOPE
 C B = LEAST SQUARES ESTIMATE OF THE Y INTERCEPT
 C SB = ESTIMATE OF THE STANDARD DEVIATION OF B

C
C
C

C THEORY IS TAKEN FROM ELEMENTS OF STATISTICAL INFERENCE BY
 C DAVID V HUNSTBERGER (PUB BY ALLYN AND BACON, 1967) ON
 C PAGES 255 TO 263.

C

DIMENSION X(N),Y(N)

```

IF (N.LT.3) GO TO 6
XN=N
XN2=XN-2.0
SUMX=0.0
SUMX2=0.0
SUMY=0.0
SUMY2=0.0
SUMXY=0.0
DO 1 I=1,N
SUMX=SUMX+X(I)
SUMX2=SUMX2+X(I)*X(I)
SUMY=SUMY+Y(I)
SUMY2=SUMY2+Y(I)*Y(I)
SUMXY=SUMXY+X(I)*Y(I)
SXY=SUMXY-SUMX*SUMY/XN
SX2=SUMX2-SUMX*SUMX/XN
SY2=SUMY2-SUMY*SUMY/XN
S=SXY/SX2
SD=(SY2-S*SXY)/(SX2+XN2)
B=(SUMY-S*SUMX)/XN
BD=(SD*SX2+SD*SUMX*SUMX/XN)/XN
SD=SQRT(SD)
BD=SQRT(BD)
RETURN
6 WRITE (6,7)
7 FORMAT('1 SUBROUTINE SLOPE REQUIRES N GREATER THAN 2')
STOP 7
END

```

CHANGE: THE FOLLOWING SUBROUTINE HAS BEEN ADDED TO
C CALCULATE INTERVAL VELOCITIES OVER A DEPTH
C INTERVAL IN EARTHMODEL. IT AVERAGES THE VELOCITIES
C (WEIGHTED BY THE THICKNESS OF EACH LAYER) TO RETURN
C INTVEL. THE DEPTH INTERVAL IS GIVEN BY DEPTH1, DEPTH2.
C SUBROUTINE INTVL(DEPTH1,DEPTH2,INTVEL)
C WRITTEN BY NICK KEEHN (1986).
LOGICAL*1 JUNK
REAL INTVEL

```

READ (10,1000) JUNK
1000 FORMAT(A1)

```

```

SUMVEL = 0.0
DEPTH = 0.0

```

```

100 READ (10,2000) THKNS, VEL
2000 FORMAT(5X,2F5.0)

```

```

DEPTH = DEPTH + THKNS
IF (DEPTH.LE.DEPTH1) GOTO 100
IF (DEPTH.GT.DEPTH2) GOTO 200
IF ((DEPTH-DEPTH1).GT.THKNS) GOTO 300

```

```

SUMVEL = (DEPTH - DEPTH1)*VEL

```

```

      IF (DEPTH.EQ.DEPTH2) GOTO 400
      GOTO 100

300  SUMVEL = THKNS*VEL + SUMVEL
      GOTO 100

200  IF ((DEPTH-THKNS).LE.DEPTH1) SUMVEL = (DEPTH2-DEPTH1)
      &*VEL
      IF ((DEPTH-THKNS).GT.DEPTH1) SUMVEL = SUMVEL +
      & (DEPTH2-(DEPTH-THKNS))*VEL

400  INTVEL = SUMVEL/(DEPTH2 - DEPTH1)

      REWIND 10
      RETURN
      END

```

```

      SUBROUTINE PLOT1(X,Y,ISA,ILA,DEPTH1,DEPTH2,YI,
      & S,SD,INTVEL,Q,DEPAVE)

```

```

C      WRITTEN BY NICK KEEHN (1986).
      DIMENSION X(257),Y(257),XVAL(257),YVAL(257),XREG(4),
      & YREG(4)
      REAL INTVEL

```

```

C      MOVE THE ORIGIN FOR THIS PLOT
C      CALL PLOT(20.0,0.0,-3)

```

```

      K = 0
      DO 333 I=ISA,ILA
          K = K+1
          XVAL(K) = X(I)
          YVAL(K) = Y(I)
333  CONTINUE
      LAST = K

```

```

C      DO THE NEXT TWO LINES IN THE CALLING ROUTINE IF MORE
C      THAN ONE PLOT IS TO BE MADE
C      CALL PLOTS
C      CALL PLOT(2.0,2.0,-3)

```

```

C      AUTOMATIC SCALING
C      CALL SCALE(XVAL,15.0,ILA,1)
C      CALL SCALE(YVAL,7.0,ILA,1)

```

```

C      MANUAL SCALING
C      XVAL(LAST+1) = LOWEST VALUE WANTED ON THE X-AXIS
C                      ITSELF
C      XVAL(LAST+2) = NUMBER OF USER UNITS/CENTIMETER ALONG
C                      X AXIS
C      YVAL(LAST+1) = LOWEST VALUE ON Y AXIS

```

```

C      YVAL(LAST+2) = NUMBER OF USER UNITS/CENTIMETER ALONG
C      Y AXIS
      XVAL(LAST+1) = 0.0
      XVAL(LAST+2) = 20.0
      YVAL(LAST+1) = 0.0
      YVAL(LAST+2) = 1.0

C      SET UP AND LABEL AXES
      CALL AXIS2(0.0,0.0,' Frequency (HZ)',-16,8.0,0.0,
$          XVAL(LAST+1),XVAL(LAST+2),1.0)
      CALL AXIS2(0.0,0.0,' Ln Amp Ratio',13,3.0,90.0,
$          YVAL(LAST+1),YVAL(LAST+2),-1.0)

C      DRAW BOX AROUND PLOT.
      CALL PLOT(8.0,0.0,3)
      CALL PLOT(8.0,3.0,2)
      CALL PLOT(0.0,3.0,2)

C      DOCUMENT THE PLOT
      CALL SYMBOL(8.5,2.5,.25,'DEPTHS:           M',
&          0.0,2)
      CALL NUMBER(10.4,2.5,.25,DEPTH1,0.0,0)
      CALL NUMBER(12.1,2.5,.25,DEPTH2,0.0,0)
      CALL SYMBOL(8.5,2.0,.25,'MID-DEPTH:       M',0.0,19)
      CALL NUMBER(11.2,2.0,.25,DEPAVE,0.0,1)
      CALL SYMBOL(8.5,1.5,.25,'SLOPE:',0.0,6)
      CALL NUMBER(10.2,1.5,.25,S,0.0,6)
      CALL SYMBOL(8.5,1.0,.25,'SLOPE STD:',0.0,10)
      CALL NUMBER(11.2,1.0,.25,SD,0.0,7)
      CALL SYMBOL(8.5,0.5,.25,'INT. VEL.:',0.0,10)
      CALL NUMBER(11.2,0.5,.25,INTVEL,0.0,1)
      CALL SYMBOL(8.5,0.0,.25,'Q-VALUE:',0.0,8)
      CALL NUMBER(10.7,0.0,.25,Q,0.0,1)

C      PLOT THE DATA
      CALL LINE(XVAL,YVAL,LAST,1,-1,75)

C      EVALUATE TWO POINTS ON THE REGRESSION LINE
C      BETWEEN X(ISA) AND X(ILA)
      XREG(1) = X(ISA)
      XREG(2) = X(ILA)
      XREG(3) = XVAL(LAST+1)
      XREG(4) = XVAL(LAST+2)
      YREG(1) = X(ISA)*S + YI
      YREG(2) = X(ILA)*S + YI
      YREG(3) = YVAL(LAST+1)
      YREG(4) = YVAL(LAST+2)

C      PLOT THE REGRESSION LINE
      CALL LINE(XREG,YREG,2,1,0,0)

C      DO THE NEXT LINE IN THE MAIN PROGRAM
C      CALL PLOT(0.0,0.0,999)

```

RETURN
END

SUBROUTINE TAPER(X,N,M)

SUBROUTINE BY DAVE GANLEY, MARCH 8, 1978.

THIS SUBROUTINE WILL APPLY A COSINE TAPER TO EACH END
END OF AN INPUT TIME SERIES.

INPUTS ARE:

X = TIME SERIES

N = LENGTH OF X

M = # OF POINTS AT EACH END OF X TO WEIGHT (MAX=25)

OUTPUT IS:

X = TAPERED TIME SERIES

DIMENSION W(25),X(1)

DATA ML/0/

IF (M.GT.25) GO TO 4

IF (2*M.GT.N) GO TO 6

IF (M.EQ.ML) GO TO 2

T1=3.1415927/(M+1)

DO 1 I=1,M

T2=T1*I

1 W(I)=.5-COS(T2)/2.0

2 NP1=N+1

DO 3 I=1,M

J=NP1-I

X(I)=X(I)*W(I)

3 X(J)=X(J)*W(I)

RETURN

4 WRITE (6,5)

5 FORMAT

& ('SUBROUTINE TAPER CAN ONLY WEIGHT UP TO 25 TERMS')

STOP 16

6 WRITE (6,7)

7 FORMAT

& ('M CANNOT BE LARGER THAN N/2 IN SUBROUTINE TAPER')

STOP 16

END

SUBROUTINE AMPPHZ (LOG2N, X, IC, PDC, PFN)

WRITTEN BY DAVE GANLEY ON MAY 19, 1977.

THIS SUBROUTINE CALCULATES AMPLITUDE AND/OR PHASE SPECTRA FROM THE REAL AND IMAGINARY PARTS OF A FREQUENCY SPECTRUM OR VICE VERSA. THE INPUT (OUTPUT) ARRAY X IS OF LENGTH $2^{*}LOG2N$ WITH THE REAL PARTS OF THE FOURIER COEFFICIENTS FOR FREQUENCIES ZERO TO NYQUIST IN THE FIRST $N/2+1$ POSITIONS OF X. THE IMAGINARY PARTS OF THE COEFFICIENTS ARE IN POSITIONS $N/2+2$ TO N AND ARE NOT STORED FOR DC OR NYQUIST FREQUENCY (WHERE THEY ARE ZERO). THE OUTPUT (INPUT) ARRAY HAS AMPLITUDES IN THE FIRST $N/2+1$ POSITIONS AND PHASES IN DEGREES IN THE LAST $N/2-1$ POSITIONS. PHASES FOR DC AND NYQUIST FREQUENCIES (0 OR 180) ARE RETURNED (SPECIFIED) IN PDC AND PFN.

IC = 1 INPUT IS FOURIER COEFFICIENTS.
 OUTPUT AMPLITUDE AND PHASE.
 = 2 INPUT IS FOURIER COEFFICIENTS.
 OUTPUT IS AMPLITUDE ONLY.
 = 3 INPUT IS FOURIER COEFFICIENTS.
 OUTPUT IS PHASE ONLY.
 = -1 INPUT AMPLITUDE AND PHASE.
 OUTPUT FOURIER COEFFICIENTS.

NO SUBROUTINES ARE CALLED.

```

DIMENSION X(1)
IF (LOG2N.LT.1) RETURN
M=1
DO 9 I=2,LOG2N
9 M=2*M
N=2*M
MP1=M+1
IF (IC.LT.1) GO TO 400
GO TO (100,200,300),IC

```

CALCULATE AMPLITUDE AND PHASE SPECTRUM

```

100 IF (X(1).GE.0.0) GO TO 105
X(1)=-X(1)
PDC=180.0
GO TO 110
105 PDC=0.0
110 IF (X(MP1).GE.0.0) GO TO 115
X(MP1)=-X(MP1)
PFN=180.0
GO TO 120

```



```

115 PFN=0.0
120 IF (LOG2N.EQ.1) RETURN
    DO 129 I=2,M
    A=X(I)
    B=X(I+M)
    X(I)=SQRT(A*A+B*B)
129 X(I+M)=57.29578*ATAN2(B,A)
    RETURN

```

C
C
C

CALCULATE AMPLITUDE SPECTRUM ONLY

```

200 IF (X(1).LT.0.0) X(1)=-X(1)
    IF (X(MP1).LT.0.0) X(MP1)=-X(MP1)
    IF (LOG2N.EQ.1) RETURN
    DO 209 I=2,M
    A=X(I)
    B=X(I+M)
209 X(I)=SQRT(A*A+B*B)
    RETURN

```

C
C
C

CALCULATE PHASE SPECTRUM ONLY

```

300 IF (X(1).LT.0.0) GO TO 305
    PDC=0.0
    GO TO 310
305 PDC=180.0
310 IF (X(MP1).LT.0.0) GO TO 315
    PFN=0.0
    GO TO 320
315 PFN=180.0
320 IF (LOG2N.EQ.1) RETURN
    DO 329 I=2,M
    A=X(I)
    B=X(I+M)
329 X(I+M)=57.29578*ATAN2(B,A)
    RETURN

```

C
C
C

CALCULATE FOURIER COEFFICIENTS FROM AMPLITUDE AND PHASE

```

400 X(1)=X(1)*COS(PDC/57.29578)
    X(MP1)=X(MP1)*COS(PFN/57.29578)
    IF (LOG2N.EQ.1) RETURN
    DO 409 I=2,M
    A=X(I)
    B=X(I+M)/57.29578
    X(I)=A*COS(B)
409 X(I+M)=A*SIN(B)
    RETURN
    END

```

SUBROUTINE FFTR2(LOG2N,X,Y)

WRITTEN BY DAVE GANLEY ON MAY 1, 1972.

THIS SUBROUTINE ACCEPTS AS INPUT TWO REAL FUNCTIONS (TIME DOMAIN) AND CALCULATES THEIR FOURIER TRANSFORMS. INPUT ARRAYS ARE OF LENGTH $N=2^{**}LOG2N$. ON OUTPUT THE REAL COEFFICIENTS FOR $N/2+1$ TRANSFORM POINTS FOR FREQUENCIES ZERO TO NYQUIST FREQUENCY ARE STORED IN POSITIONS 1 TO $N/2+1$ OF X AND Y. THE IMAGINARY COEFFICIENTS ARE STORED IN POSITIONS $N/2+2$ TO N AND APPLY TO FREQUENCIES FROM ONE ABOVE ZERO TO ONE LESS THAN THE NYQUIST FREQUENCY. THE IMAGINARY COEFFICIENTS OF ZERO AND NYQUIST FREQUENCY WOULD BE ZERO.

FOR EXAMPLE:

INPUT 8 POINTS AT 1 MILLISECOND SPACING. ON OUTPUT THE REAL COEFFICIENTS OF THE SPECTRUM ARE IN POSITIONS 1 TO 5 AND APPLY TO FREQUENCIES 0, 125, 250, 375 AND 500 HERTZ. THE IMAGINARY COEFFICIENTS ARE IN POSITIONS 6 TO 8 AND APPLY TO FREQUENCIES OF 125, 250 AND 375 HZ.

THIS SUBROUTINE WOULD BE SPEEDED UP IF IT WAS USED SEVERAL TIMES BY SUPPLYING ARRAYS OF SINE AND COSINE VALUES AND AN ARRAY OF INDICES IN BIT REVERSED ORDER.

FFTR2 AND FFTCX2 FORM A TRANSFORM PAIR.

SUBROUTINES CALLED:

1. MR1DFT
2. SW2RBO

```

DIMENSION X(1),Y(1)
IF (LOG2N.LT.1) RETURN
N=2**LOG2N
CALL MR1DFT(LOG2N,X,Y)
IF (LOG2N.EQ.1) GO TO 30
CALL SW2RBO(LOG2N,X,Y)

```

WE HAVE INPUT X AND Y TO MR1DFT AS $X + I*Y$. THE TRANSFORM OF $X + I*Y$ IS $A + B*I$ WHERE I IS ROOT OF -1 , AND A IS STORED IN X AND B IS STORED IN Y.

NOW $X(W)$ AND $Y(W)$, THE FOURIER TRANSFORMS OF X AND Y, ARE CALCULATED USING THE FOLLOWING EQUATIONS. $X(W)$ AND $Y(W)$ ARE COMPLEX AND W GOES FROM 0 TO $N/2$ IN THE FOLLOWING EQUATIONS. $W=N/2$ IS THE NYQUIST FREQUENCY.

C
C
C
C
C

$$X(W) = (A(W)+A(N-W) + I*(B(W)-B(N-W)))/2$$

$$Y(W) = (B(W)+B(N-W) + I*(A(N-W)-A(W)))/2$$

$$TWON=2*N$$

$$NBY2=N/2$$

$$N21=NBY2+1$$

$$NP2=N+2$$

DO 10 I=2,NBY2

$$J=NP2-I$$

$$XR=X(I)+X(J)$$

$$XI=Y(I)-Y(J)$$

$$YR=Y(I)+Y(J)$$

$$YI=X(J)-X(I)$$

$$X(I)=XR/TWON$$

$$X(J)=XI/TWON$$

$$Y(I)=YR/TWON$$

10 Y(J)=YI/TWON

$$X(1)=X(1)/N$$

$$Y(1)=Y(1)/N$$

$$X(N21)=X(N21)/N$$

$$Y(N21)=Y(N21)/N$$

C
C
C
C
C

THE IMAGINARY TERMS ARE NOW REVERSED IN DIRECTION
IN THEIR STORAGE AND MUST BE STORED IN THE CORRECT
ORDER.

IF (LOG2N.EQ.2) RETURN

$$NP1=N+1$$

$$N41=N/4-1$$

DO 20 I=1,N41

$$TX=X(N21+I)$$

$$TY=Y(N21+I)$$

$$X(N21+I)=X(NP1-I)$$

$$Y(N21+I)=Y(NP1-I)$$

$$X(NP1-I)=TX$$

20 Y(NP1-I)=TY

RETURN

30 DO 39 I=1,N

$$X(I)=X(I)/N$$

39 Y(I)=Y(I)/N

RETURN

END

SUBROUTINE MR1DFT(LOG2N,X,Y)

WRITTEN BY DAVE GANLEY MAY 1, 1972.

MIXED RADIX ONE DIMENSIONAL FOURIER TRANSFORM

THIS ROUTINE CALCULATES THE FOURIER TRANSFORM OF
 $X + I*Y$ AND OUTPUTS THE TRANSFORM IN THE ARRAYS X AND Y.

$$\text{OUTPUT} \quad N-1 \quad \text{INPUT} \\ X(J)+I*Y(J) = \sum_{K=0}^{N-1} (X(K)+I*Y(K)) \text{EXP}(-2*PI*I*J*K/N)$$

WHERE I IS SQUARE ROOT OF -1 AND $N=2**\text{LOG2N}$

IF THIS ROUTINE IS USED SEVERAL TIMES IT MAY BE
 SPEEDED UP BY SUPPLYING ARRAYS OF COSINE AND SINE
 VALUES.

AFTER USING MR1DFT ONE MUST CALL SW2RBO BECAUSE
 THE OUTPUT ARRAY IS SCRAMBLED AND MUST BE UNSCRAMBLED
 BY STORING SUBSCRIPTED ELEMENTS AS IF THE BIT ORDER OF
 THE SUBSCRIPT WAS REVERSED. AN ARRAY OF INDICES IN
 BIT REVERSED ORDER COULD BE SUPPLIED TO SPEED UP THIS
 PROCESS IF THIS ROUTINE WAS USED MANY TIMES IN 1 JOB.

```

DIMENSION X(1),Y(1)
N=2**LOG2N
IF (LOG2N.LE.1) GO TO 50
DO 40 I=2,LOG2N,2
MM=2**(LOG2N-I)
M4=4*MM
DO 30 J=1,MM
IF (J.EQ.1) GO TO 6
ARG=6.2831853*(J-1)/M4
C1=COS(ARG)
S1=SIN(ARG)
C2=C1*C1-S1*S1
S2=2.0*C1*S1
C3=C2*C1-S2*S1
S3=C2*S1+S2*C1
GO TO 8
6 C1=1.0
C2=1.0
C3=1.0
S1=0.0
S2=0.0
S3=0.0
8 DO 20 K=M4,N,M4
I1=K+J-M4

```

```

I2=I1+MM
I3=I2+MM
I4=I3+MM
X1=X(I1)+X(I3)
X2=X(I1)-X(I3)
X3=X(I2)+X(I4)
X4=X(I2)-X(I4)
Y1=Y(I1)+Y(I3)
Y2=Y(I1)-Y(I3)
Y3=Y(I2)+Y(I4)
Y4=Y(I2)-Y(I4)
X(I1)=X1+X3
Y(I1)=Y1+Y3
IF (J.EQ.1) GO TO 10
X(I2)=(X1-X3)*C2+(Y1-Y3)*S2
Y(I2)=(Y1-Y3)*C2-(X1-X3)*S2
X(I3)=(X2+Y4)*C1+(Y2-X4)*S1
Y(I3)=(Y2-X4)*C1-(X2+Y4)*S1
X(I4)=(X2-Y4)*C3+(Y2+X4)*S3
Y(I4)=(Y2+X4)*C3-(X2-Y4)*S3
GO TO 20
10 X(I2)=X1-X3
   Y(I2)=Y1-Y3
   X(I3)=X2+Y4
   Y(I3)=Y2-X4
   X(I4)=X2-Y4
   Y(I4)=Y2+X4
20 CONTINUE
30 CONTINUE
40 CONTINUE
50 IF (LOG2N.EQ.LOG2N/2*2) GO TO 70
   DO 60 I=1,N,2
   X1=X(I)+X(I+1)
   X2=X(I)-X(I+1)
   Y1=Y(I)+Y(I+1)
   Y2=Y(I)-Y(I+1)
   X(I)=X1
   Y(I)=Y1
   X(I+1)=X2
   Y(I+1)=Y2
60 Y(I+1)=Y2
70 RETURN
END

```

SUBROUTINE SW2RBO(LOG2M,X,Y)

WRITTEN BY DAVE GANLEY ON MAY 1, 1972.

THIS ROUTINE SWITCHES POSITIONS OF ELEMENTS IN THE INPUT ARRAYS. THIS IS DONE BY REVERSING THE BIT ORDER OF THE SUBSCRIPT OF THE INPUT ELEMENT TO CALCULATE THE SUBSCRIPT OF THE OUTPUT ELEMENT OF THE ARRAY. THE ELEMENTS IN BOTH ARRAYS ARE STORED IN BIT REVERSED ORDER. THE ARRAYS ARE OF LENGTH $2^{**}LOG2M$. LOG2M CAN'T EXCEED 13.

FOR EXAMPLE:

IF LOG2M IS 3 THEN THE SUBSCRIPTS ARE THOUGHT TO GO FROM 0 TO 7. CONSIDER THE TERM WHICH IS IN POSITION 2 ON INPUT. ITS SUBSCRIPT WOULD BE 001 IN BINARY. REVERSING THIS GIVES 100 WHICH IS THE SUBSCRIPT OF POSITION 5. THUS THE TERM IN POSITION 2 IS OUTPUT IN POSITION 5 AND VICE VERSA.

IF SW2RBO WILL BE USED SEVERAL TIMES, TIME COULD BE SAVED BY STORING THE REVERSED BIT ORDER INDICES IN AN ARRAY AND SWITCHING TERMS ACCORDING TO THIS ARRAY.

```

DIMENSION X(1),Y(1),IS(12),ID(12)
EQUIVALENCE (IS1,IS(1)),(IS2,IS(2)),(IS3,IS(3)),
*(IS4,IS(4)),(IS5,IS(5)),(IS6,IS(6)),(IS7,IS(7)),
*(IS8,IS(8)),(IS9,IS(9)),(IS10,IS(10)),(IS11,IS(11)),
*(IS12,IS(12)),(ID1,ID(1)),(ID2,ID(2)),(ID3,ID(3)),
*(ID4,ID(4)),(ID5,ID(5)),(ID6,ID(6)),(ID7,ID(7)),
*(ID8,ID(8)),(ID9,ID(9)),(ID10,ID(10)),(ID11,ID(11)),
*(ID12,ID(12))

```

```

IF (LOG2M.GT.13) GO TO 25
IF (LOG2M.LE.1) RETURN
ID12=2**(LOG2M-1)
IS12=2*ID12
DO 10 I=2,12
J=13-I
IS(J)=ID(J+1)
ID(J)=1
IF (ID(J+1).GT.1) ID(J)=ID(J+1)/2

```

10 CONTINUE

```

J=0
DO 20 I1=1, ID1
DO 20 I2=I1, IS1, ID1
DO 20 I3=I2, IS2, ID2
DO 20 I4=I3, IS3, ID3
DO 20 I5=I4, IS4, ID4
DO 20 I6=I5, IS5, ID5

```

```
DO 20 I7=I6,IS6,ID6
DO 20 I8=I7,IS7,ID7
DO 20 I9=I8,IS8,ID8
DO 20 I10=I9,IS9,ID9
DO 20 I11=I10,IS10,ID10
DO 20 I12=I11,IS11,ID11
DO 20 I13=I12,IS12,ID12
J=J+1
IF (J.LE.I13) GO TO 20
T=X(J)
X(J)=X(I13)
X(I13)=T
T=Y(J)
Y(J)=Y(I13)
Y(I13)=T
20 CONTINUE
RETURN
25 WRITE (6,26)
26 FORMAT (' LOG2M IS TOO LARGE IN SW2RBO')
STOP 8
END
```

SUBROUTINE DANIEL(X,N,FWIND,DT)

SUBROUTINE BY DAVE GANLEY DECEMBER 12, 1977.

THIS SUBROUTINE CALCULATES A DANIELL-LIKE SPECTRAL ESTIMATE FROM THE PERIODOGRAM. THIS IS DONE BY AVERAGING ALL FREQUENCIES WITHIN A WINDOW CENTRED ABOUT THE DESIRED FREQUENCY. SINCE REAL AND IMAGINARY COEFFICIENTS (OR AMPLITUDE AND PHASE VALUES) ARE AVERAGED THIS IS NOT A DANIELL POWER SPECTRAL ESTIMATE. ALSO NOTE THAT AT FREQUENCIES WITHIN HALF OF THE WINDOW WIDTH OF DC OR NYQUIST FREQUENCIES THE ESTIMATES ARE CALCULATED BY AVERAGING OVER FEWER VALUES.

INPUTS:

X = INPUT FOURIER TRANSFORM AS OUTPUT BY MY ROUTINE FFTR1 OR AMPPHZ. ON OUTPUT X CONTAINS THE SMOOTHED SPECTRAL ESTIMATE IN THE SAME FORMAT.
 N = LENGTH OF X (N IS 2**M WHERE M IS AN INTEGER)
 FWIND = WINDOW WIDTH IN FREQUENCY DOMAIN (HERTZ)
 DT = SAMPLE INTERVAL OF ORIGINAL TIME SERIES IN MILLISECONDS

```

DIMENSION X(N)
DIMENSION Y(1024)
IF (N.LE.1024) GO TO 10
WRITE (6,1)
1 FORMAT ('N CANNOT EXCEED 1024 IN SUBROUTINE DANIELL')
STOP 8
10 N2=N/2
   N22=N2+2
   NP2=N+2
   DF=1000.0/(N*DT)
   M2=FWIND/(2.0*DF)+.5
   M21=M2+1
   M=2*M2+1
   XM=M
   XM1=M-1
   FWID=2.0*M2*DF
   WRITE (6,2) M,FWID
2  FORMAT (' ',I3,' PTS USED IN DANIELL WINDOW, WIDTH = ',
   F6.2,' HERTZ')
   IF (M2.EQ.0) RETURN
   DO 19 I=1,N
19  Y(I)=X(I)
   KE=0
   DO 49 I=1,M2
   II=N22-I
   L=I+N2
   LL=II+N2
   JE=M21-I
   I21=2*I-1
   II21=N22-I21

```



```

L21=I21+N2
LL21=NP2-I21
XF=XM-JE
XF1=XF-1.0
IF (I.EQ.1) GO TO 30
KE=I-1
    DO 29 K=1,KE
        X(I)=X(I)+Y(I+K)+Y(I-K)
        X(II)=X(II)+Y(II+K)+Y(II-K)
        X(L)=X(L)+Y(L+K)
        X(LL)=X(LL)+Y(LL-K)
        IF (K.EQ.KE) GO TO 29
        X(L)=X(L)+Y(L-K)
        X(LL)=X(LL)+Y(LL+K)
29    CONTINUE
30    DO 39 J=1,JE
        X(I)=X(I)+Y(I21+J)
        X(II)=X(II)+Y(II21-J)
        IF (I.EQ.1) GO TO 39
        X(L)=X(L)+Y(L21+J)
        X(LL)=X(LL)+Y(LL21-J)
39    CONTINUE
        X(I)=X(I)/XF
        X(II)=X(II)/XF
        IF (I.EQ.1) GO TO 49
        X(L)=X(L)/XF1
        X(LL)=X(LL)/XF1
49    CONTINUE
        IE=N22-M21
        IF (M21.GT.IE) RETURN
        L=M21+N2
        DO 59 I=1,M2
            X(M21)=X(M21)+Y(M21+I)+Y(M21-I)
            IF (M.GT.N2.AND.I.EQ.M2) GO TO 59
            X(L)=X(L)+Y(L+I)
            IF (I.EQ.M2) GO TO 59
            X(L)=X(L)+Y(L-I)
59    CONTINUE
        X(M21)=X(M21)/XM
        X(L)=X(L)/XM1
        IF (M.GT.N2) X(L)=X(L)*XM1/(XM1-1.0)
        IF (IE.EQ.M21) RETURN
        L=IE+N2
        DO 69 I=1,M2
            X(IE)=X(IE)+Y(IE+I)+Y(IE-I)
            X(L)=X(L)+Y(L-I)
            IF (I.NE.M2) X(L)=X(L)+Y(L+I)
69    CONTINUE
        X(IE)=X(IE)/XM
        X(L)=X(L)/XM1
        IE=IE-1
        IS=M21+1
        IF (IS.GT.IE) RETURN
        DO 89 I=IS,IE

```

```
L=L+N2  
DO 79 J=1,M2  
X(I)=X(I)+Y(I+J)+Y(I-J)  
X(L)=X(L)+Y(L+J)+Y(L-J)  
CONTINUE  
X(I)=X(I)/XM  
X(L)=X(L)/XM  
CONTINUE
```

79

89

```
RETURN  
END
```